Catalytic graphitisation of refcoal cokes

by

Mhlwazi Solomon Nyathi

Submitted in partial fulfilment of the requirements for the degree of

Master of Science

Department of Chemistry
Faculty of Natural and Agricultural Sciences
University of Pretoria
Pretoria

July 2007

DECLARATION

I, Mhlwazi Solomon Nyathi, declare that the dissertation that I hereby submit for the degree in Chemistry at the University of Pretoria has not previously been submitted by me for degree purposes at any other university.

SIGNED ON THIS ------- DAY OF JULY 2007

Mhlwazi Solomon Nyathi

ABSTRACT

Synthetic graphite is an important industrial material, used in nuclear reactors, electrodes and many other applications. Graphitisation of coke is the solid-state transformation of the disordered carbon atoms into a well-ordered hexagonal graphite structure, requiring temperatures as high as 2 600 ºC. Catalytic graphitisation using metals or metal compounds allows the rearrangement of atoms to occur at lower temperatures. The extent of catalytic graphitisation is markedly dependent on the structural ordering of the parent coke, the catalyst concentration and the reaction conditions.

Solvent extraction of coal using dimethylformamide (DMF) as a solvent yields a refined coal solution referred to as Refcoal solution. Cokes of solvent-refined Tshikondeni coal derivatives have been found to be graphitisable. The activity of acetylacetonate and hydroxyquinolinate complexes of Al, Ca, Cu, Fe and Zr for catalysing the graphitisation of Refcoal cokes at 1 600 and 2 000 ºC was investigated. The effect of residence time on the catalytic graphitisation of Refcoal cokes was investigated by heat-treating cokes for two and six hours at 1 600 °C. For iron(III)acetylacetonate, the effect of metal concentrations was studied.

Samples were analysed using thermogravimetric analysis (TGA), scanning electron microscopy (SEM), X-ray diffraction (XRD), Raman spectroscopy and optical microscope techniques. The results show that calcium(II)acetylacetonate catalyses the graphitisation of Refcoal cokes. The degree of graphitisation increases with an increase in the iron concentration. However, iron promotes localised graphitisation, probably in the vicinity of the catalyst particles.

KEYWORDS: Refcoal, coke, carbonisation, catalytic graphitisation, catalyst, graphite

ACKNOWLEDGEMENTS

I would like to express my sincere gratitude to the following people and institutions that contributed so much towards the success of this study:

- My promoter, Prof. W. W. Focke, for his supervision, encouragement and unwavering support.

- Prof. D. L. Morgan for his assistance and contributions.

- Staff members and students of the Institute of Applied Materials for their love and support.

- The following departments in the University of Pretoria for their help with sample analysis: Chemistry, Geology, Metallurgical Engineering and Chemical Engineering.

- The Pebble Bed Modular Reactor (PBMR) project, the Department of Science and Technology (DST), THRIP and the University of Pretoria for financial assistance.

- My family and friends for their unquantifiable support, understanding and love.

Above all, thanks be to God, for allowing the grass to grow through cracks of the concrete.

CONTENTS

LIST OF FIGURES

LIST OF TABLES

LIST OF NOMENCLATURE

Al(acac)	aluminium(III)acetylacetonate
$Al(C_9H_6ON)_3$	aluminium(III)hydroxyquinolinate
Al(ox)	aluminium(III)hydroxyquinolinate
Al_2O_3	aluminium oxide
$AlCl_3$	aluminium chloride
Ca(acac)	calcium(II)acetylacetonate
$Ca(C_9H_6ON)_2$	calcium(II)hydroxyquinolinate
$Ca(NO_3)_2$	calcium nitrate
Ca(ox)	calcium(II)hydroxyquinolinate
CaO	calcium oxide
Cu(acac)	copper(II)acetylacetonate
$Cu(C_9H_6ON)_2$	copper(II)hydroxyquinolinate
Cu(ox)	copper(II)hydroxyquinolinate
CuO	copper oxide
$CuSO_4$	copper sulphate
Fe(acac)	iron(III)acetylacetonate
$Fe(C_9H_6ON)_3$	iron(III)hydroxyquinolinate
Fe(ox)	iron(III)hydroxyquinolinate
$FeCl_3$	iron chloride
NaOH	sodium hydroxide
$Zr(C_9H_6ON)_4$	zirconium(IV)hydroxyquinolinate
$Zr(NO_3)_2$	zirconium nitrate
Zr(ox)	zirconium(IV)hydroxyquinolinate
ZrO_2	zirconium oxide
Zr(acac)	zirconium(IV)acetylacetonate

LIST OF ABBREVIATIONS

CSIR	Council for Scientific and Industrial Research
DMF	dimethylformamide
DMF	dimethylformamide
DTG	derivative of thermogravimetric (analysis)
HTGR	high-temperature gas-cooled reactor
HTT	heat treatment temperature
PAH	polyaromatic hydrocarbons
PBMR	Pebble Bed Modular Reactor
ppm	parts per million
ROV	reflectance of vitrinite
SEM	scanning electron microscopy
TGA	thermogravimetric analysis
XRD	X-ray diffraction

CHAPTER 1: INTRODUCTION

1.1 The Pebble Bed Modular Reactor (PBMR)

Eskom is currently the 9th largest electricity utility in the world, producing about 95% of South Africa's electricity and 50% of the electricity consumed in Africa. Eskom has maintained an excess of power-generation capacity in the past 10 years. It has engaged itself in a massive electrification campaign in South Africa, which unfortunately goes hand-in-hand with an increase in consumption and thus also with a rapid shrinkage in the excess power-generation capacity. South Africa is now only 1 year away from the point at which the rapidly growing demand for electricity will overtake the currently installed capacity. The existing units have a capacity of up to 40 000 MW, and Eskom is aiming to produce a total capacity of 80 000 MW by 2027 to counteract the anticipated threat. This will include the electricity generated by nuclear technology. In its efforts to address the looming challenge, Eskom has chosen the Pebble Bed Modular Reactor (PBMR) as a future vehicle to meet this growing electricity demand. Eskom has therefore always played a central role in investigating the possibility of generating electricity using PBMR technology (Nicholls, 1996; Urbach, 2006).

The current PBMR project is a continuation of a long historical development that began in the 1950s in Germany. It was the idea of the German nuclear physicist, Prof. Rudolf Schultan, who intended to design a 100% inherently safe nuclear power source, which could be deployed all over the world, including the developing countries, as an efficient electricity generator. The PBMR's 165 MW electric modules are appropriate for developing countries, which lack extensive electricity grids. It is estimated that around 640 units of PBMR plants could be exported all over the world over a period of 25 years. Research has already covered substantial ground, despite the concerns of environmental activists with regard to safety considerations and spent fuel disposal.

The PBMR is a high-temperature gas-cooled reactor (HTGR). Its core will be cooled by helium gas. Helium gas was chosen as a coolant in the PBMR because of the following properties that it posses: resistance to corrosion, no condensation (giving it the possibility

of operating at any temperature), a negligible neutron-absorption cross-section and the ability to be used in a direct cycle, thus driving the turbine with high efficiency (Nicholls, 2000).

The PBMR fuel components are cricket-ball-sized graphite spheres with a diameter of 60 mm. Each sphere contains uranium dioxide particles encapsulated in coating layers of silicon carbide and pyrolytic carbon. The coatings on the uranium dioxide fuel particles are deposited by chemical vapour techniques. The inner two layers are composed of carbon with different porosities, followed by the main barrier layer of silicon carbide and finally a graphite layer. The main purpose of the coatings is to prevent the fission products from escaping. The coated beads are mixed with finely powdered graphite comprising 75% natural graphite and 25% synthetic graphite, binder resin and then moulded into a spherical shape. The pebbles are then heated to 1 900 ºC, after which they are ready for use in a reactor.

The nuclear-grade graphite in the reactor serves as the main nuclear moderator. During operation about 44 000 fuel spheres are inserted into the top of the reactor through vertical holes that are drilled into the graphite blocks. The fuel spheres are discharged at the bottom and the extent of burn-up is determined before they are returned to the reactor. The fuel becomes exhausted after a few cycles. Each pebble will pass through the reactor about six times and will last about three years before it is spent (Nicholls, 2001). Spent fuel is sent to special storage bins where the decay of the short-lived fission products takes place. Strict waste-management procedures have been decided on and put in place in order to ensure that radioactive waste material is safely stored and therefore harmless to the environment and its habitants.

The reactor is described as being inherently safe because the silicon carbide layer around the uranium oxide beads is able to contain essentially all the fission products up to a temperature of 2 000 ^{o}C. The removal of the heat generated by the decay of the fission products will be done by radiation, conduction and convection using helium gas, which serves as a coolant. The helium gas will pass out from the bottom of the reactor at a

temperature of 900 ºC. The helium gas carrying the heat is used to drive the turbines. If the coolant stops flowing, the reactor will heat up to 1 350 °C, at which point the nuclear chain reaction will come to an end, thus preventing damage to the fuel and possible explosions (Nicholls, 2001).

Graphite will be used in large quantities as the material of the reactor core. Graphite was chosen as moderator in the reactor due to its high sublimation point of more than 3 000 °C under inert conditions and its slow rate of oxidation. Furthermore, graphite is the most readily available material with a low thermal neutron capture cross-section, thus allowing efficient use of the neutrons generated. Graphite meets the basic requirements for moderators and reflector materials for thermal reactors which are: low mass number, small neutron capture cross-section, high thermal conductivity, high electrical conductivity, large scattering cross-section, high modulus and strength. Nuclear graphite is normally synthesised from petroleum pitch and Gilsonite pitch cokes. Petroleum pitch is obtained as a by-product in the oil-refining process. Petroleum pitch cokes yield anisotropic graphite, whereas Gilsonite pitch cokes yield isotropic graphite. The differences between anisotropic and isotropic nuclear graphite are given in Table 1.1.

Table 1.1: Typical properties of nuclear-grade graphite (Kirk-Othmer, 1996)

Property	Anisotropic graphite	Isotropic graphite
Density	1.71 g/cm^3	1.86 g/cm^3
Electrical resistivity	0.735 Ω/m	1 Ω/m
Tensile strength	9.9 MPa	46 MPa
Coefficient of thermal expansion with grain	2.2 x 10$^{-6°C-1}$	5.3 x 10$^{-6°C-1}$
against grain	3.8 x 10$^{-6°C-1}$	5.3 x 10$^{-6°C-1}$
Anisotropy ratio (CTE ratio)	1.73	1.00
Total ash	740 ppm	400 ppm
Boron content	0.4 ppm	0.3 ppm

The PBMR needs isotropic graphite in order to maintain a uniform thermal expansion in all directions. Anisotropic graphite blocks are made by grinding the cokes to an appropriate particle size, mixing them with pitch binder, extruding or moulding and then impregnating the mixture before graphitisation. Since South Africa does not have sufficient oil reserves to manufacture its own petroleum coke, graphite needs to be imported. It is therefore in the interests of the PBMR project to be able to use local abundant resources, such as coal, to serve as a substitute for petroleum coke, which is expensive and in short supply. Coal is an abundant source of carbon in South Africa. It is a highly aromatic and inexpensive precursor of carbon. Suitable coal extracts can rearrange to graphite on heating (Kgobane, 2005). Isotropic graphite, which is derived from purified and carbonised coal and meets all the essential requirements for moderators, could therefore be of use in the PBMR project. This work looks at the ability of different metals in catalysing graphitisation of coal derived cokes.

Catalytic graphitisation was heavily studied in the early sixties by various researchers. A metal catalysed or high pressure graphitisation results in the production of a graphitic carbon structure at temperatures lower than normal graphitisation temperatures. A metal catalytic graphitisation is believed to involve a chemical reaction between the ungraphitised carbon and the metal or inorganic compound that constitutes the graphitisation catalyst (Oya & Otani, 1979). A high pressure catalysed graphitisation is assumed to be due an enormously increased kinetic energy of atoms due to high temperatures and pressures. Catalytic graphitisation is normally done at heat treatment temperatures between 1 000 °C and 2 600 °C. As in the graphitisation process, catalytic graphitisation should be performed under an inert atmosphere; argon or nitrogen gas is usually used. Catalytic graphitisation is markedly dependent on the structural ordering of the parent coke, the catalyst concentration and the reaction conditions (Oya & Marsh, 1982).

1.2 Aims and Objectives of the Study

Synthetic graphite is an important industrial material used in nuclear reactors, electrodes, high-temperature processes and many other applications. Graphite is usually

manufactured as a composite of petroleum, Gilsonite pitch cokes or coal-tar pitch cokes. During graphitisation a pre-ordered coke is heat-treated at 3 000 °C under inert conditions for a selected reaction time. Unfortunately, the demand for graphite is growing with the rapid decrease in the production of the above-mentioned precursors. Solvent-refined coal derivatives, known as *Refcoal cokes*, were investigated as potential precursors of graphite. The research work was initiated at the CSIR and is being continued at the Institute of Applied Materials at the University of Pretoria. It has been proved that cokes of solvent-refined Tshikondeni coal derivatives are graphitisable (Kgobane, 2005). The results indicate that the degree of graphitisation is dependent on the extraction conditions.

This study was a follow-up of the work done on the cokes obtained by carbonisation of Tshikondeni coal derivatives extracted at 95 °C. Since these cokes are graphitisable at high temperatures only, this study considered metal complexes for the catalytic graphitisation of these cokes. The aim of the study was therefore to graphitise Refcoal-derived cokes using metal complexes as catalysts for graphitisation. Generally, such catalysts are expected to allow the rearrangement of carbon atoms at lower temperatures. The following catalysts were considered: acetylacetonate and hydroxyquinolinate complexes of Fe, Al, Ca, Cu and Zr. For iron(III)acetylacetonate, the effect of metal concentrations was studied. Acetylacetonate complexes have been used previously in catalytic graphitisation studies (Park *et al.*, 2005). They feature relatively high vapour pressures and conveniently low decomposition temperatures. Hydroxyquinolinate complexes were chosen for this study because they have a higher thermal stability and contain aromatic structures that might make them compatible with the constitution of Refcoal. The study also investigated the effect of heat-treatment temperature and reaction time on the catalytic graphitisation of Refcoal cokes.

CHAPTER 2: LITERATURE SURVEY

2.1 Coal

2.1.1 Origin and formation of coal

Coal is not just another form of carbon, such as graphite and diamond, but is a highly amorphous organic rock or can be viewed as a solid colloid. It is considered to be composed of numerous molecules whose molecular mass is widely distributed, which means that it may potentially have molecules that can be used as raw materials for high-performance carbon materials. Different coals vary significantly due to their geographical location and age (Valkovic, 1983; Marsh, 1989).

Coal is believed to originate predominantly from plants that died millions of years ago, which were buried underground and then decomposed following the chemical processes they had undergone underground. These processes result from the action of temperature and pressure on plant debris. In fact, the individual plants are recognisable in today's coal as discrete fossilised plant fragments called *macerals* (Van Krevelen, 1961). The formation of coal comprises two stages, namely biochemical and geochemical. The dead plants were subjected to high temperatures and pressures to form peat, which is a product of the first stage – the biochemical decomposition stage. There was then a subsequent intervention in the bands of peat by the action of temperature and pressure during the second stage, resulting in the formation of coals found today (Bouska, 1981). That second stage is called the geochemical stage. In time there was a further alteration in the horizontal coal seams as they became folded, tilted and eroded (Given, 1960). 'Coalification' is the term for the development of the series of different types of coal, resulting from the alterations made by the environment to the buried plant remains. The series is: living material > peat > lignite > bituminous coal > anthracite. This progress of coalification with increasing coal rank from living material to anthracite is called metamorphism (Marsh, 1989; Davidson *et al*., 1974).

2.1.2 Coal classification and its composition

Coal is a heterogeneous solid originating from plant materials that have undergone biochemical and geochemical coalification. Studies have proved that coal is a sedimentary rock that is composed of a number of distinct organic entities and inorganic constituents, called *macerals* and *minerals* respectively. Microscopy results show that the minerals are normally found at the boundaries of macerals. The minerals that are observed in abundance fall into the following classes: aluminosilicates, carbonates, sulphides and quartz.

Coal comprises various amounts of essentially all the elements. It is believed to contain more than 50% by weight and more than 70% by volume of carbonaceous material (Fuchs, 1942). This carbonaceous material is normally referred to as the 'organic matrix'. The organic matrix makes up most of the coal weight and consists mainly of carbon, with smaller units of hydrogen, oxygen, nitrogen and sulphur. As the biochemical and geochemical processes take place, the different coals are formed, with different physical and chemical properties which determine their coal rank. As the rank increases, so the carbon content increases, whereas the oxygen, hydrogen and nitrogen contents decrease, as indicated in Table 2.1 (Valkovic, 1983).

Table 2.1: Coalification through time, pressure and heat (dry ash-free values)

Coal type	% C	% H	% O	% N	% ROV
Wood	50.0	6.0	43.1	-	-
Peat	58.9	5.1	33.1	2.6	0.20 – 0.30
Lignite	71.0	4.4	23.1	1.2	0.30 - 0.50
Bituminous	81.4	5.4	10.1	1.9	0.50 – 2.0
Anthracite	92.9	3.1	2.4	0.9	2.0 – 6.0

Note: ROV = Reflectance of vitrinite

The reactivity of the series decreases from lignite to anthracite. As the coal rank increases, the moisture content and the porosity decrease (Starch et al., 1982). The

volatile matter decreases with increasing rank as a result of these processes (volatile matter consists of gaseous substances that are driven off by heat during the coalification process). The other parameter that increases with an increase in coal rank is vitrinite reflectance (ROV), as shown in Table 2.1.

This succession of changes in the properties and structure of coal is called *metamorphism*. The most important factor in the metamorphism of peat to anthracite is temperature. The temperature of earth increases as the depth increases; research indicates that the temperature increases by 2 to 5 °C per 100 m of depth (Valkovic, 1983). Current studies show that the formation of anthracite could be effected even at temperatures as low as 200 °C. Tectonic pressures and movements lead to a severe increase in the temperature, which enhances the coalification process. It is thought that frictional forces which increase the temperature from 300 to 800 °C result in the transformation of anthracite to graphite (Francis, 1961). During the progress of metamorphism (coalification), the chemical changes produce the coal rank series: living material (wood)> peat > lignite > bituminous > anthracite.

2.1.3 Solvent extraction of coal

Solvent extraction of coal is one of the techniques most widely used to study the composition of coal. The understanding of the composition of coal can only be achieved by separating the bulk mineral matter from the carbonaceous matter (organic matrix). In early studies, much attention was directed to ‘solvolysis’, which is simply the solvent extraction of coal under conditions in which the coal undergoes incipient or thermal decomposition. The primary objective of coal extraction is the isolation of the material from which coal derives its coking properties; this is still of great interest, even in recent studies (Hoffman, 1978). The solvent extraction of coal ensures the reduction of the mineral matter content, the sulphur content and the volatile matter content, and also permits control of the extract’s microstructure. Early studies laid the foundations for much of the modern work on solvent refining of coal and hydrogenation in the hydrogen-donor (H-donor) system.

Solubilisation of coal may be achieved by both physical and chemical methods. The physical properties of both the minerals and the carbonaceous material determine the success of the physical methods. The chemical methods involve the solution of the organic part of coal in various solvents using different additives. Research has shown that due to the direct action of the solvent on the coal, there are some molecular rearrangements that are irreversible. Renganathan, *et al.*, 1987) discovered that the yield of extract could be greatly enhanced by thorough crushing of the coal; this is because the coal particle size has some effect on the degree of extraction achieved. Heat-treated coals show the dependence of the coking properties on the extraction yield (Dryden, 1945). Research has proved that for a given type of coal there is an optimum temperature for solvent extraction. The optimum temperature for the extraction process is at the decomposition temperature of that specific type of coal (Dryden, 1945)

The structure of coal is three-dimensional and cross-linked by closely packed molecules. The major form of bonding between the molecules is hydrogen bonding. During the sequence of stages involved in solubilisation, depolymerisation and repolymerisation take place. Both of these processes are dependent on the temperature of the reaction. When hydrogen is added to the mixture, this terminates the pattern of rearrangement (Dryden, 1945). The soluble products consist of oils, fats, acids, alcohols, esters, resins, hydrocarbons and waxes, which may be occluded within the solid structure of the system. The extract from bituminous coals will yield aliphatic hydrocarbons rather than acids, alcohols, esters and carbohydrates. It is believed that hydrocarbons are produced from the hydrolysis of the waxes, followed by splitting. Another part of the soluble product appears to result from the thermal depolymerisation of the coal. Extracts from low-rank coals contain only solid materials, with no oily material (Kiebler, 1945).

Research has shown that the solvent penetrates the organic matrix, resulting in the swelling of the coal. This leads to a bigger surface area and greater possibilities for the selective cleavage of bonds. Swelling is thought to put a strain on the coal matrix, leading to the rupture of the hydrogen bonds. However, only solvents that are strongly basic are capable of breaking all the hydrogen bonds in coal. Following the preliminary breaking

of the bonds, the coal matrix will be reorientated due to the reorientation of the hydrogen bonding structure. It is the combined actions of swelling and bond breaking that appear to allow included mineral matter to drop out of the coal structure, while the coal matrix is weakened. The solvent removals from the extraction phase leave mostly products of the same type as the original but smaller in molecular size due to a mild pyrolysing effect of the solvent (Dryden, 1945).

2.1.3.1 Classification of solvents

There are different classes of solvents, namely non-specific solvents, specific solvents, degrading solvents, reactive (hydrogen donor) solvents and highly reactive solvents. All these classes differ from one another in their actions on coal and their operational temperatures. The solvents in each class behave in a similar way to other solvents in the same class, even though there are slight differences within the class. Specific solvents have the ability to penetrate coal, swell it and then break the bonds.

Degrading solvents are known for their high temperature demand during solvent extraction; they depend mainly on the thermal degradation of coal to smaller and more soluble fragments.

Reactive solvents react chemically with coal and donate hydrogen. This is conveniently detected from chemical changes in the recovered solvents, which are dehydrogenated. Coal becomes degraded to small soluble fragments just after the catalytic transfer of hydrogen from solvent to coal. Reactive solvents have the ability to remove more mineral matter with increasing extraction temperature, resulting in a more highly purified coal extract. Highly reactive solvents cause a massive degradation of coal to small molecules. Specific reactive solvents are widely employed in industry because of their chemical properties and their coal extraction abilities (Kiebler, 1945).

2.1.3.2 Solvent extraction of coal using N,N-dimethylformamide

The Council for Scientific and Industrial Research (CSIR) undertook work on coal solubilisation and came up with a refined coal solution referred to as *Refcoal solution* (Morgan, 1996). Polar aprotic solvents are ideal for this method due to their polarity and their natural aprotic properties, thus effectively extracting fairly large amounts of the organic material in coal. Besides their chemical properties, these solvents are said to be common and also easy to recover after the process. The coal solubilisation developed by the CSIR involves a mixture of N,N-dimethylformamide, coal and sodium hydroxide in a ratio of 100:10:1. The alkali (sodium hydroxide) moves into the solution by means of a phase-transfer catalyst and the coal appears to act in this capacity. This is due to the fact that sodium hydroxide does not dissolve in dimethylformamide until there is a small amount of dissolved coal in solution (Shoko, 2005). The addition of alkali (NaOH) during the extraction process improves the amount of organic material dissolved in polar aprotic solvent.

The mixture is heated in an oil-bath jacketed reactor with effective stirring for five hours under a nitrogen atmosphere. After heating, centrifugation for one hour is used to separate the bulk of the inorganic minerals from the organic material dissolved in solution. This method leaves most of the inorganic impurities in the residue. The Refcoal is separated from the solution by precipitation in water, which is effective in recovering the solvent. The Refcoal solution is therefore mixed with water and centrifuged for twenty minutes. The procedure of water addition and centrifugation is repeated five times, and this has proved to be capable of removing substantial amounts of the solvent from the Refcoal. The Refcoal samples are then dried overnight at 60 °C in an oven (Morgan, 1996).

2.2 Carbonisation

Carbonisation is the destructive heating of coal or any source of carbon in the absence of air, resulting in a solid porous carbonaceous residue with a certain degree of structural ordering, called *coke*. Carbon materials such as coal, coal tar pitch, petroleum pitch and polycyclic aromatic hydrocarbons are normally used in the synthesis of high-performance

carbon materials. Knowing the composition of these precursors makes it possible to track the molecular changes that take place during carbonisation. The nature of a coke determines to a large extent the properties of the product that will be obtained by graphitisation of that particular coke. During carbonisation, the complex organic molecules of coal are decomposed with the evolution of volatile compounds, thus enhancing the formation of a highly carbonaceous residue which has the nature of an aromatic polymer. The volatile products of carbonisation consist essentially of a mixture of gases, tar and light oil. The process of volatile diffusion should take place at a slow rate so as to avoid the interruption and breakage of the carbon network.

The most prominent reactions that take place during carbonisation are as follows:

1. Cleavage of C-H and C-C bonds for the formation of free radicals
2. Molecular rearrangements
3. Polymerisation, whereby the cyclisation of short chains to form aromatic compounds takes place
4. Condensation of aromatic rings (thermal polymerisation) to form polycyclic aromatic compounds which constitute the mesophase spheres that eventually coalesce to form the mesophase
5. Elimination of side-chains (Marsh, 1989).

The above-mentioned reactions occur during the three stages that constitute the complete carbonisation process. These three stages are: the pre-carbonisation stage, the mesophase formation stage and the transformation of semi-coke to coke. A good coke is formed when the coal has passed through a liquid-crystalline phase forming the mesophase during carbonisation (Wilson & Wells, 1950). Studies have shown that, generally, bituminous coal is the only coal that can undergo mesophase formation, whereas coals of lower rank decompose when heated and coals of higher rank do not soften when heated, which is the major requirement of a coking process. On heat treatment of bituminous coal, the vitrinite mineral melts or fuses, whereas the inertinite mineral remains unchanged. As a result, the vitrinite forms a binder phase and the inertinite forms a filler phase. The binder phase binds the filler phase, resulting in the formation of a cohesive

continuous material. For a strong coke to be formed, both the binder phase and the filler phase are needed. For this reason, the mesophase formation stage does not occur in all carbon precursors.

For carbonisation to be successful the process should take place under an inert atmosphere, for which nitrogen or argon is normally used. The two principal classes of carbonisation process are high-temperature coking and low-temperature coking. In high-temperature carbonisation the final temperature of the coke is above 900 °C, whereas for low-temperature carbonisation the final temperature is no more than 700 °C, depending on the nature of the carbon parent and the experimental objectives. Research in the United States has shown that chars from low-temperature formed cokes are more reactive than those from high-temperature formed cokes (Marsh, 1989).

2.2.1 Mechanism of carbonisation

At temperatures up to 450 °C, pre-carbonisation takes place. Pre-carbonisation is initiated by the C-C and C-H bond cleavages which result in the formation of reactive free radicals. At temperatures below 200 °C, the volatile products consist mainly of water, carbon dioxide, carbon monoxide and methane, presumed to have been naturally adsorbed on the surface of a precursor. Some radicals may react with the hydrogen from the system to form high-molecular-weight compounds which have high stability (Marsh, 1989). Pre-carbonisation is accompanied by molecular rearrangements and the initial cyclisation reactions. In this temperature range, there is an increase in the evolution of hydrogen. The temperature accompanying this stage is called the ‘first critical temperature’, and the stage is normally characterised by the oily compounds in the volatile products (Wilson & Wells, 1950). The nitrogen compounds are observed to be evoluted during the pre-carbonisation stage.

Research has shown that during the carbonisation process some of the nitrogen compounds in the coal are converted into ammonia; other portions also appear in the gas as nitrogen and hydrogen cyanide. The tar in the volatiles contains the nitrogen in the form of organic bases, such as pyridine, quinoline and aniline.

The stage that follows right after the pre-carbonisation stage is the mesophase formation stage, during which a discotic nematic (unstable) liquid crystal, called the *mesophase*, is formed. The mesophase formation stage occurs in the temperature range of 450 to 600 °C. This stage starts with the completion of cyclisation of the formed short chains. The termination of the mesophase is identified by the development of anisotropic domains and the formation of a semi-coke (Marsh & Menendez, 1988). The amount of hydrogen gas released at this stage has been found to be very minimal. This stage is discussed at length in the next section.

The sulphur compounds have been found to be evoluted during carbonisation in the form of hydrogen sulphide and other organic-sulphur compounds in the temperature range of 500 to 800 °C. The sulphur in both the mineral matter and the coal substance contributes to the formation of the volatile sulphur compounds (Gollmar, 1945).

The stage that follows the mesophase formation stage is the transformation of semi-coke to coke. The major process occurring during this stage is the elimination of side-chains. With an increase in temperature some compounds are subjected to pyrogenic cracking reactions, resulting in an increase in the evolution of hydrogen and methane gases. The temperature accompanying this stage is called the ‘second critical temperature’ and during this stage the release of hydrogen gas increases rapidly until it becomes the main constituent of the products.

To summarise the sequence of events discussed above, the mechanism of carbonisation can be viewed as a process that occurs in three stages. The first stage is a cleavage reaction in which a precursor decomposes. This is followed by cyclisation reactions which result in the formation of aromatic compounds. The second stage is the condensation reactions, which form high-molecular-weight polycylic aromatic compounds resulting in an unstable intermediate crystal responsible for the plastic behaviour. This is followed directly by resolidification of the metaplast into a semi-coke, accompanied by foaming of the residue due to the evolution of primary gases. The last

stage is the transformation of a semi-coke into a coke due to the evolution of secondary gases, usually methane and hydrogen (Wilson & Wells, 1950).

2.2.2 Mesophase formation stage

At about 500 °C during carbonisation, the liquid crystal called the mesophase is formed. The mesophase has been found to be the intermediate stage for the formation of anisotropic cokes. The mesophase is formed when the fusing point of a carbon precursor is reached; the thin layer then softens and fuses to form a plastic-like material. The formation of the mesophase is found to be favoured by the loss of bonding during heating, the development of aromaticity, the formation of carbon-carbon bonding, increased viscosity, and a decrease in reactive functions. It is during these intermediate stages that the aromatic molecules rearrange themselves to create an anisotropic nematic liquid-crystal phase. Destructive-distillation reactions occur rapidly in the plastic layer, resulting in the evolution of volatile products.

The condensation reactions that take place during this stage lead to the formation of polycyclic aromatic molecules with large molecular masses, hence the process is called *thermal polymerisation*. This thermal polymerisation results in the formation of small, well-ordered droplets called *mesophase spheres*. Mesophase spheres can be simply described as planar aromatic compounds with high molecular weights, separated in the isotropic liquid as droplets. On heat treatment, mesophase spheres undergo coalescence, resulting in the formation of a continuous liquid crystal phase (called the mesophase). Coalescence is dependent on the viscosity of the liquid crystal. The viscosity of the liquid crystal facilitates the mobility of the aromatic molecules so that they may arrange themselves to form a disc-like anisotropic nematic liquid crystal. (This means that the lamellar arrangement is along the long axis in parallel lines, i.e. orientational order with no positional order). As the volatile matter is driven off, the precursor remains highly porous and swells up. The final reactions that take place during the carbonisation process appear to be the splitting of hydrogen from the extremely complex high-molecular-weight hydrocarbons, and the volatilisation of non-carbon elements (Wilson & Wells, 1950).

As the temperature increases, the plastic layer resolidifies and there is continual evolution of volatile matter. After all these complex reactions, the semi-coke shrinks to form a final coke.

2.2.3 Effect of additives in carbonisation

Both inorganic and organic compounds are added to carbon during carbonisation for a wide range of purposes, amongst which are:

- reduction of char-formation reactions during pyrolysis
- enhancement of mesophase formation during carbonisation
- development of isotropic cokes
- anti-puffing purposes
- desulphurisation
- synthesis of mesophase pitch
- catalytic graphitisation (Wang *et al*., 1995; Forrest & Marsh, 1983; Khan *et al*., 1988; Guan *et al*., 2003).

All the additives composed of organic or inorganic compounds affect the coal's thermoplastic properties through their actions. Studies show that the effect of these additives is dependent on the nature and concentration of the specific additive used. However, the effect is also dependent on the physical properties of the carbon's source and on the conditions of pyrolysis. The ability of a chemical additive to influence the condensation reactions at pre-coking temperatures and the evolution of free radicals at increasing carbonisation temperature is manifested at the active centres of the coal's macromolecules, such as functional groups and labile hydrogens (Shevkoplyas, 2002). Mochida *et al.* (1979) concluded that the degree of interaction between coal and additive depends on the characteristics of the coal, the characteristics of the additive, the ratio of mixing and the carbonisation conditions.

Reports show that the mesophase nucleation initiates homogeneously, thus resulting in the carbonaceous mesophase spheres. Taylor *et al.* (1993) found that carbon blacks and

quinoline insolubles are adsorbed on the surface of the mesophase spheres of a coal tar pitch, thus producing a large number of smaller spheres by limiting growth and coalescence. Carbon black (1 wt %) has been found to delay the appearance of liquid crystals but promote the clustering of the spheres, which causes an apparent reduction in the size of the optical texture in the coke. The interaction between carbon black and carbon is believed to take place at the early stages of carbonisation, with carbon black initiating pyrolysis at lower temperatures, thus preventing the intense evolution that results in poor swelling (Kanno *et al*., 1994; Kanno *et al*., 1997).

Since carbonisation starts with the cleavage of the C-C and C-H bonds to form free radicals, the additives begin to react at this stage. If these thermally induced radicals are not stabilised by transferable hydrogen from the system, they may rapidly combine or react with the additives present in the highly viscous system to form isotropic carbon and small-sized anisotropic carbon structures. In the case of systems with low viscosity, such as petroleum pitch, this kind of reaction does not occur and thus the anisotropic coke is formed. Rapid stabilisation of these radicals through hydrogen transfer depends on the chemical composition of the starting material (Ellington, 1977).

According to a study conducted by Wang *et al*. (2001), at the heat treatment stage Fe_2O_3 oxidises the mesogens, and in the process is itself reduced to Fe_3O_4. Iron oxide is believed to enhance the oxidative polymerisation of the lighter fraction in the pitch, thus promoting dehydrogenative polymerisation. It therefore increases the yield of the insoluble fraction through the aromatic condensation reaction. Greater polymerisation of the carbon compounds with less hydrogen reduces the extent to which they swell during carbonisation. These authors found that heat-treated pitch without the additive swelled to about 17 times its original height after carbonisation, whereas the addition of 6% Fe_2O_3 decreased its swelling height to 12 times. Highly dispersed particles release the evolved gases from the molten mesophase pitch along their surface and are thought to physically inhibit the swelling of the pitch by providing a pathway for the evolving gases. Heat-treated pitch without the additive showed anisotropic texture with flow domains, while iron oxide changed the texture to a mosaic one of variable sizes. Of course, the size of the

mosaic domain depended on the amount added, because 6% gave a coarse mosaic texture, while 17 and 25% gave a fine mosaic texture. Devolatilisation is said to be better under viscous conditions, which result in increased porosity as the concentration of the additive increases (Wang et al, 2001).

2.3 Graphitisation

Graphitisation is the solid-state transformation of a thermodynamically unstable carbon into graphite by high-temperature heat treatment (Schilnder, 1989). Increasing interest in the use of graphite as a moderator in nuclear reactors and many other applications has led to an extensive study of the graphitisation process, graphite itself and its properties. The use of modern techniques has led to a much better understanding of the conversion of carbon materials to graphite with specific, desirable properties. Graphite is normally manufactured as a composite: the coke is calcined, ground to an appropriate particle size, and mixed with pitch binder.

The main objective in the application of this method is to order the carbon atoms within the carbon matrix towards the perfect structure of hexagonal graphite. Heat treatment of a carbon material to a temperature of 3 000 °C can produce these changes, with the vibrational energy of the lattice being increased sufficiently to enhance the atomic displacements. As a result graphitisation was initially viewed as the migration of atoms or rings from one layer to another. But later it was recognised as both migration of atoms or rings, and the annealing and healing of defects within the structure (Franklin, 1951).

Carbon compounds can be either graphitisable carbon or non-graphitisable carbon. Non-graphitisable carbons are not converted to graphite by heat treatment, whereas the graphitisable carbons are so converted. During the graphitisation process, the non-graphitisable carbons are converted to a carbon with a small proportion of graphitic carbon, which shows turbostratic order. This concept simply means that they contain a number of graphite layers stacked together, roughly parallel and equidistant, but with each layer having a completely random orientation about the normal layer (Marsh, 1989). This is presumably due to localised crystallisation taking place within the sample.

Graphitisation is industrially performed at a heat-treatment temperature of 3 000 °C under inert conditions. The reaction time and the heating rate are dependent on the experimental intentions and the reaction conditions. The reaction time can be as long as 14 days (Mantell, 1968). The graphitisation process can be accelerated by the addition of a catalyst in a process called *catalytic graphitisation*, inasmuch as it can be accelerated by the use of high pressures. It is believed that a higher degree of graphitisation can be achieved with a shorter reaction time or lower heat treatment temperatures through these techniques of acceleration (Jenkins & Kawaramura, 1976). The most important reactions that occur during the process are summarised below:

1. Removal of most defects within each graphite layer plane, as well as between the planes
2. Gradual shifting and growth of the crystallites
3. Removal of cross-linking bonds
4. Evolution of the ABAB stacking sequence
5. Shifting of carbon rings or single atoms to fill vacancies and eliminate dislocations.

The major weight loss in a material has been found to occur in the early stages of the process. This is attributed to the removal of the interlayer species, mostly interstitial carbon. During heat treatment many elements are evolved in the form of gaseous by-products. Research has shown that most oxides are reduced, resulting in the metallic impurities that are then driven off. At 1 500 °C, the material is almost completely carbon because most of the hydrogen has evolved, except for some metallic impurities. Above 1 800 °C, the conversion from a turbostratic structure to a graphitic structure begins. This occurs slowly at first, then more rapidly as the temperature passes 2 200 °C. Most elements, including sulphur, are gradually removed through evolution, but at 2 000 °C virtually none remains (Inagaki *et al.*, 1989). At temperatures above 2 500 °C, diffusion and annealing of imperfect crystallites take place because crystals grow slowly, with imperfections in their internal crystallite structures. The increase in the crystal size concomitantly with the decrease in the interlayer spacing has been found to be

responsible for the high density of graphite. The process of graphitisation is well described by the following schematic presentation (Figure 2.1).

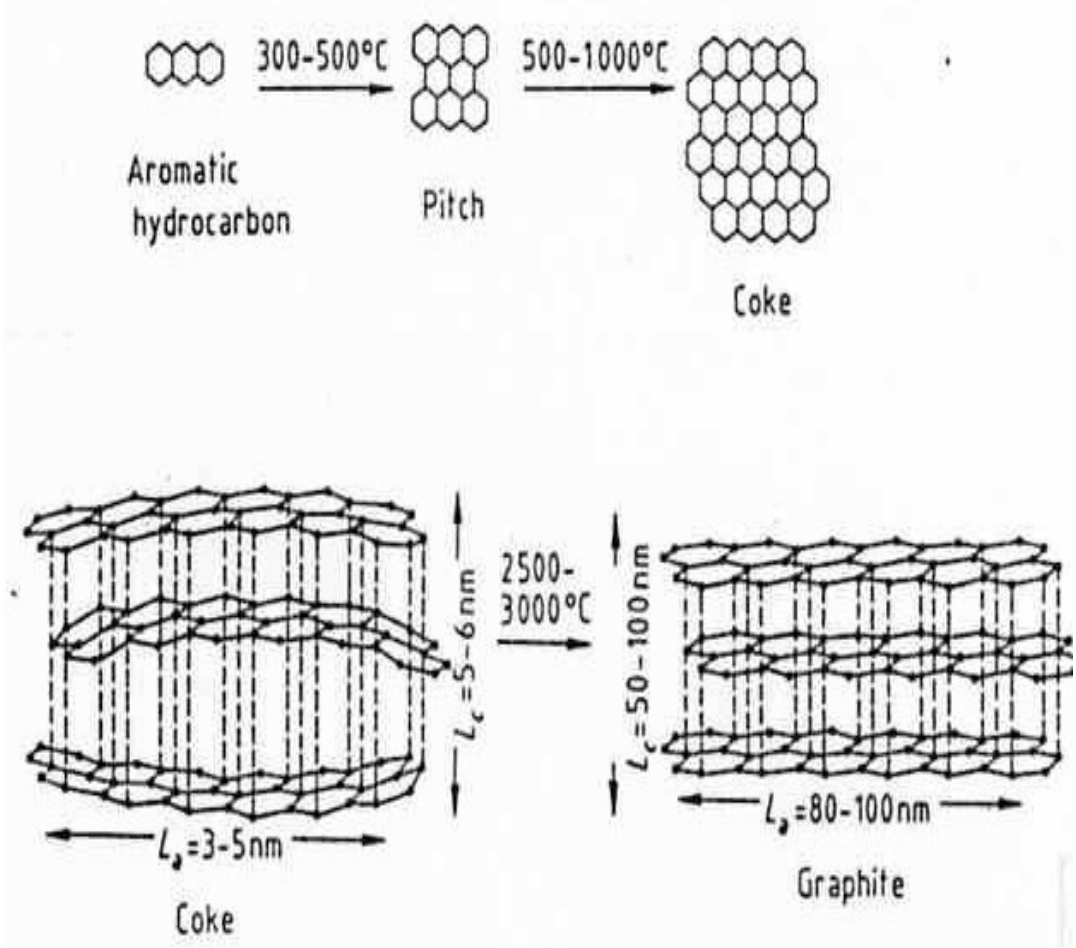

Figure 2.1: Conversion of a carbon precursor to graphite (Gerhartz, 1986)

2.3.1 Graphite

Carbon is a non-metal element with two allotropes that are regularly ordered, and two allotropes that do not show any significant degree of ordering. The ordered allotropic forms are graphite and diamond, while the other two are carbynes and fullerenes. Carbon nanotubes are the newly emerging form of carbon. Graphite is the most thermodynamically stable form at ambient temperatures and pressure. For the conversion of graphite to diamond, the pressure and temperature have to be elevated. The stability of

graphite under irradiation, as well as its thermal and mechanical properties, allows it to be used in nuclear technology applications. It has a slow rate of oxidation and a high sublimation temperature, which is the reason it is used for high-temperature purposes.

Graphite is formed in many parts of the world as a natural material, with its quality dependent on its location. Graphite is also synthesised from many resources, in which case the quality varies widely depending on the availability of the resources. Synthetic graphite is an important industrial material used in nuclear reactors, electrodes, as a refractory material in chemical and high-temperature applications, and in many other applications. Most of the synthetic graphite employed in engineering applications is a granular composite consisting of a filler and a binder carbon formed from pitch (Marsh, 1989).

Graphite is made up of a series of continuous parallel carbon layer planes and has a density of 2.25 gcm^{-1}. Each carbon atom is covalently bonded to three other surrounding carbon atoms. The structure of graphite crystal is the carbon layer plane which is an extended hexagonal array of carbon atoms. This hexagonal unit has both σ and π bonding holding the atoms in hexagonal two-dimensional networks. The layers are an electronic structure, with each carbon atom possessing sp^2 σ orbital hybridisation and the π bonding being delocalised across the hexagonal unit. The covalently bonded electrons in-plane make graphite thermally conductive and the delocalised electrons make it electrically conductive because they are free to move. As a result, the thermal and electrical conductive properties of graphite are more pronounced in-plane than perpendicular to the planes. Therefore, the layers are rather held loosely together by van der Waals' forces. This is due to the hybridised fourth valence electron being paired with another delocalised electron from the adjacent plane as a result of much weaker van der Waals' forces. Thus all the layers are held together by these forces. The stacking of the layers is principally ABABAB, the hexagonal form. The structure is a hexagonal unit, with cell dimensions of a = 0.24615 nm and c = 0.6708 nm and an interlayer spacing (d) of 0.3354 nm. The atoms are hexagonally arranged in layers such that the interatomic distance is 0.142 nm, as shown in Figure 2.2.

Graphite is also obtained in a rhombohedral form in which the stacking of the layers is principally ABCABC, as also shown in Figure 2.2. It is believed that this rhombohedral form constitutes a small portion of graphite in comparison with the hexagonal form. It has been suggested that the rhombohedral form could be converted to the hexagonal form at elevated temperatures because it is not possible to separate its crystals from hexagonal-form crystals (Marsh, 1989).

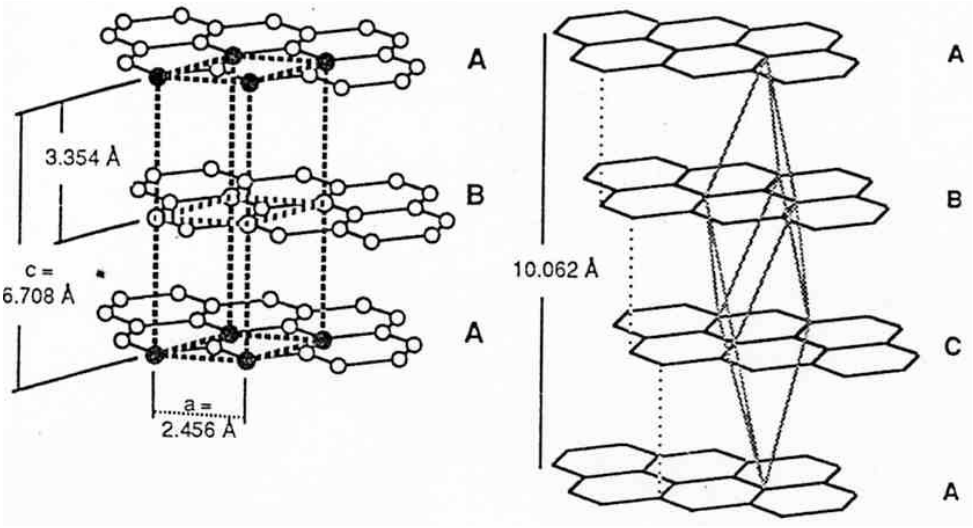

Hexagonal unit cell Rhombohedral stacking

Figure 2.2: Structure of graphite

2.4 Catalytic Graphitisation

Due to the increasing demand for graphite for use in various industrial applications, ways and means of producing graphite by cost-effective methods have been developed. This is simply a commercial concern, with efforts being made to reduce the energy consumption during the graphitisation process. This demand for the economical and energy-efficient production of graphite is receiving special attention and ensures a continuing interest in catalytic graphitisation processes.

To acquire the graphite structure at lower temperatures, many studies have been carried out on carbonisation and graphitisation in the presence of catalysts. Catalytic graphitisation is one of the most effective methods of obtaining graphite nanostructure, such as nanotubes and nanoparticles. As a result, most studies of catalytic graphitisation focus on making graphite nanotubes. Unfortunately, the yield of carbon nanotubes is too low, approximately 2% (Tohji *et al*., 1996). This process has not been extensively applied in industry because of the undesirable characteristics of graphite containing amounts of residual catalyst material. There are also concerns regarding the poor employment of catalytic graphitisation for purposes other than carbon nanotubes synthesis.

Catalytic graphitisation using metal or metal compounds allows the atomic rearrangement of graphite to occur at the lower heat-treatment temperature (HTT) of cokes (Marsh & Warburton, 1970). Catalytic graphitisation can be due to either the addition of organic or inorganic additives, or to increased pressure. Enhancing the crystallinity of carbon by catalytic graphitisation therefore involves a chemical reaction between the ungraphitised carbon and the metal or inorganic compound that constitutes the graphitisation catalyst. Carbon materials containing graphitic structures can be obtained at HTTs between 1 000 °C and 2 600 °C when catalytic graphitisation is employed (Oya & Marsh, 1982). As in the graphitisation process, catalytic graphitisation should be performed under an inert atmosphere; argon or nitrogen gas is usually used (Oya & Otani, 1979).

Catalytic graphitisation has also been used in carbon aerogels. However, the resultant carbons have poor porosity because the catalyst particles tend to fill up the pores, thus inhibiting the large surface area and dominant porosity. In some studies the use of metal-impregnated polymeric gels was found to overcome the problem of poor porosity (Sevilla & Fuertes, 2006).

The success of catalytic graphitisation is based on many factors, namely the properties of the carbon parent, the chemical and physical properties of the metal (catalyst) source, the concentration of a catalyst, the method of catalyst dispersion, the HTT, the reaction time and the experimental conditions. The notable influences of these factors have been

reported (Otani *et al*., 1975; Firtzer & Kegel, 1968). The extensive studies on exploiting the various aspects of catalytic graphitisation have led to the identification of four types of catalytic graphitisation (Oya & Otani, 1978; Oya & Marsh, 1982).

2.4.1 Four types of catalytic graphitisation

2.4.1.1 The G-effect

The G-effect is a type of catalytic graphitisation that results in the successful formation of well-ordered graphite from amorphous carbon. The G-component that is formed has a d_{002} interlayer spacing of approximately 0.335 nm and a crystallite height, L_c >500 Å. The studies have emphasised the need for a catalyst to be present in appreciable amounts in order to effect the formation of the G-component. The X-ray diffraction pattern of such graphitised material gives a composite of a broad profile from the parent carbon and a sharp profile from the G-component at an angle 2θ of 26º and 26.5º before and after graphitisation respectively (Oya & Marsh, 1982).

2.4.1.2 The A-effect

The A-effect is a type of catalytic graphitisation that results in the formation of a less-ordered carbon material. When a parent carbon material is heated with a very finely divided catalyst, such as a vaporised metal, or by elemental substitution in the carbon crystallite, for example O_2 and CO_2, a more homogeneous catalytic graphitisation occurs, resulting in an A-component. The X-ray diffraction pattern of such a product shows a very broad profile – almost as broad as for the parent carbon (Oya & Marsh, 1982).

2.4.1.3 The T_s-effect

The T_s-effect is a type of catalytic graphitisation that leads to a turbostratic carbon (T_s-component). The T_s-component is an ordered carbon structure, but not a three-dimensionally ordered graphitic structure. This happens if a non-graphitising parent carbon is heat-treated with a finely divided catalyst. This kind of carbon component has a

d_{002} interlayer spacing that varies from 0.338 to 0.342 nm and a crystallite height, L_c that varies from 60 to 200 Å, depending on the catalyst used. The X-ray diffraction pattern of this compound is broad to sharp at an angle $2\theta = 26°$ (Oya & Marsh, 1982).

2.4.1.4 The T_n-effect

The T_n-component has a well-ordered turbostratic structure, but not a three-dimensionally ordered graphitic structure. The T_n-component has a d_{002} interlayer spacing of 0.342 nm and a crystallite height, L_c of 900 Å. The X-ray diffraction pattern of this component gives a very complicated profile in which there is a small sharp peak situated at an angle $2\theta = 26°$ (T_n-component) and another small sharp peak situated at an angle $2\ \theta = 26.5°$ (G-component). This carbon compound remains turbostratic because the T_n-component peak is more pronounced than the G-component peak (Oya & Marsh, 1982).

2.4.2 Mechanism of catalytic graphitisation

Extensive studies on this subject have been done to develop a broader understanding of the mechanism of catalytic graphitisation (Marsh & Warburton, 1970; Derbishire *et al*., 1975; Lamber *et al*., 1988). These studies show that the mechanism of catalytic graphitisation varies from system to system, depending on the nature of the carbon (hard/soft) and the catalyst used. Even though these researchers went the extra mile in efforts to exploit the subject, the mechanism is still not fully understood. In accordance with the carbon and catalyst properties, three mechanisms have been identified, namely

(i) the dissolution-precipitation mechanism
(ii) the metal carbide formation-decomposition mechanism
(iii) the dissolution-precipitation that occurs via carbide formation.

2.4.2.1 Dissolution-precipitation

This mechanism results in bulky graphite crystals (thickness $L_c \geq 500$ Å). Essentially, the catalyst melts, dissolves the carbon agglomerates and finally precipitates graphite crystal. In detail, the metal flows into the capillary-like network of very fine pores in the

disordered carbon, dissolving it and precipitating it as non-reactive small graphite crystallites. As a result, the catalysis of graphitisation in this mechanism corresponds to the melting state of the catalyst used. After precipitation, the free metal continues to diffuse in the disordered carbon. The rate of penetration depends on a number of factors, such as the pore structure and the viscosity of the melted catalyst. The precipitated graphite crystallites grow slowly in size with continued heat treatment. The driving force of the reaction is the favourable change in free energy in going from the disordered amorphous carbon to a highly ordered graphitic carbon (Austerman *et al*., 1968).

This mechanism is only applicable to metals of Group VIII because they have a d-shell occupied by six to ten electrons. The energy levels of these metals change little on acceptance of electrons from carbon, whereas metals of Group IIb cannot react with carbon because of a full d-electron shell. In the case of non-transition metals the electrons' configuration cannot explain the catalytic ability, but the ionisation energy and atomic number are somewhat related to the ability, even though they do not give a complete elucidation of it (Oya & Otani, 1979).

Studies show that the solubility of carbon in a metal is of great importance in the success of this mechanism, which yields graphitic carbon and the catalyst in the form of metal crystals. It is reasonable to conclude that when catalysts are retained as metal crystals by quenching, they belong to this mechanism. Research proves that the metal may sublime at a certain temperature, thus terminating any further graphitisation, but this is, of course, dependent on the nature of the catalyst used (Fischbach, 1972). This mechanism is normally found in the production of a G-component. For a T_s-component, this mechanism is also applicable, although the phenomenon of a graphite component suggests the elemental substitution of carbon in a crystallite. This is suspected because in some studies the catalyst particles were found in the turbostratic carbon structure.

2.4.2.2 Metal carbide formation-decomposition

This mechanism has drawn a lot of attention, and efforts have been made to understand and improve it. The metal reacts directly with the carbon to form a metal carbide. At increased HTTs, the metal carbide decomposes to graphite crystals and metal crystals. The metal carbide formation is reported to take place at an HTT of 1 000 °C. Metal compounds may also react with carbon to form unstable metal carbides (Oya & Marsh, 1982). These compounds are said to catalyse graphitisation in their recrystallisation states. The formed metal carbides are considered to be intermediates of the graphite formation. The driving force in this mechanism is the difference in the free energy of formation between a disordered carbon and ordered graphite.

This mechanism is only possible when metals of Group IVb to VIIb are used because they have 2 to 5 electrons in their d-shell. These metals form strong chemical bonds with carbon to result in the metal carbide. It is reasonable to conclude that metals that are retained as carbides by quenching belong to the carbide formation-decomposition mechanism. It has been observed that the ease of metal carbide formation is an important factor for the carbide formation-decomposition mechanism. This mechanism forms a G-component with either large or fine crystals. The catalyst should be added in large particles. For the formation of a T_s-component, this mechanism can also occur; the only difference here is that the metal reacts preferentially at the boundaries of the turbostratic structure that constitutes these non-graphitising carbons. Droplets of metal carbides are formed, on the surfaces of which float detached elementary domains. On decomposition of the carbide, a shell of carbon is formed which is graphitisable because the carbon lamellae are parallel to the external surface of the spherical hollow shell. This mechanism also applies in the catalytic graphitisation that forms the A-component. In this case, hyperfine metal carbides must be formed through the preferential reaction of gaseous metal with cross-linked carbon, followed by decomposition. The resulting carbon, however, may be too fine to result in the T- or G-components (Oya & Marsh, 1982).

2.4.2.3 Dissolution-precipitation via carbide formation

Due to the fact that some metals were catalysing graphitisation through an ambiguous mechanism that did not fully belong to either of the two mechanisms discussed above, a closer look was taken to understand how it worked. The conclusion was reached that some of the metals took an intermediate path between the dissolution and precipitation mechanisms, going via metal carbide formation. These metals dissolve the carbon and react with it directly to produce metal carbides, followed by decomposition to produce a G-component. Although this mechanism has been successfully identified, more work still needs to be done so as to develop a complete understanding of it (Oya & Marsh, 1982). Metals of Group VIIb, including Al, Ti and Zr, have shown some characteristics of this mechanism (Oya & Otani, 1978). These studies have shown that the metal carbide bond gets weaker as the atomic number increases.

2.4.3 Graphitisation catalysts

It is known that the addition of certain metals or inorganic compounds to carbon accelerates graphitisation through the formation of graphitic carbon at HTTs. Many elements are known to be able to catalyse the graphitisation of carbon (Marsh & Warburton, 1970; Fischbach, 1972). Some investigators have attempted to systematise the elements having catalytic ability using the Periodic Table (Ishikawa & Yoshizawa, 1963). However, such attempts have been unsuccessful because the conclusions were drawn from inconclusive results (Oya & Otani, 1979). This is because there was effectively no balance or consistency between the following factors:

(i) The kind of carbon used
(ii) The use not only of metals, but also of their oxides and carbonates
(iii) The concentration of the catalyst used
(iv) The particle size of the catalyst used
(v) The catalyst dispersion method
(vi) The heat treatment temperature (HTT).

Consequently, different results were often reported for the same element by various investigators. Despite all the resulting confusion, Oya & Otani (1979) undertook a very careful study and observed that most of the graphitisation catalysts have an atomic number of less than 40 and a first ionisation potential of between 6 and 8 eV, with the exception of tungsten (W) (Otani *et al.*, 1981).

At present there is no theory available to explain catalytic graphitisation by non-transition elements, except that from the studies reported, there appears to be a relation between an element's ionisation energy, atomic number and catalytic ability. Oya and Otani (1979) found that the ability of transition metals to catalyse graphitisation corresponded to their ability to synthesise diamond. As a result the reactivity of transition metals with carbon was classified into three groups:

1. Group IIb metals cannot react with carbon because of a completely filled with d-electron shell.
2. Group VIII metals have a d-electron shell occupied by six to ten electrons. The energy level of a such configuration is scarcely changed by the acceptance of additional electrons from carbon and therefore these metals can dissolve carbon.
3. Group VIb – VIIb metals have two to five electrons in the d-electron shell. These metals form strong chemical bonds with carbon, resulting in metal carbide formation. Although metal carbides are formed, the chemical bond between a metal and carbon appears to become weaker as the atomic number increases.

When choosing a catalyst from the whole list of options available, care should be taken because some elements are not ideal since they have negative impacts on the functioning of the resultant graphite in certain applications. For example, even though boron is a highly effective catalyst in graphitisation, it cannot be employed in the production of nuclear-grade graphite because it promotes neutron absorption. In this study the catalytic ability of iron, aluminium, calcium, copper and zirconium was investigated.

2.4.3.1 Iron

Iron is a transition metal with an atomic number of 26. Its electron configuration is $[Ar]3d^6 4s^2$, its melting point is 1 538 ºC and its oxidation states are II, III and VI. Due to its chemical properties, it is one of the metals used to catalyse the synthesis of high-performance carbon materials. It has been widely used for catalysing the synthesis of both single-wall and multiple-wall carbon nanotubes. Iron and its compounds and oxides have been reported to catalyse the graphitisation of the various carbon precursors (Weisweiler *et al*., 1971). It has been used to catalyse the graphitisation of pitch in order to prepare highly graphitisable carbon grains of spherical shape, which have proved to be the best anodes for lithium ion secondary batteries (Wang *et al*., 2001). In short, iron has been used for the catalytic graphitisation of amorphous carbon, coal-derived cokes, electron acrylic nanofibres, polymers, hydrocarbon gases, etc. Catalytic graphitisation by iron is believed to involve the dissolution of carbon by the metal, followed by the precipitation of graphite. In this mechanism, carbide formation takes place prior to precipitation. Wang *et al.* (1995) confirmed the formation of carbide through the X-ray diffraction pattern, after which the cementite Fe_3C was formed during the graphitisation of amorphous carbon.

In another study, Wang and co-workers (2001) introduced FeO_2 into a coke and then heat treated that coke at 1 600 ºC for 1 hour in the presence of nitrogen gas. The samples were characterised using X-ray diffraction, optical microscopy and Raman microprobe spectroscopy. The most noticeable spectral difference between the graphite produced and the original coke was that the second-order Raman G' band of the former occurred in an overlapping doublet, whereas the latter had only a single symmetrical peak.

Another mechanism of action of iron(III)acetylacetonate as a catalyst during graphitisation has been proposed recently. However, this mechanism is coupled to assumptions in the research work done by Hong and colleagues (2007). They used iron(III)acetylacetonate in the graphitisation of poly(vinylidene fluoride)-based carbon fibres, within a temperature range of 800 to 1 800 ºC. Graphite nanofibres were obtained which showed sharp peaks at approximately 26º and 44º, corresponding to the d_{002} and

$d_{100/101}$ planes respectively. The graphite nanofibres obtained at 800 ºC showed additional peaks at 36º and 48º, corresponding to Fe_3O_4, whereas the one obtained at 1 300 °C showed an αFe peak at 42º to 44º (110) and 65º (200). They therefore assumed that iron(III)acetylacetonate was converted into Fe_3O_4 via αFeO(OH) and that the reduction of Fe_3O_4 resulted in the production of an αFe catalyst which was still able to induce the graphitisation reaction. This study showed that graphitisation was accelerated at temperatures higher than 1 300 ºC, even though a turbostratic structure in the graphite nanofibres was obtained (Hong *et al*., 2007)

2.4.3.2 Aluminium

Aluminium is a Group III element with an atomic number of 13. Its electron configuration is [Ne] $3s^2 3p^1$, its melting point is 660 ºC and it has an oxidation state of III and I. Aluminium has been used mainly in the catalytic graphitisation of non-graphitisable carbons. Aluminium triisopropoxide has been compared to aluminium oxide in its ability to catalyse the carbonisation of wood charcoal. In a study by Warburton (1973), these two compounds, with a particle size of 40 µm, were separately suspended in biomass carbon and plasma-sintered for five minutes under an argon pressure of 50 MPa at temperatures up to 2 200 ºC. Plate-like catalytic graphitisation developed in both cases through the formation and dissociation of plate-like Al_4C_3. The formed carbide dissociated at increased temperatures to aluminium vapour and solid carbon. It was concluded that the difference between aluminium triisopropoxide and Al_2O_3 is a matter of the intensity of the graphite reaction versus the size of the graphite patches. Both samples had a turbostratic carbon structure with little character of a G-component.

In another study of catalytic graphitisation (Hata *et al*., 2004), highly purified graphite was obtained by adding Al_4C_3 to an amorphous carbon and heat-treating it to 1 100 ºC in a stream of chlorine. The carbide was found to have decomposed to graphite, whereas the metal was removed as a volatile chloride. The graphitisation process was completed by

heat-treating samples at 2 000 ºC for two hours. This study showed that the addition of Al_4C_3 led to an increase in crystallite dimensions.

2.4.3.3 Calcium

Calcium is a Group II element with an atomic number of 20. Its electron configuration is [Ar] $4s^2$, its melting point is 842 °C and it has an oxidation state of II and I. Calcium has been used in the catalytic graphitisation of both low- and high-rank coals. Studies have shown that the Ca^{2+} ions inherently present in coals can promote the transformation reaction of A-component to T-component. Calcium is one of the elements that catalyse the graphitisation of carbon precursors. In a study in which they examined the nitrogen release during coal pyrolysis at high temperatures of greater than or equal to 1 000 ºC, Tsubruchi *et al*. (2003) found that calcium and its compounds promoted the transformation of amorphous carbon to crystallised carbon. Four different coals with different coal ranks were impregnated with CaO and heat-treated at 1 000 ºC to 1 350 ºC in a fixed-bed quartz reactor. The interlayer spacing and the crystallite size of T-carbon were not changed significantly among their products. As a result, they formed a turbostratic carbon structure, with the T-carbon depending on the coal rank. This study showed that the smaller particles of CaO readily migrate in the char substrate and consequently agglomerate. The following reaction was observed to be the result of the interaction between carbon and the catalyst:

$$CaO + C(\text{A-carbon}) \rightarrow CaC_x \text{ (or } CaO_\alpha C_\beta) + CO \qquad (1)$$

CaC_2 as the carbide could also be formed, even though the formation of this compound by reaction of CaO and carbon was thermodynamically unfavourable under the conditions of this particular work. At increased temperatures, the non-stoichiometric intermediates may subsequently be decomposed to yield crystallised carbon with turbostratic structures. The formation of this kind of carbon is observed in the following reaction:

$$CaC_x \text{ (or } CaO_\alpha C_\beta) + CO \rightarrow CaC_y \text{ } (CaO_\alpha C_y) + C \text{ (T-carbon)} \quad (2)$$

A similar reaction was observed in a study by Oya and Otani (1979), in which phenolic resin carbon was catalysed using CaO. These two researchers observed the formation of CaC_2 as an intermediate when the samples were heat-treated at 2 000 ºC for five hours. This study proved that the fine particle sizes of CaO give a T-component and that bulky particle size results in a graphitic carbon. Research shows that the formed CaC_2 may also react with the nitrogen in carbon, thus resulting in the formation of $CaCN_2$ and graphitic carbon (Noda *et al*., 1965; Oya & Otani, 1979).

2.4.3.4 Copper

Copper is a transition element with an atomic number of 29. Its electron configuration is $[Ar]3d^9 4s^1$, its melting point is 1 084 ºC and its oxidation number varies from 0 to II. According to the literature, copper has not been widely studied for catalytic graphitisation purposes. However, its application for other objectives in carbon materials has been noted. Yokokawa *et al.* (1967) did a study regarding its catalytic activity towards graphitisation. The intention was to gain an understanding of the process kinetically. Although hard carbon was used, positive results were obtained. Amberlite IRC-50 and furfural-furan resins produced at 800 ºC from divinyl benzene polymer were mixed with cupric oxide and heat-treated between 1 450 and 1 525 ºC for 30 to 180 minutes. Copper catalysed the graphitisation of Amberlite IRC-50. It was assumed that the mechanism was cleavage of the cross-linking carbon-carbon bonds.

Copper has also been used to enhance the catalytic activity of Ni in the synthesis of carbon nanotubes in a process called ‘catalytic chemical vapour deposition’. In a study conducted by Nasibulin *et al*. (2003), copper(II)acetylacetonate was used to successfully synthesise the carbon anion particles from carbon monoxide. Carbon anions are described as quasi-spherical carbon nanoparticles consisting of concentric graphitic shells. In their study, copper(II)acetylacetonate decomposed at between 705 and 1 216 ºC, with the copper particles being covered by amorphous carbon at low temperature and by the

graphitic carbon layers at high temperature. However, copper does not react directly with carbon, except in direct chemical methods in which unstable Cu_2C_2 and CuC_2 are the only known carbides that are formed. The presence of copper as a catalyst resulted in the formation of carbon nanoparticles that ranged from 5 to 30 nm in diameter and consisted of carbon layers surrounding a hollow core.

Furthermore, copper has been used in the modification of carbon-carbon composites (Macherzysnska & Blazewicz, 2004). The composite was made out of graphite fibre and a matrix (mesophase pitch and phenol-formaldehyde resin). Copper chloride was used to intercalate the composite, which changed the electrical and mechanical properties on intercalation. The decrease in electrical properties was caused mainly by stress, induced during synthesis of the intercalation composite.

2.4.3.5 Zirconium

Zirconium is a transition element with an atomic number of 40. Its electron configuration is [Kr] $4d^2 5s^2$, its melting point is 1 855 ºC and its oxidation number varies from II to IV. Zirconium is used in the cladding of nuclear fuel elements, which under irradiation can produce zirconium-93 (Maitre & Lefort, 1997). Although not much work has been done on the catalytic ability of this element in graphitisation, zirconium oxides and compounds are accepted as catalysts for graphitisation. According to results obtained by Otani and Oya (1979), zirconium is amongst the elements that catalyse graphitisation through dissolution-precipitation via the carbide formation mechanism.

Maitre and Lefort (1997) confirmed this kind of mechanism in their examination of the solid-state reaction of zirconium with carbon. These two researchers found that at HTTs above 1 500 ºC, the reaction that takes place is as follows:

$$ZrO_2 + 3C \rightarrow ZrC + 2CO \qquad (3)$$

As the temperature was increased, an appreciable amount of graphite was precipitated.

Zirconium and titanium have been used in the catalytic graphitisation of carbon prepared form Gilsonite pitch, acenaphthylene and a phenol-hexamine resin (Marsh & Warburton, 1976). Different concentrations of these elements were used and the samples were heat-treated in a graphite resistance furnace up to 1 600 ºC at a rate of 20 ºC/min. The results of optical microscopy of polished surfaces of the three carbons showed the granular, mosaic anisotropy of Gilsonite carbon, the larger, flow-type anisotropy of acenaphthylene carbon and the isotropic carbon from the resin.

The catalytic ability of zirconium has also been shown in a study conducted by Preiss *et al*. (1996), in which a carbonaceous gel obtained from a coal tar pitch and a zirconium gel were combined. The samples were carbonised and then graphitised at 1 600 ºC, and analysed using thermogravimetric analysis and X-ray diffraction techniques. Fine crystallites with particle sizes of 1 µm and less were obtained. The formation of these sub-micrometre crystallites was explained by the homogeneity and reactivity of the gel-derived carbon reactant.

2.4.4 Factors affecting catalytic graphitisation

2.4.4.1 Catalyst composition

Different elements in various forms have shown different catalytic abilities in graphitisation. Not surprisingly, the catalytic activity of a compound is different from that of the constituent metal or other compounds containing the same metal (Oya & Marsh, 1982). The same principle applies to the use of the alloys as catalysts. Alloys are believed to enhance graphitisation through their lower melting points. The catalytic activity of the minerals is attributed to their high reactivity resulting from decomposition. This is because if two or more graphitisation catalysts are present in one mineral, they will make a combined effort to enhance the process. For example, when aluminium and titanium are present together, the conversion of coke into G-component graphite is more complete than when aluminium alone is used, although the mechanism is not clear. Noda *et al.* (1965) observed that both $CaCO_3$ and $Ca(OH)_2$ produce G-component graphite at their

recrystallisation temperatures under high pressure, but CaF_2 has a lower catalytic ability. Parker *et al.* (1965) used Fe, FeO, Fe_2O_3, Fe_3O_4 and $FeSiO_3$ to catalyse the graphitisation of needle coke. They found that Fe_2O_3 was the most effective catalyst, yielding graphite of high density and large crystallite size, compared with other forms of iron.

In this study the metal acetylacetonate and hydroxyquinolinate complexes of Fe, Al, Ca, Cu and Zr were investigated. Metal acetylacetonate complexes have suitable vapour pressures and are unstable because of convenient decomposition temperatures (Parker *et al.*, 1965). Metal hydroxyquinolinate complexes were used in this study because they are stable and contain a large amount of aromatic carbon, thus giving the best possibility of their being compatible with the Refcoal carbon structure.

2.4.4.2 Catalyst concentration

With regard to the concentration of the catalyst to be used in catalytic graphitisation, the degree of graphitisation increases with the increase in the concentration of a catalyst in carbon, unless the metal is completely inactive. The concentration of the catalyst also influences the rate of graphitisation and thus controls the properties of the final product. The structure of the graphite may improve from isotropic to lenticular or even flow structure, depending on the nature of the catalyst, as the concentration of the catalyst increases. However, the formation of the T_s-component can be replaced by the formation of a G-component, as a result of the coalescence and growth of finely divided particles in the catalyst. Some catalysts can form the A-, T_s or G-component, depending on the concentration of the catalyst used (Oya & Marsh, 1982).

2.4.4.3 Properties of carbon sources

Carbon is found abundantly in nature as coal, natural graphite and diamond. Moreover, it is readily obtained from the pyrolysis of hydrocarbons such as resins and pitches, and can be deposited from the vapour phase by cracking hydrocarbon-rich gases. The degree of graphitisation is highly dependent on the physical and chemical properties of the parent carbon. This is because graphitisation itself is viewed as the progressive improvement of

the initially very defective structure that exists in the carbon. The pre-orientation existing in the carbon facilitates the process, no matter how limited it is (Fischbach, 1972).

The success and extent of graphitisation vary widely with different types of carbon. The many forms of carbon have a great diversity of structural and electronic properties.

Carbons are classified into two classes, namely hard and soft carbons. Hard carbons are non-graphitising carbons, such as glassy or vitreous carbon, cellulose carbons, and several types of carbon fibres and chars. This class of carbons retains a very imperfect structure even after prolonged treatment at high temperatures because of the strong cross-linking within and between the planes, which gives them a high degree of imperfection in their structures. These carbons do not undergo plastic deformation during heat treatment. Catalysis or high pressures at high temperatures can improve the degree of graphitisation for these carbons. The effectiveness of graphitisation depends mainly on its ability to promote a significant rearrangement of the carbon atoms in the structure. The effectiveness of catalysis in this class of carbons is due to the excess free energy of the disordered structure.

Soft carbons are graphitising carbons that exhibit a perfect graphite structure under thermal treatment and ordinary pressures. This class of carbons includes conventional petroleum pitch, pyrolytic carbons, coal tar pitch, diamond, etc. They undergo plastic deformation under thermal treatment, hence satisfying the primary requirement for structural improvement. Unlike hard carbons, structural rearrangement is not a principal objective with soft carbons because the structure of graphitising carbons is such that only a small proportion of the atoms in the disordered carbon needs to be rearranged to produce parallel, perfectly stacked layers. In soft carbons the principal objective is the healing of defects within the layers and the removal of interlayer and intercrystallite defects, such as cross-links or distorted bonds. During catalytic graphitisation both classes of carbon form metal carbides or metal complexes as intermediates whenever a metal catalyst is used (Oya & Otani, 1979).

2.4.4.4 Heat-treatment temperature

Various graphitisation catalysts behave differently throughout the range of graphitisation temperatures. Different catalytic graphitisation temperatures can be used because of the structural diversity of carbon materials. At low temperatures, in most cases a non-graphitic carbon is produced. This is due to the fact that the low temperatures inhibit the completion of the entire process, thus resulting in premature graphite. With catalysts that favour the dissolution-precipitation mechanism, at low temperature the catalysts only sinter, agglomerate and melt, without any further completion of the process, i.e. the precipitation of graphite. On the other hand, with catalysts that favour the metal carbide or metal complex formation mechanism, if low temperatures are employed, the metal carbide or complex may be formed without any further decomposition in order to produce graphite.

High temperatures of catalytic graphitisation obviously allow the production of graphite with a certain significant degree of ordering, and it is believed that at very high temperatures the metal will be evolved, leaving graphite as the only product. An increase in graphitisation temperature can lead to a cessation in the production of the T_s-component or T_n-component. This is replaced by the G-component, which is triggered by the sintering and agglomeration of the catalyst particles as the temperature increases. Research has proved that the metal may sublime at a certain temperature, thus terminating any further graphitisation, but this is, of course, dependent on the nature of the catalyst used (Fischbach, 1972). The structural variations that result from the heat treatment temperatures may vary from isotropic to a flow structure in catalytic graphitisation of the same carbon under fixed conditions but with variations in temperature.

2.4.4.5 Reaction time

Previously the effect of reaction time in graphitisation and catalytic graphitisation was considered to be less important as a factor that determines the extent of graphitisation of the carbon precursors. Heat treatment temperature was always considered the most

influential parameter. Not surprisingly, studies that took reaction time into consideration proved that the reaction time could have a great influence on the extent of improvement in graphite precursors (Oya & Otani, 1979). Of course, the longer the reaction time in catalytic graphitisation, the better the chances of a well-ordered carbon product. Even a non-graphitising carbon can yield a much-improved product when given an adequate reaction time at the heat treatment temperature of interest. Chemical reactions may not go to completion if a short reaction time is employed, whereas a long reaction time allows all the reactions to complete. In this study various reaction times were employed in order to understand their effect on catalytic graphitisation.

2.5 Analytical Techniques

2.5.1 Thermogravimetric analysis

Thermogravimetric analysis is an analytical technique used to determine a material's thermal stability and degradation as a function of temperature. Through this technique, the decomposition of the material can be used to determine its fraction of volatile components and the stoichiometry of the reaction. Measurements are normally carried out under a controlled atmosphere, which can be either air, a vacuum or an inert gas, such as nitrogen, helium or argon. Decomposition of the sample can also occur in a self-generated atmosphere; this is normally observed when the sample is heated in a small container with a restricted opening. The temperature range is usually large, ranging from room temperature to 1 000 ^{o}C or even higher depending on the properties of the sample or the experimental intentions. Basically, the maximum temperature is selected such that the residual weight will be stable at the end of the measurement, indicating that all chemical reactions have been completed. The heating rate must be carefully chosen because it has a profound effect on the final results. Studies show that rapid heating rates may result in less-detailed information on decomposition by not showing all the decomposition events (Brown, 1988).

Thermogravimetric analysis can be coupled with other analytical techniques, such as chromatography, mass spectrometry and Fourier transform infrared spectrometry. The

combination with other techniques can be used for qualitative and quantitative purposes. The main thermal events that take place during the measurement are phase transition, melting, sublimation and decomposition. These events give information about the composition and the stoichiometry of the reaction.

Thermal events fundamentally originate from sintering and changes in crystal structure. The resultant increase in the average kinetic energy of molecules, atoms or ions leads to the decomposition of the sample, thus forming new molecular fragments. The increase in motion takes place if the intramolecular forces are weaker than the intermolecular forces. The stability of the newly formed fragments varies, depending on the volatility with increased temperature, which is the reason they are termed 'intermediates'. If there is more than one solid substance in the process, there may be interaction between them on heating and new phases, such as a solid solution or a eutectic mixture, may form. Depending on the chemical properties of the sample, multi-stage or single-stage decomposition may take place with relatively stable or non-stable intermediates. It is noted that heating a carbon-containing sample under air results in combustion, thus forming gaseous carbon dioxide, with some weight gain at the end of the curve due to the oxidation of residual metal into solid metal oxides (Brown, 1988).

2.5.2 Scanning electron microscopy

Scanning electron microscopy (SEM) is a technique that is used to study the surface of chemical samples. SEM uses electrons rather than light to form an image. It offers higher magnification, greater depth of focus and greater resolution. Greater depth of focus allows a larger portion of the sample to be in focus at a time. Furthermore, high magnification allows the closely spaced features of the material to be imaged properly and clearly. The signals obtained from specific emission volumes within the sample can be used to examine many characteristics of the sample, such as sample composition, surface topography, crystallography, etc.

SEM utilises a focused beam of highly energised electrons that systematically scans across the surface of the sample. When the electron beam strikes the sample, a large

number of signals are emitted, including photon and electron signals. The signals most commonly detected in SEM are electron signals. These are assigned to two categories: secondary electrons and backscattered electrons. Both secondary and backscattered electrons are produced through the interaction between the energetic electrons of a beam and the electrons of the sample. Secondary electrons are the electrons of the sample that undergo an inelastic interaction with the electrons of the beam, whereas backscattered electrons undergo an elastic interaction with the electrons of the beam. The low energy of the secondary electrons makes them a conveniently collected signal for SEM since they are easily drawn to the detector system. Normally, there are fewer backscattered electrons than secondary electrons, but they play a major role in detecting contrast between areas with different chemical compositions. This generally happens when the average atomic numbers are different in various regions of the sample. The electron detector is then used to convert the radiation of interest into an electrical signal for manipulation. SEM therefore provides information about chemical composition (elementally), structural morphology, density and orientation/crystallinity (Gerhartz, 1986).

2.5.3 Optical microscopy

Polarised light optical microscopy is usually used in geology for studies of minerals in rocks, but it is also used to study many other materials. Basically, it elucidates the structure and composition of the material. It provides information on the reflection of polarised light on the boundaries between minerals of various diffraction indices in the material under analysis. Optical microscopy can be used with either reflected or transmitted light. The most important features of optical microscopy are the polariser situated below the sample and the analyser situated perpendicularly above it. The polariser and analyser are positioned at right angles to each other. By nature, light waves vibrate at right angles to the direction of a travelling light, but the polariser can transform circular travelling light into linear (one direction of vibration) travelling light. The contrast image obtained is due to the interaction between the plane-polarised light and the sample which produces two separate wave components that are each polarised in perpendicular planes.

Polarised light optical microscopy is also used to distinguish between anisotropic and isotropic materials. Distinction between an optical anisotropic and isotropic texture is made possible by using a reflected polarised microscope equipped with a rotating analyser. Reflectance is the proportion of the direct light that is reflected by the polished surface. Isotropic materials have only one refractive index or simply demonstrate the same optical properties in all directions. This means that they have a three-dimensional lamellar arrangement in all directions, with no preferred orientation. Isotropic materials therefore place no restriction on the vibration direction of light passing through them. Consequently, isotropic materials show no colours under optical microscopy analysis (Marsh, 1989).

Anisotropic materials, on the other hand, have optical properties that vary with the orientation of the crystal lattice with respect to the incident light since they exhibit a range of refractive indices, depending on the propagation direction of light with regard to the sample. The classification of the material's degree of anisotropy depends on the size and shape of the anisotropic layers. Consequently, anisotropic materials give colourful images. The colour arises when the crystal's orientation results in the reflection of light. Reflection of light occurs when the molecular orientation of the surface in the polished block is perpendicular to a symmetry fold, thus giving colour, while domains with molecules lying flat or parallel to the light disappear. It is also possible to introduce a retarder plate in order to cause interference colours that will change with the orientation of the layers, resulting in all the layers observed on the polished block being represented by individual colours. Normally, a half-wave retarder plate is used for retardation.

Polarised light entering an optically active anisotropic crystal is resolved into components that vibrate in two perpendicular planes because of the differences in crystal orientations and refractive indices. The components are then merged with construction and destruction interference as they pass through the analyser. However, one component is retarded by a certain amount, depending on the length of the optical path (Parker *et al.*, 1965).

2.5.4 X-ray diffraction

X-ray diffraction is a versatile, non-destructive analytical technique that reveals detailed information about chemical composition, phase composition and the crystallographic structure of materials. It is used mainly for the determination of the various crystalline forms, known as phases, of compounds present in powdered and solid samples. It probes the repeating planes of atoms (Klug, 1984). As a result every sample gives a unique X-ray diffraction pattern. Identification is achieved by comparing the X-ray diffraction pattern obtained from the unknown sample with an internationally recognised database containing reference patterns for more than 70 000 phases

A crystal lattice is a regular three-dimensional distribution of atoms in a space. These atoms are arranged such that they form a series of parallel planes separated by distance d, which varies according to the nature of the material. For any crystal, planes exist in a number of different orientations, each with its own specific d-spacing. The nature of the crystal makes it possible to obtain the diffraction pattern. The d-spacing of the lattice planes depends on the size of a unit cell and determines the position of the peaks, whereas the intensity of each peak is caused by the crystallographic nature of the material's structure, i.e. the position of the atoms within the unit cell and their thermal vibration (Oya & Marsh, 1982). The line width and shape of the peaks may be derived from the conditions of measuring and from properties such as the particle size of the sample material.

The diffraction of X-rays by a material, either crystalline or amorphous, results from a scattering process in which the X-rays are scattered by the electrons of the atoms without changing the wavelength (coherent or Bragg scattering). The electrons of the atoms interact with the incoming X-ray photons, resulting in either absorption or scattering. Accordingly, the sample must be correctly oriented with respect to the incoming beam. A monochromatic X-ray beam with wavelength λ is projected onto a material at angle θ. Diffraction occurs only when the distances travelled by the X-rays as reflected by the planes differ by a complete number n of wavelength, which results in constructive interference (Madswen *et al.*, 2000). Scattering of the X-rays by the material can only be

observed when Bragg's law is satisfied. By varying the angle θ, the conditions of Bragg's law are satisfied by different d-spacings in the planes of the material. Bragg's law can be easily expressed by Bragg's equation:

$$n\lambda = 2d\sin\theta \quad (4)$$

By using the Rietveld refinement method, the crystallite size and c-dimension can be determined. For powder X-ray diffraction, a sample consists of a collection of many small crystallites with random orientations. Orientation is averaged over a crystal and the scattered intensity is measured as a function of outgoing angle. This technique is widely used to study carbon materials ranging from amorphous carbon to crystalline carbon. This technique is especially helpful for studying the behaviour of carbon materials on graphitisation. The degree of graphitisation can be calculated using the Marie and Meiring equation (Marsh, 1989):

$$G = (3.440 - d_{002}) (3.440 - 3.354) \quad (5)$$

A sharp peak is observed for graphite with high crystallinity and an interlayer spacing of 0.3354 nm, whereas for amorphous materials this peak is very broad. The broadening of diffraction peaks may be due to lattice strain, defects in the structure and finite crystal size. However, the instrumental calibration and resolution are of the utmost importance to the pattern obtained. In carbon materials an internal standard (silicon) is required. The use of this internal standard is essential because carbon materials have a low absorption coefficient for X-rays, such that it penetrates deeply into the sample, which causes a shift of diffraction peak to the lower angle side and also a broadening of the observed profile (Marsh, 1989).

2.5.5 Raman spectroscopy

Raman spectroscopy is an analytical technique which gives vibrational information that is very specific to the chemical bonds in molecules. It is commonly used in chemistry and

condensed physics since it provides the 'fingerprint' by which a molecule can be identified. This type of spectroscopy gives the chemical and phase composition of materials, ranging from amorphous to highly crystalline structures. Consequently, a molecule and its environment determine the Raman signals to be observed. It is named after the Indian physicist who discovered it in 1928, C. V. Raman.

Raman spectroscopy gives the measurement of the wavelength and intensity of the light inelastically scattered by a molecule. The scattering process can be explained using the concept of molecule polarisability. When the light strikes a molecule, it interacts with the electron cloud of the bond of that molecule. The extent to which the electron cloud is deformed is the polarisability of the molecule. Polarisability depends on how tightly bound the electrons are to the nuclei. When electrons vibrate, they vibrate either symmetrically or asymmetrically. Raman scattering is favoured by symmetrical stretches of electrons. In symmetrical stretch the strength of the electrons is the difference between the minimum and maximum internuclear distances. As a result, polarisability changes during vibration and the vibration mode scatters Raman light. Because in asymmetrical stretch the electron expanding away from the nucleus is more easily polarised than the electron that is compressing, there is no overall polarisability (Schrader, 1995).

The induced dipole moment then emits a photon, leading to either Raman or Raleigh scattering. The Raman effect occurs when the incident light excites a molecule to a virtual state (less than the excited electronic state), which subsequently scatters the light and relaxes back to the first vibrational energy state. Elastically scattered light is the light that is scattered at the same wavelength as the incident light (Raleigh scattering), whereas inelastically scattered light is the light that is scattered at a different wavelength from the incident light (Raman effect). The energy difference between the incident light and Raman scattered light is equal to the energy that causes the molecules to vibrate. In Raman spectroscopy Raleigh scattering is filtered out and Raman light is dispersed onto a detector. Since Raman transitions are relatively weak, exciting radiation with a higher intensity, normally laser light, is used.

Raman spectroscopy is a non-destructive technique and is used to characterise carbon materials such as disordered, turbostratic and diamond-like carbons, or polymers such as carbon films and graphite. In 1970 Tuinstra and Koenig discovered the Raman spectra of a single crystal of graphite and of microcrystalline graphite samples (Tuinstra & Koenig, 1970). For single-crystal graphite the spectra showed a fairly sharp peak at 1 575 cm^{-1} although not as sharp as the one for diamond. Because it was known that graphite has carbon layer planes stacked in a hexagonal crystal structure corresponding to the space group $P6_3/mmc$ ($=D_{6k}^4$), therefore possessing two vibrational modes (E_{2g1} and E_{2g2}), a sharp peak was assigned to the Raman active mode E_{2g2}. This peak is commonly called the G-peak, with G referring to graphite. It apparently shifts according to the stress and temperature involved. The E_{2g1} mode at 42 cm^{-1} is assigned to the interplanar "rigid-layer" shear. Both of these vibrational modes are associated with the in-plane vibrations of carbon atoms in the layer.

For microcrystalline graphite an additional peak emerged at 1 355 cm^{-1}. This peak was assigned to the first-order scattering of photons by the disordered zone of the structure. It appears when the long-range order of graphite is disrupted (lattice distortion) and when the material has a finite crystallite size. This peak is generally called the D-peak, with D referring to disordered. The bond angle, bond length disorder, lattice disruption and crystallite size have a strong influence on the Raman intensity. However, the proximity of the laser wavelength to electronic transition enhances the bands. The average size of the crystallites can therefore be determined in terms of changes in the position, width and intensity ratio of two Raman peaks (Cottinet *et al.*, 1988).

CHAPTER 3: EXPERIMENTAL

Chemical and reagents used

The chemicals, all pure grade, used were: N, N-dimethylformamide (DMF) 99.9 % AR (Samsung Fine Chemicals); NaOH CP in pearl (Bio-Zone Chemicals). The following chemical were supplied by Merck (Pty) Ltd: oxine, 99% acetic acid, 55% nitric acid, ferric chloride, ammonium nitrate, aluminium chloride, calcium nitrate, copper sulphate and zirconium nitrate.

3.1 Analysis of Coal

The coal that was used in this study was obtained from Tshikondeni Mine in the Limpopo Province. The coal was submitted for analysis to Coal and Mineral Technologies (Pty) Ltd, a subsidiary of the South African Bureau of Standards. The results of the ultimate and proximate analyses, on an air-dry basis, and of the major petrographic analysis are given in Tables 4.1, 4.2 and 4.3 respectively.

3.2 Coal Solvent Extraction

The method developed by the CSIR was employed in this study for coal solvent extraction (Morgan, 2000). In a 3 ℓ steel oil-jacketed reactor, 2 800 g of DMF and 280 g of coal were charged in a reactor and heated up to 95 °C under a nitrogen atmosphere. The mixture was stirred effectively at 700 r/min until the temperature reached 95 °C. When it reached the operating temperature, 24 g of NaOH was added to the mixture. To follow the progress of extraction, samples were taken at suitable time intervals. The samples were centrifuged for five minutes at a speed of 4 000 r/min. About 0.1g of the supernatant solution was weighed accurately to a 50 ml volumetric flask and diluted up to the mark with DMF. The absorbance was measured at a wavelength of 600 nm on a spectrophotometer. The absorbance was then corrected to 0.1 g of each sample. The progress of extraction was followed for five hours. The mixture of Refcoal solution and the inorganic components was then transferred to a centrifuge bottle and centrifuged for one hour at a speed of 3 000 r/min. After centrifugation, the supernatant was separated

from the residue by decanting the upper layer. The Refcoal solution was then ready to be mixed with the catalyst and precipitated.

3.3 Dispersion of Complexes in Refcoal Solution

The complexes used were metal acetylacetonates and hydroxyquinolinates of iron, aluminium, calcium, copper and zirconium. The metal acetylacetonates were obtained commercially, whereas the metal hydroxyquinolinates were synthesised according to the procedures outlined below. Each complex was added to the Refcoal solution separately such that after carbonisation, a coke would have a 3 wt % loading of the metal which would serve as a catalyst on graphitisation. The catalyst solution was prepared by dissolving the calculated mass of each metal complex into a small amount of DMF, and then mixing the solution with 200 g of Refcoal solution. The mixture was shaken for five minutes to ensure proper and uniform mixing. The modified Refcoal was then precipitated by mixing it with 600 g of distilled water and centrifuging it for twenty minutes at a speed of 3 000 r/min. The supernatant was removed by decantation and the washing process was repeated five times in order to effectively remove the DMF and the alkali. The residue was then filtered and dried in the oven under nitrogen gas at a temperature of 60 °C overnight. For comparison, a sample with no complex added was prepared following the same procedure.

3.4 Synthesis of Metal Hydroxyquinolinate Complexes

3.4.1 Preparation of iron(III)hydroxyquinolinate

About 0.4 g of ferric chloride ($FeCl_3$) was dissolved in 50 ml of 4N acetic acid and diluted with water to 100 ml. The $FeCl_3$ solution was then heated to 70 °C, followed by the drop-wise addition of 20 ml of 2M ammonium acetate solution with constant stirring. Thereafter, 200 ml of the reagent (hydroxyquinoline acetate) was added in portions with constant stirring over a two-hour period. During the addition of the reagent, the temperature was kept at a range of 60 to 70 °C. When the precipitate started forming, the pH was measured immediately. After the total volume of the reagent had been added, the pH was measured again. The solution was then heated further up to 80–90 °C for

30 minutes in order to coagulate the precipitate. The solution was allowed to cool and then filtered through a sterile membrane filter (0.45 µm pore size). The precipitate was washed with hot water (60 °C) until a clear filtrate was obtained. The product was dried at 130 °C in the oven for two hours and weighed as $Fe(C_9H_6ON)_3$ (Jeffery *et al.*, 1989).

3.4.2 Preparation of aluminium(III)hydroxyquinolinate

About 0.4 g of aluminium chloride ($AlCl_3$) was dissolved in 20 ml of 4N acetic acid and diluted to 100 ml with water. The $AlCl_3$ solution was heated up to 70 °C with constant stirring. About 133 ml of the reagent solution was added in small portions over a period of one-and-a-half hours. During the addition of the reagent, the temperature was kept at a range of 60 to 70 °C. After about 80 ml of the reagent had been added, the precipitate started forming and the pH was measured immediately. After the total volume of the reagent had been added, 20 ml of 2M ammonium acetate solution was introduced drop wise while stirring until the pH reached 4.21. The mixture was then heated at a temperature range of 60–70 °C for an additional hour in order to coagulate the precipitate. The solution was allowed to cool and then filtered using a sterile membrane filter. The product was washed with hot water, dried in the oven at 120 °C for two hours and weighed as $Al(C_9H_6ON)_3$ (Erdey, 1965).

3.4.3 Preparation of calcium(II)hydroxyquinolinate

About 0.725 g of 8-hydroxyquinoline was weighed and dissolved in 100 ml of distilled water. Five ml of 1M NaOH solution was added to the hydroxyquinoline solution dropwise while stirring. The resulting mixture was stirred at room temperature using a stirrer bar for one hour. Thereafter 2.5 ml of 1M $Ca(NO_3)_2$ was added dropwise to the solution with continued stirring at room temperature. The mixture was then stirred for an additional hour, after which the product was allowed to settle for 30 minutes. The product was filtered using a sterile membrane filter and washed with hot water. It was dried at 130 °C for three hours to ensure complete dehydration, and then weighed as $Ca(C_9H_6ON)_2$ (Charles, 1961).

3.4.4 Preparation of copper(II)hydroxyquinolinate

About 0.4 g of copper sulphate ($CuSO_4$) was dissolved in 20 ml of distilled water. Ammonium acetate solution was prepared by dissolving 3 g of ammonium acetate in 12 ml of glacial acetic acid with 5 ml of distilled water. The ammonium acetate solution was then added to the copper sulphate solution. The mixture of the two solutions was made up to the mark with distilled water. The solution mixture was heated up to 70 °C. The reagent was then added dropwise to the solution mixture with constant stirring until there was a slight excess in the temperature range of 60 to 70 °C. The pH was measured immediately as the precipitate started forming. Twenty-five ml of 2M ammonium acetate solution was added dropwise to complete the precipitation. The solution was heated to 80 to 90 °C for 30 minutes in order to evaporate the excess precipitant. It was allowed to cool and then filtered using a sterile membrane filter. The product was washed with boiling water until a colourless filtrate was obtained and then dried in an oven at 105 to110 °C for two hours and weighed as $Cu(C_9H_6ON)_2$ (Jeffery *et al.*, 1989).

3.4.5 Preparation of zirconium(IV)hydroxyquinolinate

About 0.2 g of zirconium nitrate ($Zr(NO_3)_2$) was dissolved in 20 ml of distilled water. The zirconium nitrate solution was heated up to 80 °C in order to effectively concentrate the solution. This was followed by the dropwise addition of 2 ml of concentrated nitric acid with constant stirring. The solution was then diluted up to 100 ml with distilled water. The resulting solution was heated up to 70 °C. The reagent solution was added in small portions while stirring until there was an excess. During the addition of the reagent, the temperature was kept in the range of 60 to 70 °C. The pH was measured immediately as the precipitate started forming. Ammonium acetate solution was then introduced dropwise with stirring until the pH of the solution was found to be 3.72. Thereafter the solution was further heated at 60 to70 °C in order to coagulate the precipitate. It was allowed to cool and then filtered through a sterile membrane filter, washed with hot water, dried at 120 °C for 2 hours and then weighed as $Zr(C_9H_6ON)_4$ (Hollingshead, 1954). The reaction of the metal(III) with 8-hydroxyquinoline is illustrated in Figure 3.1.

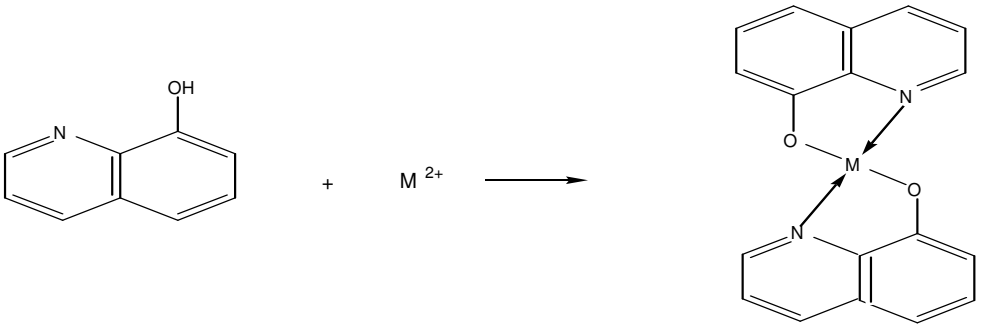

Ligand Metal ion Complex

(Metals: Ca and Cu)

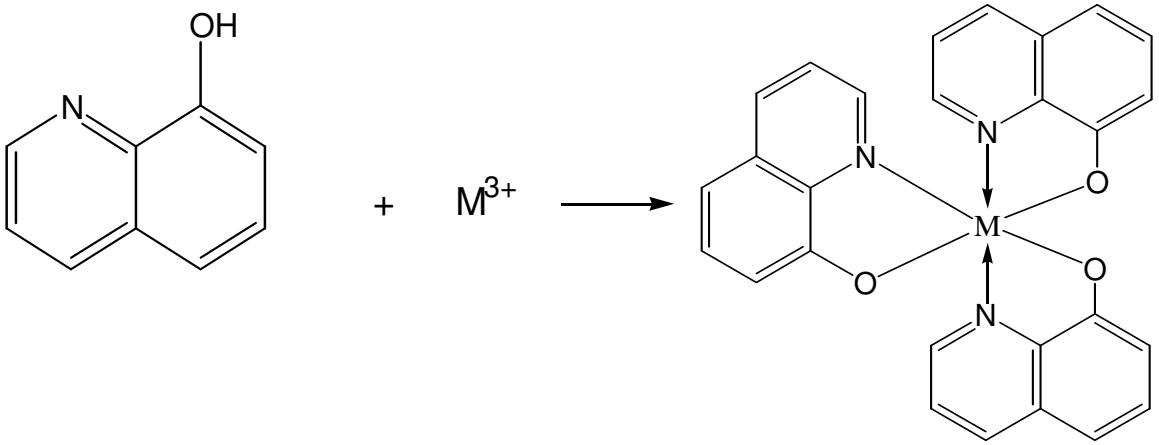

Ligand Metal ion Complex

(Metals: Fe and Al)

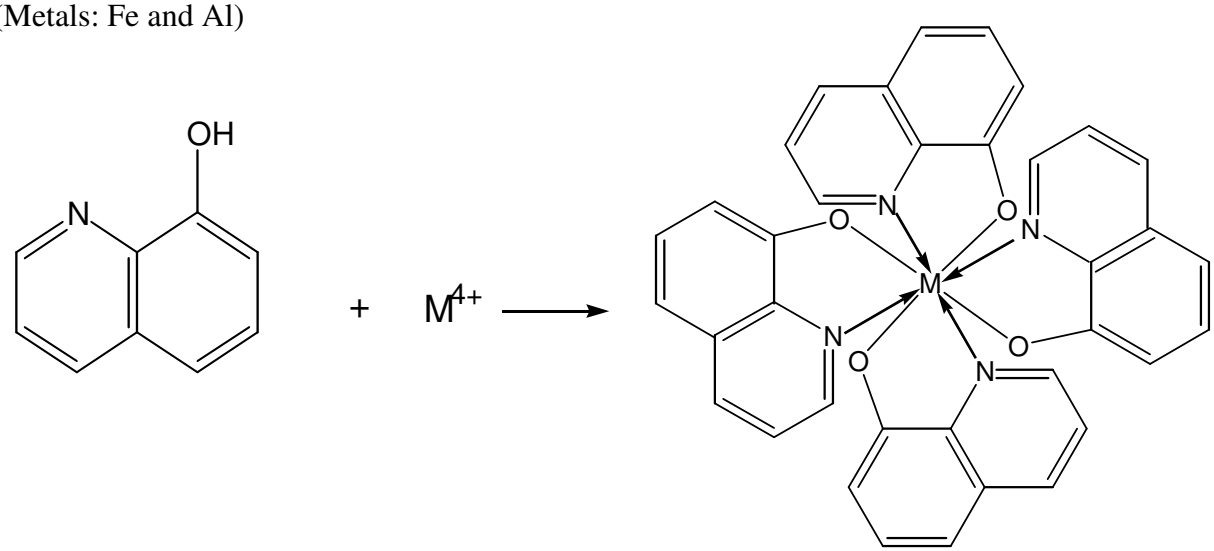

Ligand Metal ion Complex

(Metal: Zr)

Figure 3.1: Reaction scheme between metal ion and hydroxyquinoline ligand

3.5 Analysis of Metal Hydroxyquinolinate Complexes

3.5.1 Solubility

The solubility of the complexes was determined for six solvents in both cold and hot conditions, and the results are given in Table 4.4 in Chapter 4.

3.5.2 Thermogravimetric analysis

Thermogravimetric analysis (TGA) was done on the metal hydroxyquinolinate complexes in order to study their thermal stability and decomposition. The analyses were carried out in a Mettler Toledo TGA/SDTA 831^e thermal analyser, using the following procedure. About 10 mg of each sample was placed in a 70 µl capacity aluminium crucible with no lid. The samples were heated up to 1 000 °C at a rate of 10 °C/min under nitrogen gas flow of 50 ml/min. The weights of the residues were determined from the TGA curves. The samples were run under an air atmosphere at 50 ml/min and the residue weights were obtained from the TGA curves corresponding to the metal oxides. The results showing the fixed carbon in the complexes and the residues obtained by TGA are given in Table 4.5 in Chapter 4.

3.6 Carbonisation of Refcoal Samples

Dried Refcoal samples were ground into fine powder, weighed and loaded on aluminium boats. A twin-tube furnace was used for the carbonisation of the Refcoal samples under nitrogen gas flow. The samples were heat-treated at a heating rate of 10 °C/min up to 500 °C. The temperature was held at 500 °C for one hour to allow mesophase formation to take place, and then increased to 900 °C at a heating rate of 10 °C/min. The temperature was kept at 900 °C for two hours. The Refcoal solids were weighed before and after carbonisation, and the masses are given in Table A1 in the Appendix. The total yield of the neat coke is more than 100%, and this is attributed to instrumental errors.

3.7 Graphitisation of Cokes

The induction furnace from Solid State Induction Heating (Pty) Ltd, connected to the Vulcan induction generator, was used for graphitisation runs. The cokes were heat-treated at 1 600 ºC under a nitrogen atmosphere for two hours and six hours at a heating rate of 15 ºC/min under the following conditions: power output of 4 kW, frequency output of 2 500 Hz and voltage output of 250 V. The cokes were also graphitised at 2 000 ºC for two hours at a heating rate of 25 ºC/min under the conditions given above, except that the power output was 2.5 kW. The cokes were weighed before and after graphitisation, and the masses are given in Tables A2, A3 and A4 in the Appendix.

3.8 Analysis of Cokes and Graphitised Samples

3.8.1 Thermogravimetric analysis of cokes

Thermogravimetric analysis (TGA) was applied to the cokes in order to determine their volatile content, fixed carbon content and catalyst concentration. About 10 mg of each sample was placed in a 70 µl capacity aluminium crucible and heated from room temperature at a heating rate of 40 °C/min up to 110 °C under nitrogen at a flow rate of 50 ml/min. The samples were kept at that temperature for five minutes and then heated to 900 °C at a heating rate of 80 °C/min. They were then kept at that temperature for five minutes under nitrogen at a flow rate of 50 ml/min. The nitrogen gas was then closed off and air was allowed in at a flow rate of 50 ml/min. The samples were kept at 900 °C under an air atmosphere for 25 minutes.

3.8.2 Scanning electron microscopy

The SEM technique was applied to the cokes and graphitised cokes in order to study their morphology and to identify the catalyst particles. Samples were prepared for analysis by adding a small volume of ethanol to each sample. The mixture was shaken for a short while and then doped with a dropper in a small carbon disc. This was allowed to dry and was then ready for analysis. The samples were analysed using a JSM-6000F Scanning Electron Microscope, Jeol, first using only secondary electrons detector imaging,

followed by backscattered electrons detector imaging on each sample. Magnification of 6500 was used.

3.8.3 Optical microscopy

Optical microscopy was used to analyse both the cokes and graphitised cokes. For sample preparation, blocks with highly reflecting polished surfaces were prepared. To facilitate the polishing of brittle samples, a cross-section of each sample was mounted in Bakelite resin. In order to expose the sample and prepare a flat surface, the initial grinding was carried out on a grinding disc fitted with 120, 600 and 1200 grades of diamond disc, over which water was flowing continuously. Grinding was carried out with the successive disc grades until a flat, even surface ready for polishing had been obtained. The samples were then mounted on glass slides with plasticine using a manual mounting press to enhance evenness, with the polishing surface being protected during the mounting by a lens tissue. The samples were analysed using an Olympus PMG3 microscope with a rotation stage under polarised light. Magnification of 50 x 000 was used.

3.8.4 X-ray diffraction

The X-ray diffraction (XRD) technique was used to analyse both the cokes and graphitised cokes. For sample preparation, about 0.6 g of each sample was mixed with silicon (internal standard) that is 99.9% pure as supplied by Merck laboratories, with a crystallite size up to 43 μm. The masses that were used for sample preparation are given in Tables A5, A6, A7 and A8 in the Appendix. The sample and the silicon were mixed thoroughly by grinding, using a mortar and pestle. The mixture was then loaded into the sample holder using the back-loading preparation method. The mixture was analysed using a PANalytical X`Pert Pro powder diffractometer with X`celerator detector, variable divergence and receiving slits with Ni-filtered Cu-Kα radiation. The phases in the material were identified using X`pert Highscore Plus software.

3.8.5 Raman spectroscopy

This technique was used to analyse both the cokes and graphitised cokes. The Raman spectra were recorded with an XY Raman spectrometer from Dilor®, using the = 14.3 nm laser line of a Coherent Innova®90 Ar^+-laser, with a resolution of 2 cm^{-1} at a range of 600 to 1 800 cm^{-1}. The samples were recorded in a backscattering configuration under the microscope attached to the instrument, using a 30-x objective. A liquid-nitrogen-cooled CCD detector was used, with the laser power at 200 mW at the laser exit, resulting in a laser power of 45 mW at the sample. The spectra were baseline-corrected, using the Labspec software program supplied by Dilor®.

CHAPTER 4: RESULTS AND DISCUSSION

4.1 Coal Studied

Tables 4.1, 4.2 and 4.3 show the petrographic characteristics, ultimate analysis and proximate analysis of Tshikondeni coal. Based on the petrographic analysis data, it is classified as a meta-bituminous medium rank B coal (Mthembi, 2003).

Table 4.1: Petrographic characteristics of Tshikondeni coal

Rank (degree of maturity)	Bituminous
Seam classification	Medium rank A
Mean random reflectance	1.42 %
Vitrinite-class distribution	V 12 to V16
Standard deviation	0.078
Evidence of heating effects	None observed
Vitrinite content	94 %
Liptinite content	<1 %
Total inertinite	6 %

Table 4.2: Ultimate analysis of Tshikondeni coal

Moisture (air dry)	0.6 %
Ash (dry basis)	9.4 %
Volatile matter (dry basis)	23.3 %
Fixed carbon (dry basis)	67.4 %
Total sulphur (dry basis)	0.81 %
Calorific value (air-dry basis)	33.50 (MJ/kg)
Free swelling index	9.0
Roga index	86

Table 4.3: Proximate analysis of Tshikondeni coal

Element in the coal	Wt %
Carbon	81.5
Hydrogen	4.38
Nitrogen	1.86
Oxygen	1.15

4.2 Metal Hydroxyquinolinate Complexes

4.2.1 Colour

Table 4.4 gives the colour of the synthesised metal hydroxyquinolinate complexes. The synthesised complexes are colourful, whereas the free ligand is a cream-white powder. This is an indication that the colour does not emanate from the ligand, but derives from the metal ion and its oxidation state.

4.2.2 Solubility

Table 4.4 also shows the solubility data of the complexes. Solubility testing of the complexes was carried out in polar solvents such as methanol, chloroform and butanol, as well as in non-polar solvent (toluene) and a highly coordinating solvent dimethylformamide (DMF). The latter is the solvent medium used for coal extraction in this study. The complexes are soluble in chloroform and DMF, possibly due to coordination with solvents. On the other hand, the complexes are completely insoluble in water, as the literature indicates (Erdey, 1965).

Table 4.4: Colour and solubility of metal hydroxyquinolinate complexes

Complex	Colour	Solvents											
		$CHCl_3$		DMF		CH_3OH		Butanol		Toluene		H_2O	
		C	H	C	H	C	H	C	H	C	H	C	H
$Fe(C_9H_6ON)_3$	Black	S		S		SS	SS	SS	SS	SS	S	IS	IS
$Al(C_9H_6ON)_3$	Lime	S		S		SS	SS	SS	S	SS	S	IS	IS
$Ca(C_9H_6ON_2$	Yellow	S		S		SS	SS	SS	SS	SS	S	IS	IS
$Cu(C_9H_6ON_2$	Green	S		S		SS	SS	SS	S	SS	S	IS	IS
$Zr(C_9H_6ON)_4$	Green	S		S		SS	SS	SS	SS	SS	S	IS	IS

Note: C = cold, H = hot, S = soluble, SS = sparingly soluble and IS = insoluble

4.2.3 Thermogravimetric analysis

Table 4.5: Summary of thermogravimetric analysis results

Complex	Metal in complex (%)	Carbon in complex (%)	Expected metal oxide	Expected metal oxide residue (%)	Experimental TGA residue (%)
$Fe(C_9H_6ON)_3$	11.44	66.41	FeO	16.35	16.15
$Al(C_9H_6ON)_3$	5.87	70.58	Al_2O_3	11.09	6.21
$Ca(C_9H_6ON)_2$	12.25	65.77	CaO	17.07	17.23
$Cu(C_9H_6ON)_2$	18.06	61.44	CuO	22.60	22.26
$Zr(C_9H_6ON)_4$	13.65	64.74	ZrO_2	18.45	20.81

4.2.3.1 Iron(III)hydroxyquinolinate

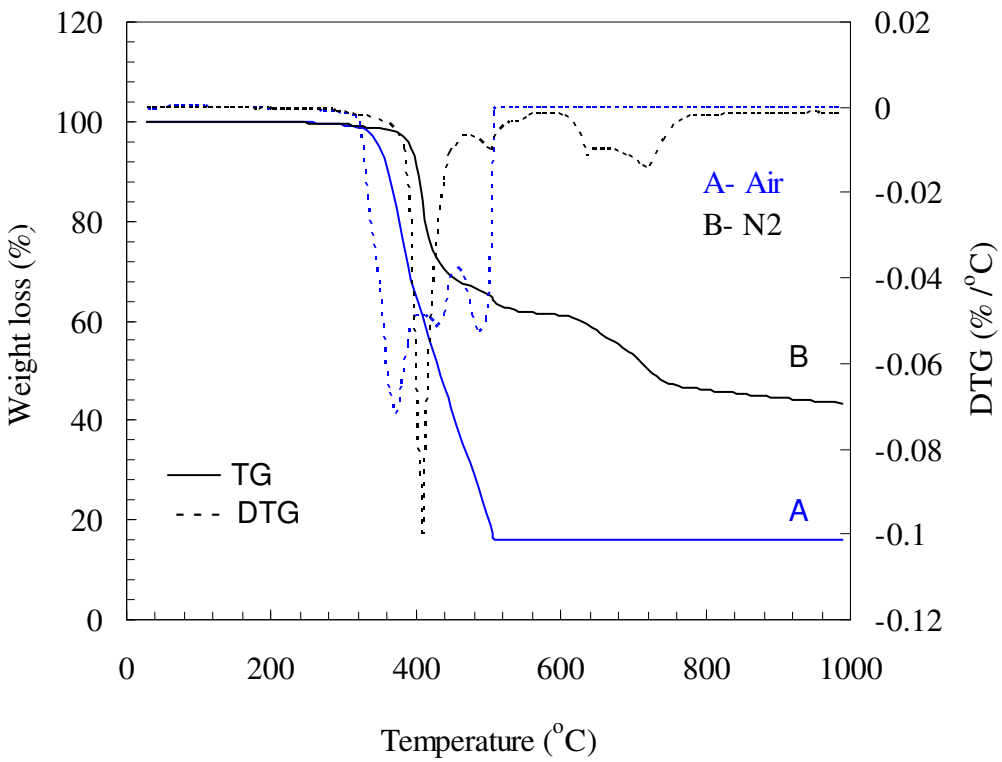

Figure 4.1: Thermogravimetric mass loss and derivative mass loss (DTG) curves for iron(III)hydroxyquinolinate obtained under air and nitrogen

Figure 4.1 shows the thermogravimetric (TG) and DTG curves of $Fe(C_9H_6ON)_3$ in both an N_2 atmosphere and air. Through TG analysis of the complex it was verified that the composition of the synthesised complex is $Fe(C_9H_6ON)_3$. In an N_2 atmosphere the curve shows that the dry complex is stable up to about 320 °C. Thereafter mass loss occurs in at least four separate steps, indicated by the DTG peaks centred at ca. 408, 505, 644 and 623 °C. The mass loss between 350 and 480 °C might be due to partial volatilisation. That mass loss is followed by partial thermal decomposition of the complex to a mixture of carbonaceous and oxide residues in the temperature range of 480 to 995°C. In an air atmosphere the DTG curves indicate three separate thermal events centred at ca. 372, 428 and 487 °C. The final residue is composed of FeO (Erdey, 1965). Experimental value for the metal oxide of the synthesised complex as determined using TGA is given in Table

4.5. The table also give the calculated theoretical value for expected metal oxide, thus allowing comparison between theoretical and experimental values. The experimental value for the iron oxide obtained under air corresponds closely to the theoretical value.

4.2.3.2 Aluminium(III)hydroxyquinolinate

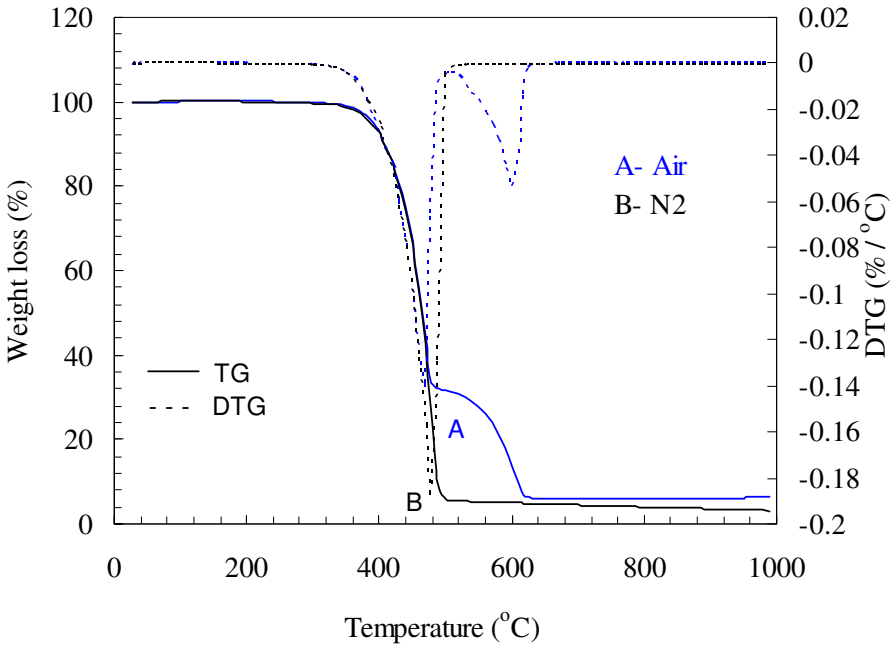

Figure 4.2: Thermogravimetric mass loss and derivative mass loss (DTG) curves for aluminium(III)hydroxyquinolinate obtained under air and nitrogen

Figure 4.2 shows the TG and DTG curves of $Al(C_9H_6ON)_3$ in both an N_2 atmosphere and air. Through TG analysis of the complex it was verified that the composition of the synthesised compound is $Al(C_9H_6ON)_3$. The curve obtained in N_2 shows that the dry complex has a constant weight up to about 350 °C. Thereafter mass loss occurs in one sharp event, indicated by the DTG peak centred at ca. 479 °C. The weight loss between 350 °C and 500 °C is attributed to loss of the complex, assumed to be due to volatilisation in the form of sublimation and vaporisation. The weight loss is followed by partial thermal decomposition of the complex to a mixture of carbonaceous and oxide residues in the temperature range of 500 to 995 °C. In an air atmosphere the DTG curves

indicate two separate thermal events centred at ca. 469 and 602 °C. The TG curve of the complex obtained in an air atmosphere shows partial volatilisation of the complex between 350 and 500 °C, followed by thermal decomposition at 500 to 620 °C, which results in the formation of Al_2O_3 (Kokkonen *et al.*, 1987). Experimental value for the metal oxide of the synthesised complex as determined using TGA is given in Table 4.5. The table also give the calculated theoretical value for expected metal oxide, thus allowing comparison between theoretical and experimental values. The theoretical and experimental values do not compare very well, but the value obtained corresponds to that obtained by previous researchers (Kokkonen *et al.*, 1987). An increase in temperature up to 1 000 °C had no further effect on the resultant residue.

4.2.3.3 Calcium(II)hydroxyquinolinate

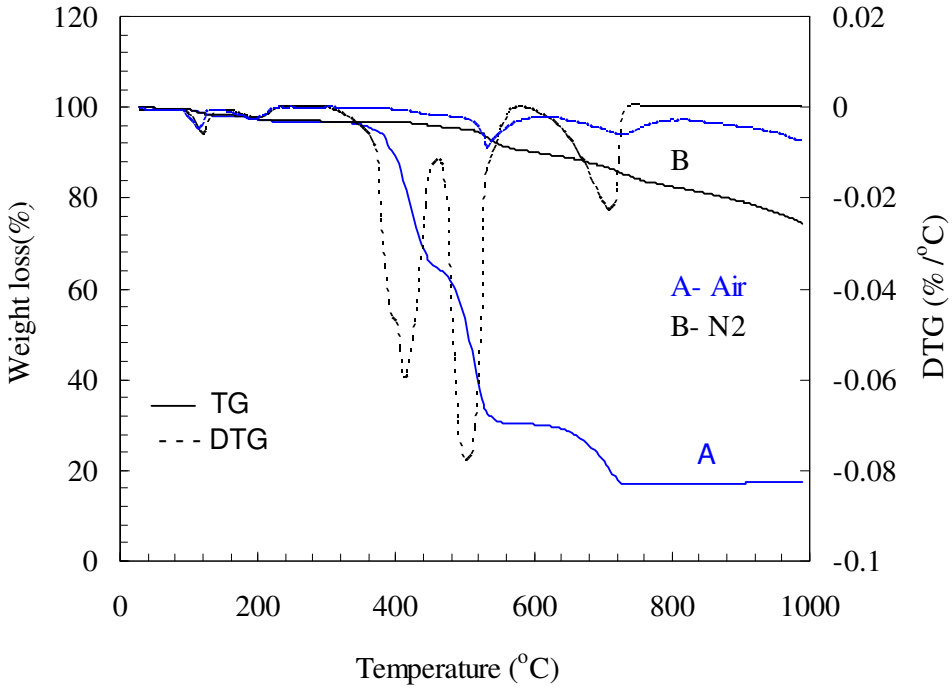

Figure 4.3: Thermogravimetric mass loss and derivative mass loss (DTG) curve for calcium(III)hydroxyquinolinate obtained under air and nitrogen

Figure 4.3 shows the TG and DTG curves of $Ca(C_9H_6ON)_2$ in both an N_2 atmosphere and air. The TGA results show that the composition of the synthesised complex is $Ca(C_9H_6ON)_2$. The curve obtained in an air atmosphere shows mass loss occurring in four

separate events, indicated by the DTG peaks centred at ca.115, 417, 506 and 714 °C. The event between 180 and 200 °C corresponds to dehydration of the complex. It is assumed that the mass loss between 200 and 500 °C is due to volatilisation. This event is followed by partial thermal decomposition of the remaining compound to a mixture of carbonaceous and oxide residues in the temperature range of 500 to 815 °C. The curve obtained in an air atmosphere also shows the dehydration step in the temperature range of 180 to 380 °C, followed by partial volatilisation of the complex at 380 °C. Thermal decomposition taking place between 560 and 730 °C results in the formation of CaO. Experimental value for the metal oxide of the synthesised complex as determined using TGA is given in Table 4.5. As can be seen, the residue yield from the TGA obtained in air is comparable to the theoretical yield of CaO in the complex. An increase in temperature up to 1 000 °C had no effect on the chemical composition of the residue (Charles, 1961).

4.2.3.4 Copper(II)hydroxyquinolinate

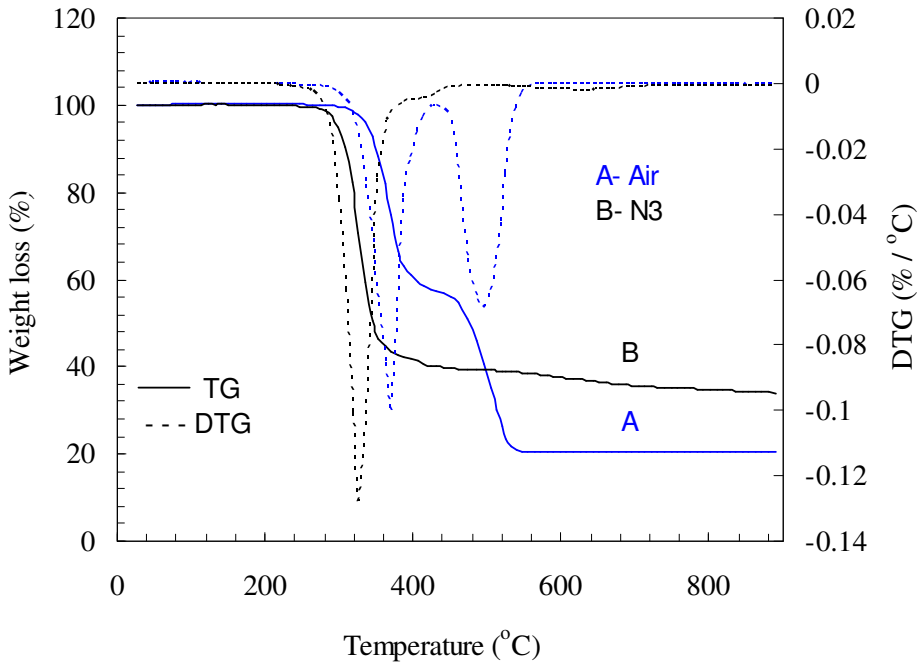

Figure 4.4: Thermogravimetric mass loss and derivative mass loss (DTG) curve for copper(III)hydroxyquinolinate obtained under air and nitrogen

Figure 4.4 shows the TG and DTG curves of $Cu(C_9H_6ON)_2$ in both an N_2 atmosphere and air. Through TG analysis of the complex it was verified that the composition of the synthesised complex is $Cu(C_9H_6ON)_2$. The curve obtained in N_2 shows that the dry complex has a constant weight up to about 280 °C, with an unchanged chemical composition. Thereafter mass loss occurs in one event, indicated by the DTG peak centred at ca. 326 °C. The weight loss between 280 and 430 °C is attributed to loss of the complex by partial volatilisation in the form of sublimation and vaporisation. Partial thermal decomposition of the complex to a mixture of carbonaceous and oxide residues takes place in the temperature range of 430 to 995 °C. In an air atmosphere the DTG curves indicate two separate thermal events centred at ca. 370 and 795 °C. It is assumed that partial volatilisation of the complex takes place between 280 and 615 °C, followed by thermal decomposition at 615 to 995 °C, which results in the formation of CuO (Crespi *et al.*, 1999). Experimental value for the metal oxide of the synthesised complex as determined using TGA is given in Table 4.5. The theoretical and experimental values of the metal and metal oxide correspond fairly well.

4.2.3.5 Zirconium(IV)hydroxyquinolinate

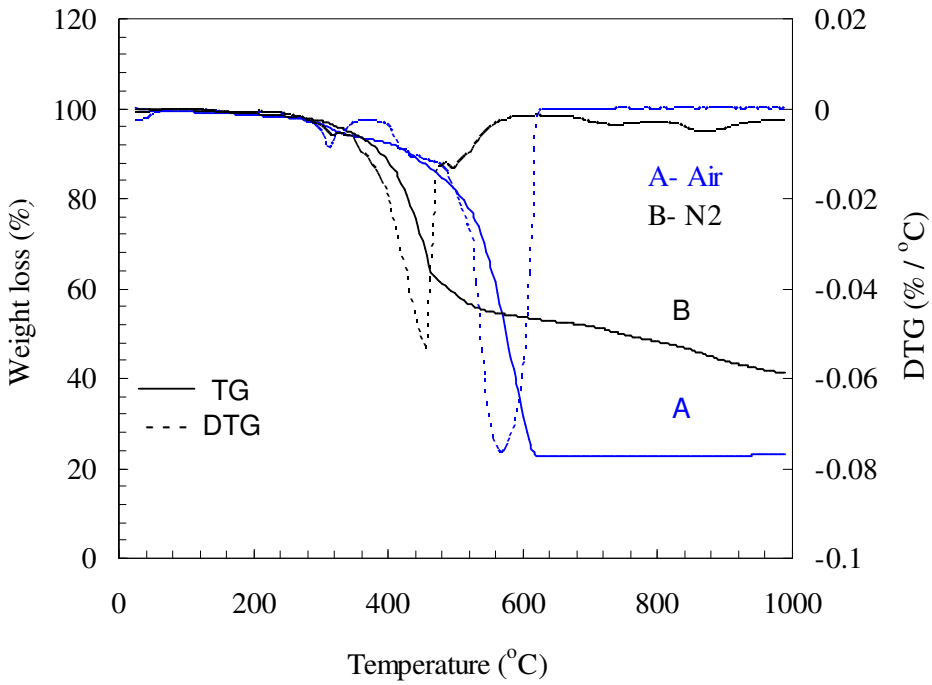

Figure 4.5: Thermogravimetric mass loss and derivative mass loss (DTG) curve for zirconium(III)hydroxyquinolinate obtained under air and nitrogen

Figure 4.5 shows the TG and DTG curves of $Zr(C_9H_6ON)_4$ in both an N_2 atmosphere and air. TG analysis of this complex shows that the composition of the compound is $Zr(C_9H_6ON)_4$. The curve obtained in N_2 shows that the dry complex has a constant weight up to about 190 °C. Thereafter mass loss occurs in two separate events, indicated by the DTG peaks centred at ca. 457 and 880 °C. The TG curve shows that between 190 and 470°C the complex undergoes mass loss. This event is followed by partial thermal decomposition of the complex to a mixture of carbonaceous and oxide residues in the temperature range of 470 to 994°C. In an air atmosphere the DTG curves indicate two separate thermal events centred at ca. 316 and 575 °C. The curves show mass loss of the complex between 260 and 380°C, followed by thermal decomposition at 380 to 600°C, which results in the formation of ZrO_2. An increase in temperature up to 1 000 °C had no further effect. Experimental value for the metal oxide of the synthesised complex as determined using TGA is given in Table 4.5. The table also give the calculated theoretical value for expected metal oxide, thus allowing comparison between theoretical and experimental values. As can be seen, the residue yield of the TG analysis obtained in air is comparable to the theoretical yield of ZrO_2 in the complex (Hollingshead, 1954).

4.3 Analysis of Cokes

4.3.1 Thermogravimetric analysis

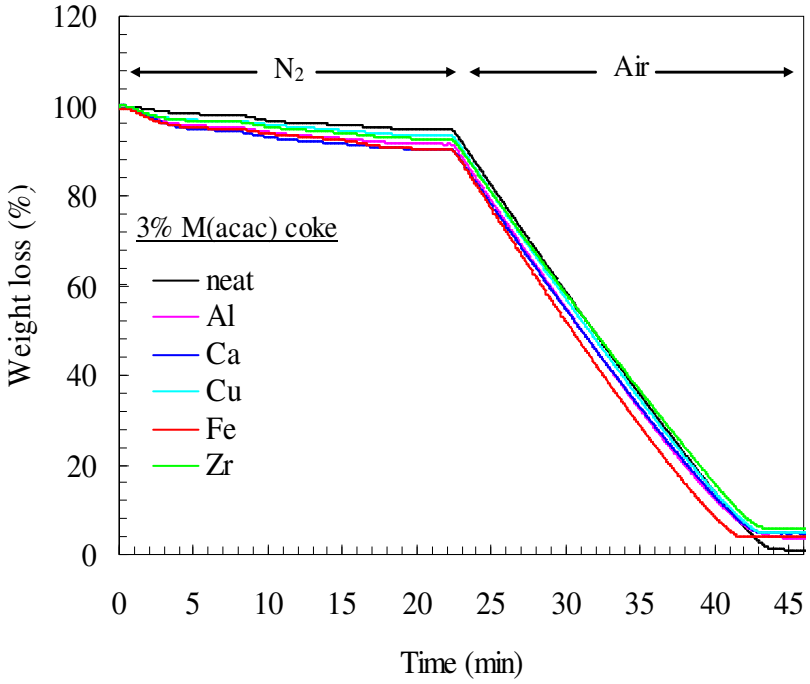

Figure 4.6(a): Thermogravimetric curve of Refcoal carbonised for 2 hours at 900 ºC

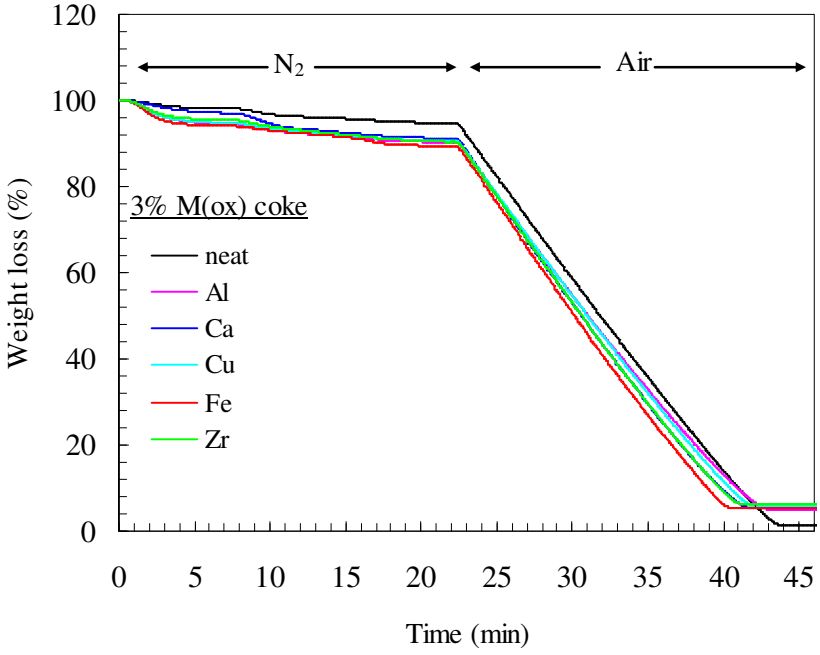

Figure 4.6(b): Thermogravimetric curve of Refcoal carbonised for 2 hours at 900 ºC

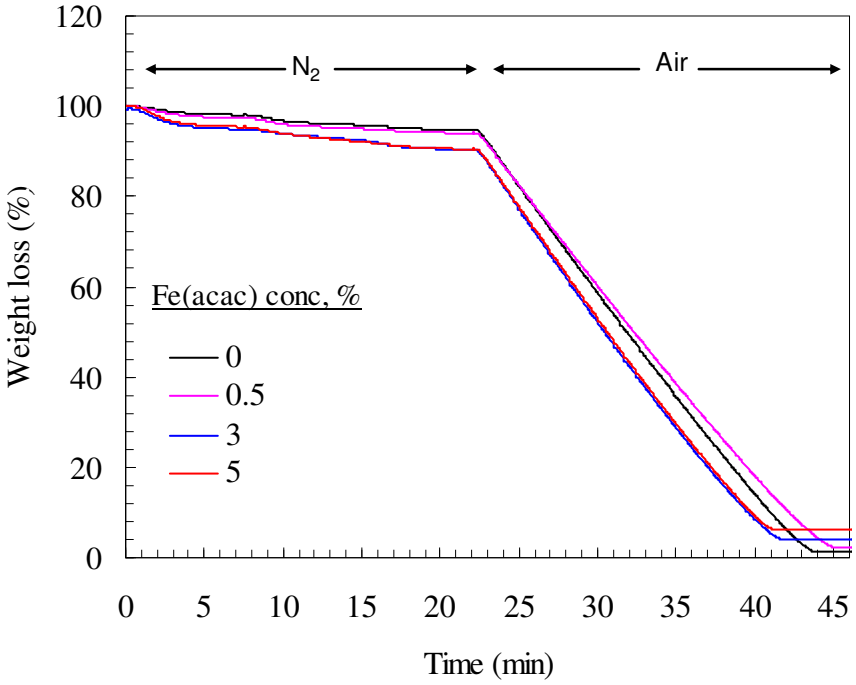

Figure 4.6(c): Thermogravimetric curve of Refcoal carbonised for 2 hours at 900 ºC

Figures 4.6 (a) and (b) depict the TGA curves of cokes obtained by carbonisation of Refcoal. The cokes were heated under N_2 up to 900 °C at a scan rate of 40 °C/min, and held isothermally at this temperature for 25 minutes before switching to air. They were kept isothermally under an air atmosphere for 25 minutes. The moisture and volatile contents correspond to the mass losses obtained when the samples were heated under nitrogen. The fixed carbon and ash contents were determined from the runs done isothermally in air. Table 4.6 summarises the results given in the graphs. All the cokes show slight dehydration, which is assumed to be the moisture that the cokes capture when exposed to air. The cokes containing catalysts show high moisture, volatile matter and ash contents compared with the neat coke owing to the presence of the catalyst. However, the neat coke shows high fixed carbon content compared with the metal-containing cokes.

When the nitrogen gas is closed off and an air atmosphere is allowed into the instrument, the samples undergo combustion. On combustion during thermal analysis of a coke with

an acetylacetonate complex, carbon is lost; while the metal oxide remains in the crucible, thus contributing to the ash content obtained. This is based on the assumption that after oxidation of the cokes, only the corresponding metal oxide remains. The latter constitutes the "ash content" of the sample. Figures 4.6 (a) and (b) also show the effect of the additives on the rate of combustion of the cokes. The metal-containing cokes had a fast rate of combustion compared with the neat cokes. The iron-containing cokes had the fastest rate of combustion, indicating the catalytic oxidation of iron. The cokes containing aluminium and calcium show a slow rate of combustion, whereas the copper and zirconium-containing cokes have an intermediate rate of combustion. Figure 4.6(c) shows the TGA curve of the cokes obtained by carbonisation of Refcoal treated with different concentrations of iron. These cokes show different ash content values due to the different concentrations of iron in each coke.

Table 4.6: Summary of TGA results obtained in cokes carbonised at 900 °C

Sample	Moisture (%)	Volatile matter (%)	Fixed carbon (%)	Ash content (%)
Neat coke	1.93	3.37	93.09	1.11
3%Fe(acac) coke	4.06	4.76	86.31	3.95
3%Al(acac) coke	4.58	3.93	87.48	3.47
3%Ca(acac) coke	2.64	3.90	91.14	4.71
3%Cu(acac) coke	3.29	3.33	88.19	4.79
3%Zr(acac) coke	3.41	3.91	85.62	5.78
3%Fe(ox) coke	5.87	4.67	82.46	5.42
3%Al(ox) coke	5.41	4.19	84.64	4.67
3%Ca(ox) coke	2.89	5.87	84.56	5.47
3%Cu(ox) coke	5.15	4.11	83.59	5.54
3%Zr(ox) coke	4.57	5.00	83.96	6.35
0.5%Fe(acac) coke	2.51	3.46	92.54	2.18
5%Fe(acac) coke	3.03	4.14	82.02	6.37

4.3.2 Scanning electron microscopy

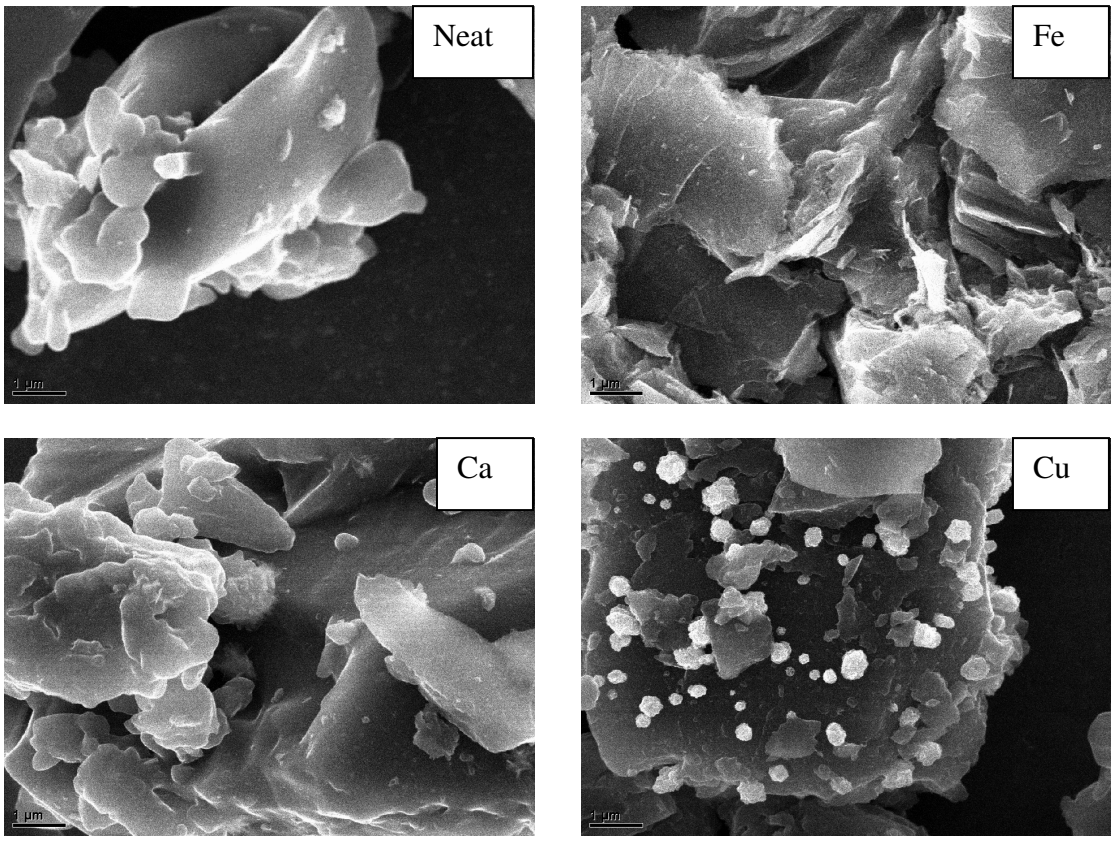

Figure 4.7(a): Scanning electron micrographs of 3% M(acac)-containing cokes obtained at 900 °C

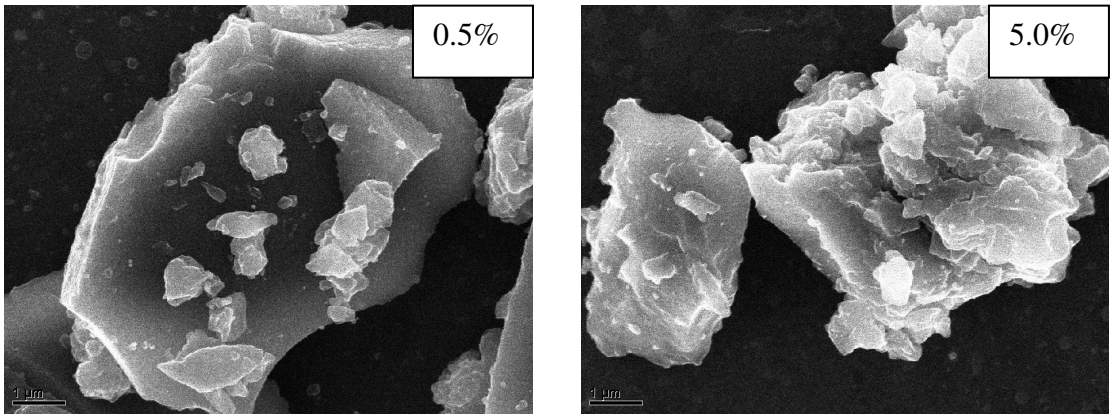

Figure 4.7(b): Scanning electron micrographs of cokes obtained by carbonisation of Refcoal at 900 °C at different concentrations of Fe(acac)

Figure 4.7(a) shows the scanning electron micrographs of the cokes obtained by carbonisation of Refcoal for two hours at 900 ºC. This technique was applied to the cokes in order to study their morphology and to identify the metal catalyst particles. The presence of the metal in the cokes modified the morphology of the cokes. The micrograph of the neat coke shows a fine and smooth surface, indicating that the coke has passed through more of the mesophase stage than the treated samples. The neat coke also shows balloon-shaped particles. The structure of these particles means that the neat cokes have foamed during volatilisation more than treated samples (Park *et al.*, 2005). The micrographs of the treated cokes show rough surfaces compared with the smooth fine texture of the neat coke. However, the degree of roughness varies from system to system. For example, the micrographs of the iron-containing cokes show carbon with rough surfaces, with some regions showing flaky structures.

The interaction between the metal and the carbon resulted in the formation of clustered particles, although not all the metals interacted well with carbon. For example, the micrographs of the copper-containing cokes show the presence of copper crystals on the carbon surface. The micrograph of the calcium-containing coke is typical of the micrographs that were obtained for the aluminium- and zirconium-containing cokes. No major difference was observed between the micrographs of the cokes containing metal acetylacetonate and those containing metal hydroxyquinolinate complexes.

Figure 4.7(b) shows the micrographs of the cokes obtained by carbonisation of Refcoal with different concentrations of iron(III)acetylacetonate. An increase in the iron concentration led to rougher coke fracture surfaces morphology, clearly indicating a difference in the material structures. This can be related to the X-ray diffraction results which show that iron reacts with carbon to form iron carbide, as will be discussed in Section 4.4.

4.3.3 Optical microscopy

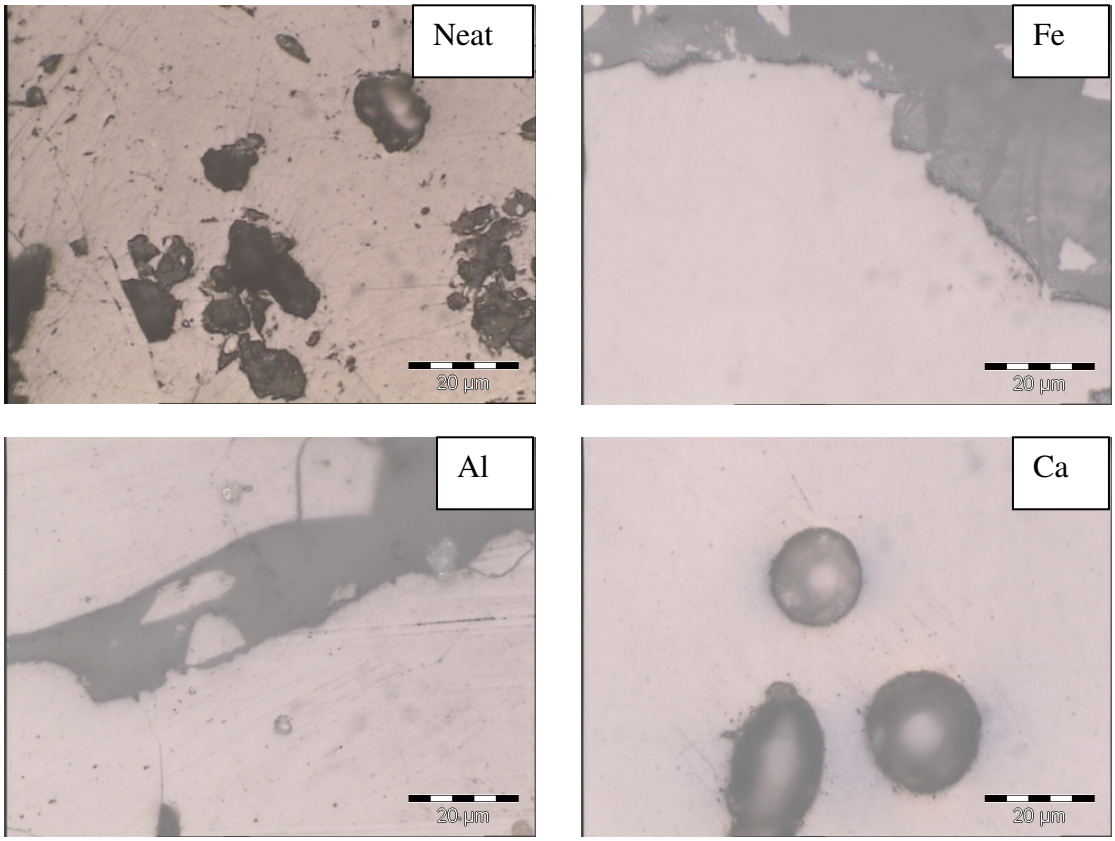

Figure 4.8(a): Optical micrographs of 3% M(acac)-containing cokes obtained at 900 ºC

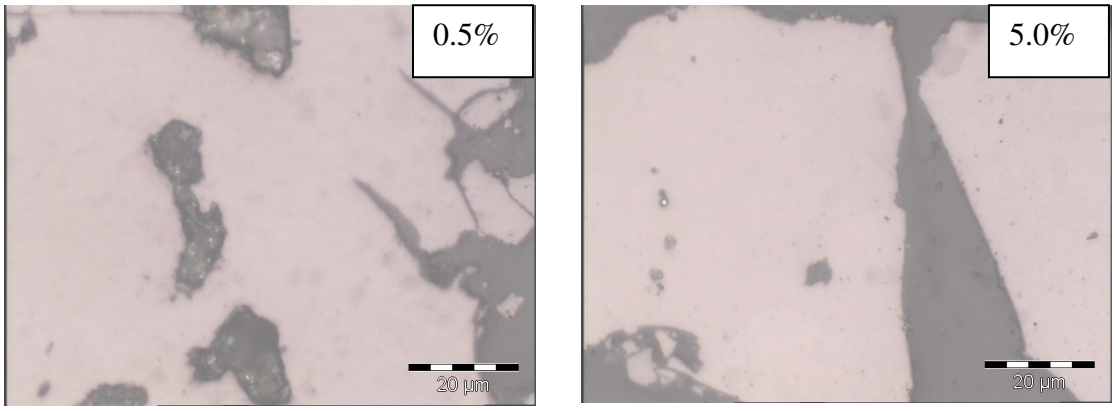

Figure 4.8(b): Optical micrographs of cokes obtained by carbonisation of Refcoal with different concentrations of Fe(acac), at 900 ºC

Figure 4.8(a) shows the optical micrographs of the cokes obtained on carbonisation of Refcoal for two hours at 900 ºC. Optical microscopy was used to study the texture of cokes. It is generally expected that a carbon sample that undergoes a complete mesophase formation stage during carbonisation will have an anisotropic texture. An isotropic texture indicates that a sample did not pass through a complete mesophase formation stage, meaning that mesophase spheres did not coalesce into large mesophase droplets. The micrograph of the neat coke shows a different texture compared with those of the metal-containing cokes, suggesting modification of the cokes' texture by the additives. Although the micrograph of the neat coke shows a region with fine-grained anisotropic texture, it still has a large region that remains isotropic. The micrographs of the metal-containing cokes are entirely isotropic. This is probably because the metal residues contained in the Refcoal retarded the coalescence of the mesophase spheres.

These observations correspond to previous findings that the additives may be adsorbed on the mesophase surfaces, thus producing a large number of smaller spheres by limiting growth and coalescence (Taylor *et al.*, 1993). It is, however, noted that the neat coke and the coke containing calcium(II)acetylacetonate showed devolatilisation pores.

Figure 4.8(b) shows the optical micrographs of the cokes obtained by carbonisation of Refcoal with different concentrations of iron(III)acetylacetonate. These micrographs of these cokes show isotropic texture. The coke containing 0.5% iron(III)acetylacetonate is, however, not completely isotropic. It has a few fine anisotropic grains, which is an indication that it has undergone the mesophase formation stage better than the cokes containing high concentrations of iron.

4.3.4 X-ray diffraction

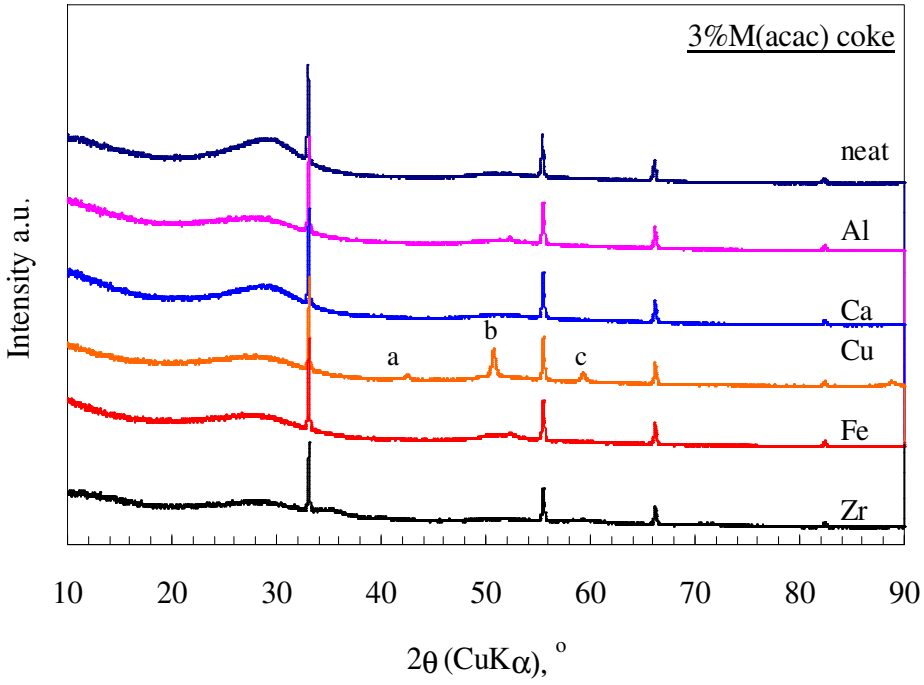

Figure 4.9(a): X-ray diffraction patterns of Refcoal carbonised for 2 hours at 900 °C

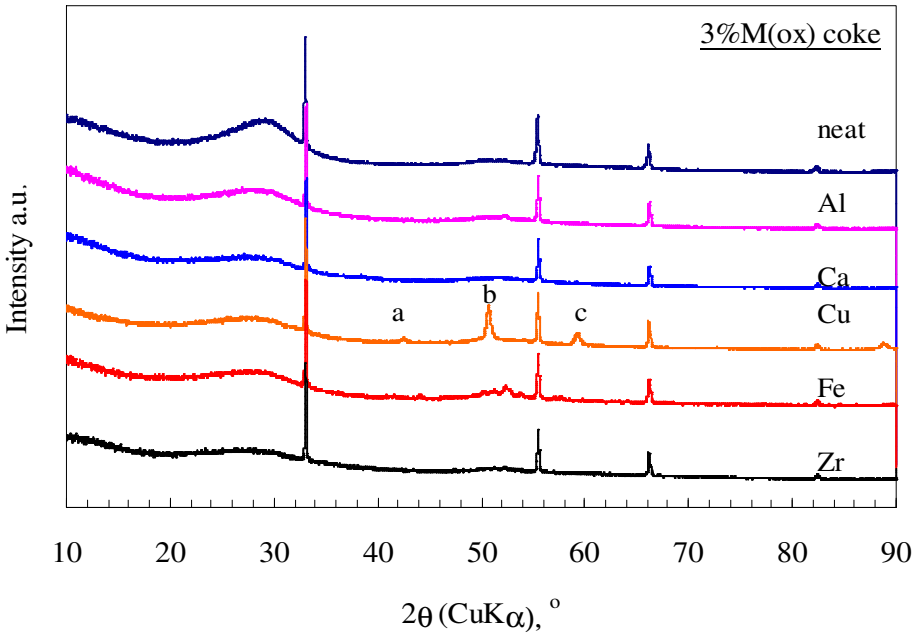

Figure 4.9(b): X-ray diffraction patterns of Refcoal carbonised for 2 hours at 900 °C

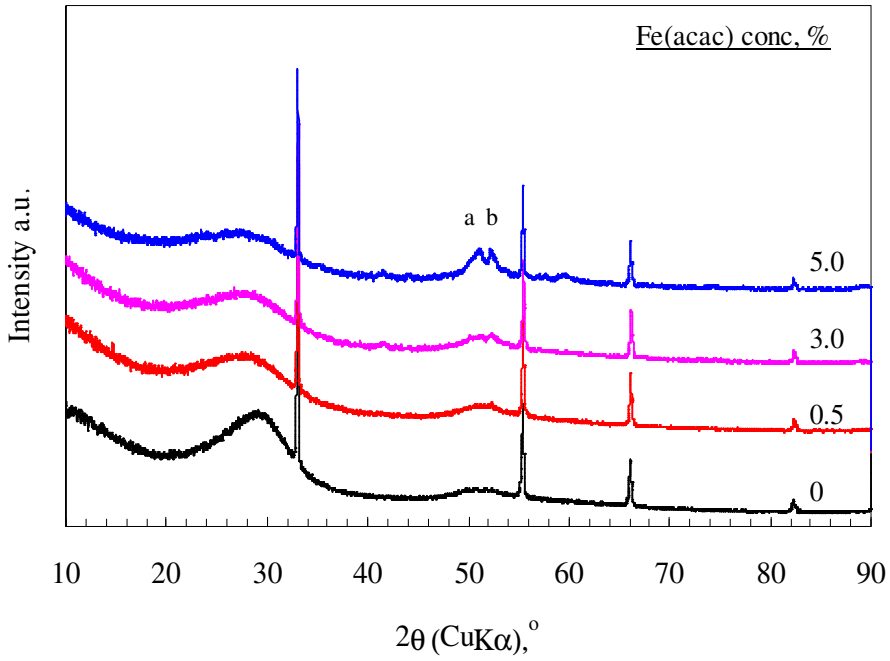

Figure 4.9(c): X-ray diffraction patterns for Refcoal treated with different concentrations of iron(III)acetylacetonate and carbonised for 2 hours at 900 °C

Figures 4.9(a) and (b) show the X-ray diffraction patterns of the cokes obtained by carbonisation of Refcoal. All the samples show peaks at approximately 26° and 52°, corresponding to diffraction by (002) and (004) graphite planes. The (002) graphite peak in the neat coke has a higher intensity than the metal-containing cokes; this because the additives reduce the purity of the cokes. The graphs show a broad (002) peak, indicative of structural imperfection. Both Figures 4.9(a) and (b) have peaks labelled (a), (b) and (c). The peak labelled (a) represents cuprite (CuO), whereas the peaks labelled (b) and (c) both match metallic copper, indicating reduction and crystallisation of copper.

Figure 4.9(c) shows a decreasing trend in the intensity of the (002) peak with an increase in the catalyst concentration. The X-ray diffraction pattern of the 5% Fe(acac) coke has peaks labelled (a) and (b), representing cementite (Fe_3C) and Fe respectively. The development of the same peaks is seen on the 3%Fe(acac) coke pattern. This behaviour manifests the effect of the catalyst concentration on the reaction between the carbon

structure and iron. This is in agreement with previous results obtained by Hong *et al.* (2007), namely that, on carbonisation, iron(III)acetylacetonate is converted to Fe_3O_4 via α-FeO(OH), which is then further reduced, resulting in the formation of metallic iron (α-Fe). Metallic iron reacts with carbon to form a metal carbide that is unstable on high-temperature treatment, thus decomposing to graphite crystal and metal crystal (Hong *et al.,* 2007; Park *et al.,* 2005). The phases present in the cokes are thought to be responsible for catalysing the graphitisation of the cokes. Based on the X-ray diffraction analyses of the cokes, the catalyst composition appeared to have no effect in the present study.

4.3.5 Raman spectroscopy

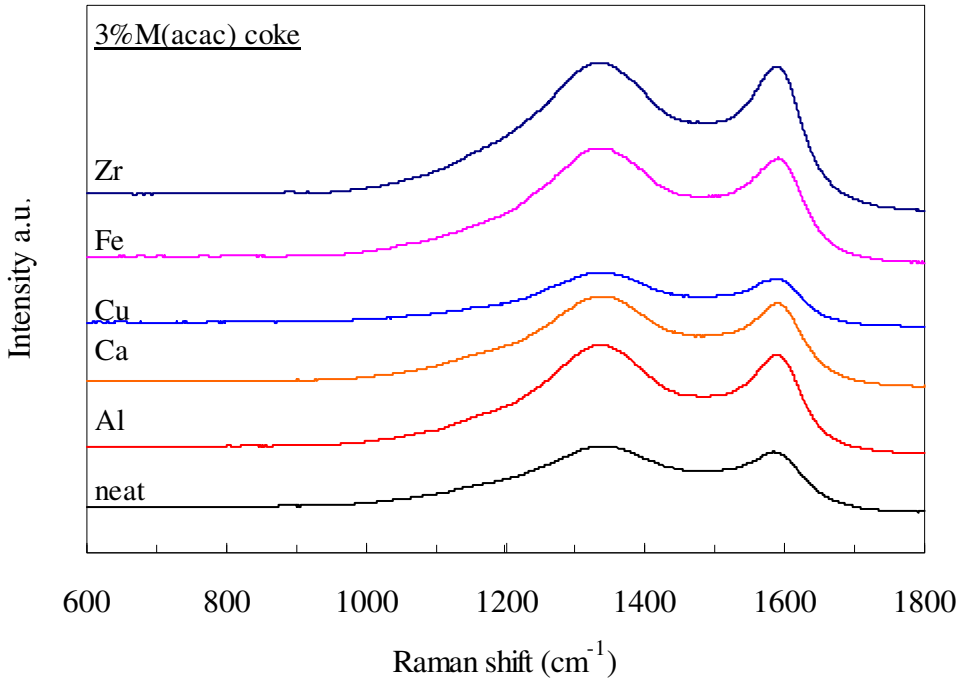

Figure 4.10(a): Raman spectra of Refcoal carbonised for 2 hours at 900 °C

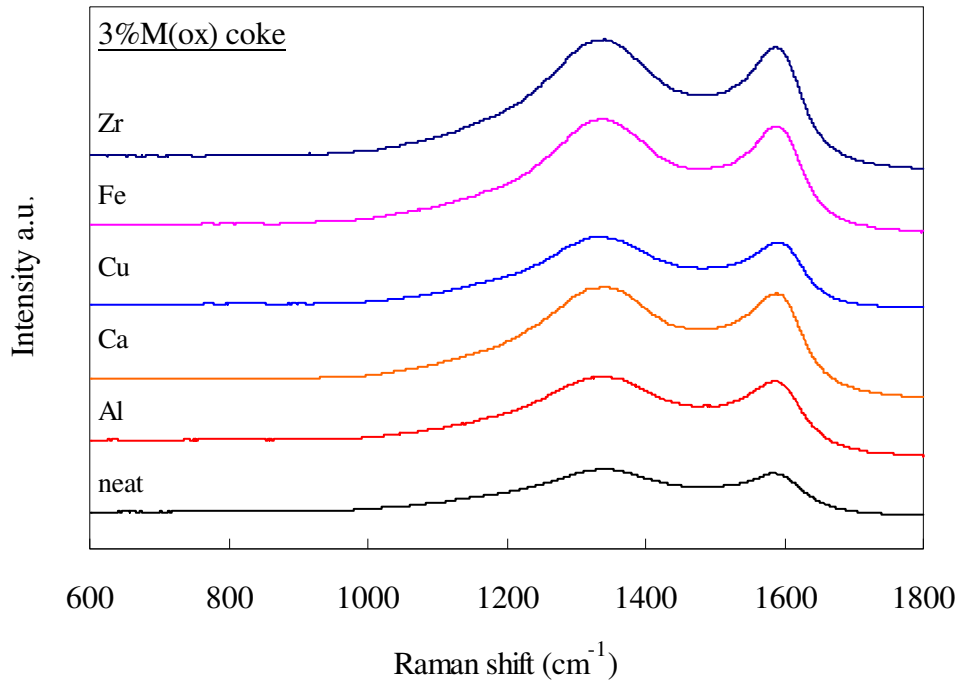

Figure 4.10(b): Raman spectra of Refcoal carbonised for 2 hours at 900 °C

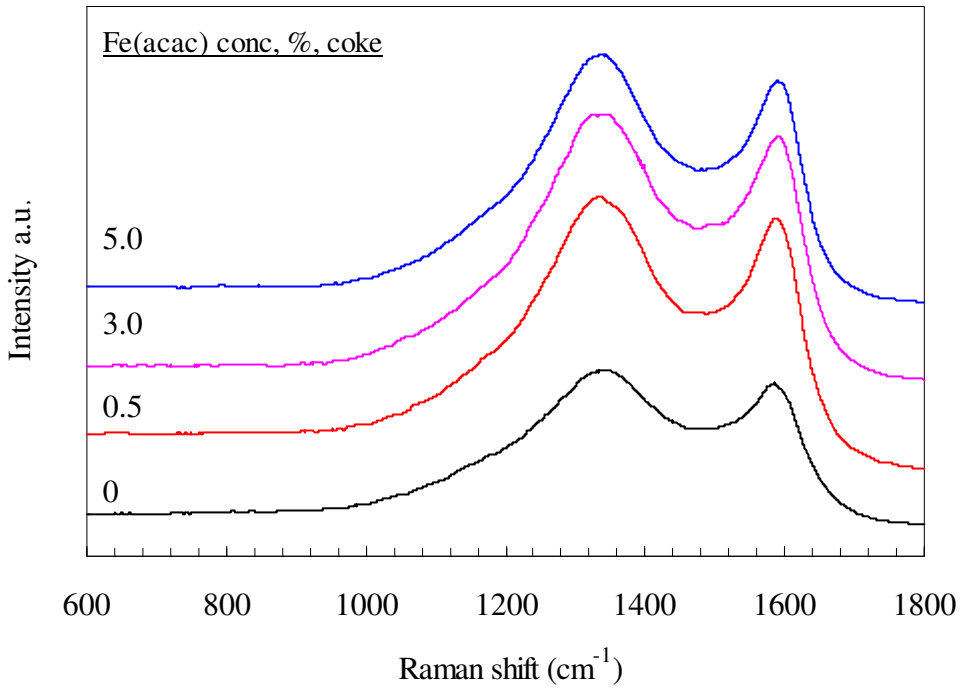

Figure 4.10(c): Raman spectra of Refcoal treated with different concentrations of iron(III)acetylacetonate and carbonised for 2 hours at 900 °C

Figures 4.10(a) and (b) show the Raman spectra of the cokes obtained by carbonisation of Refcoal for two hours at 900 ºC. The cokes show a pair of peaks at the regions around 1345 and 1580 cm^{-1}, representing the D-peak and G-peak respectively. The G-peak is associated with the graphitic structure, so the development of this peak is indicative of the improvement in the structural ordering. The D-peak is due to disordered structure in carbon. However, all the cokes (metal-containing and neat) show broad D- and G-peaks with almost equal intensities. This behaviour indicates the lattice strain on the cokes caused by the presence of metals and impurities, thus resulting in structural imperfection. Figure 4.10(c) shows the Raman spectra of Refcoal treated with different concentrations of Fe(acac). Basically, Raman spectroscopy reveals no definite effect of the additives on cokes on carbonisation.

4.4 Analysis of Graphitised Cokes

4.4.1 Scanning electron microscopy of cokes heat-treated at 1 600 °C

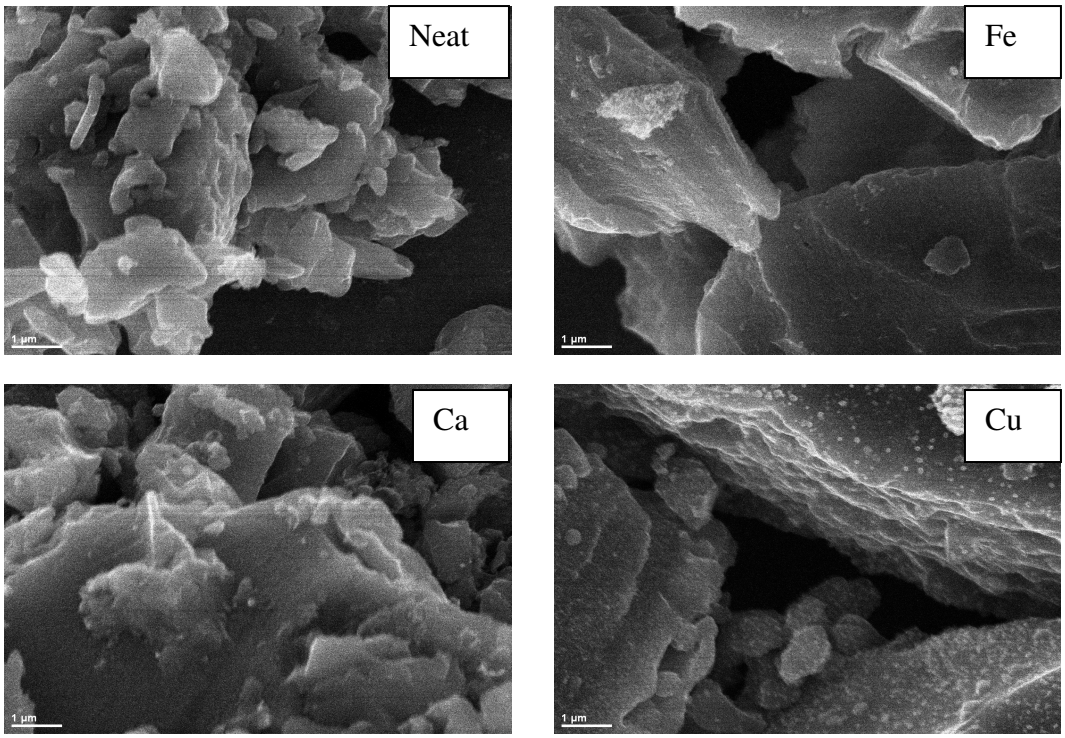

Figure 4.11(a): Scanning electron micrographs of 3% M(acac)-containing cokes heat-treated for 2 hours at 1 600 ºC

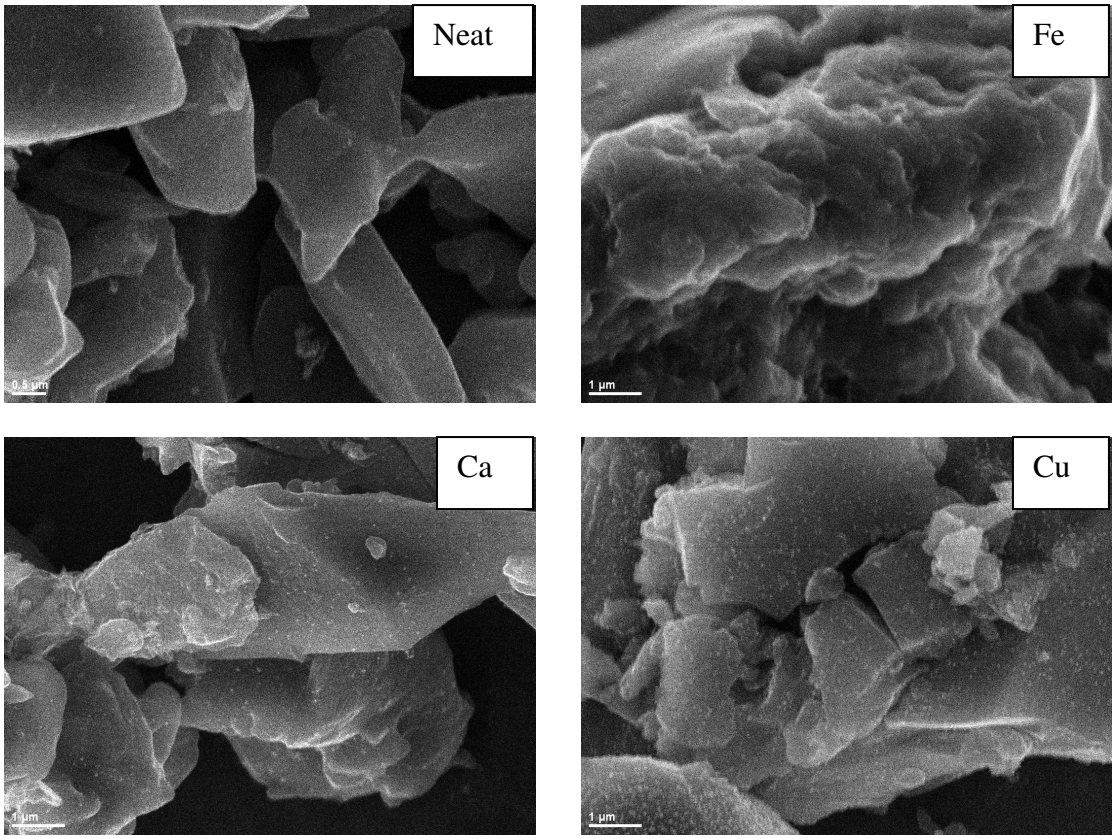

Figure 4.11(b): Scanning electron micrographs of 3% M(acac)-containing cokes heat-treated for 6 hours at 1 600 ºC

Figures 4.11(a) and (b) show the scanning electron micrographs of the cokes heat-treated at 1 600 ºC. The micrograph of the neat coke shows fine particles. The micrographs of the cokes heat-treated for two hours do in fact show smaller particles compared with those of the cokes heat-treated for six hours. This implies that the cokes treated for six hours might have undergone more structural ordering compared with those graphitised for two hours. This is a demonstration of the effect of reaction time on the structural improvement of cokes. Furthermore, it is apparent that the iron-containing cokes show differences in morphology because of the different reaction times employed. The micrograph of the iron-containing coke heat-treated for six hours shows a cloud-like appearance, which is not observable on the micrographs of the iron-containing coke heat-treated for two hours. This is assumed to be due to agglomeration as the iron reacts with carbon to form iron carbide.

The micrograph of the copper-containing cokes heat-treated for six hours does not show the bright spots that are observed in the copper-containing coke heat-treated for two hours. This is possibly due to the evaporation of copper metal as the reaction time is increased. The observations relating to the copper- and iron-containing cokes as discussed above suggest that if a short reaction time is employed, the reactions are terminated before completion. This has an effect on the structure of the resultant product. The micrograph of the calcium-containing coke is also typical of the micrographs of aluminium- and zirconium-containing cokes.

4.4.2 Optical microscopy of cokes heat-treated at 1 600 °C

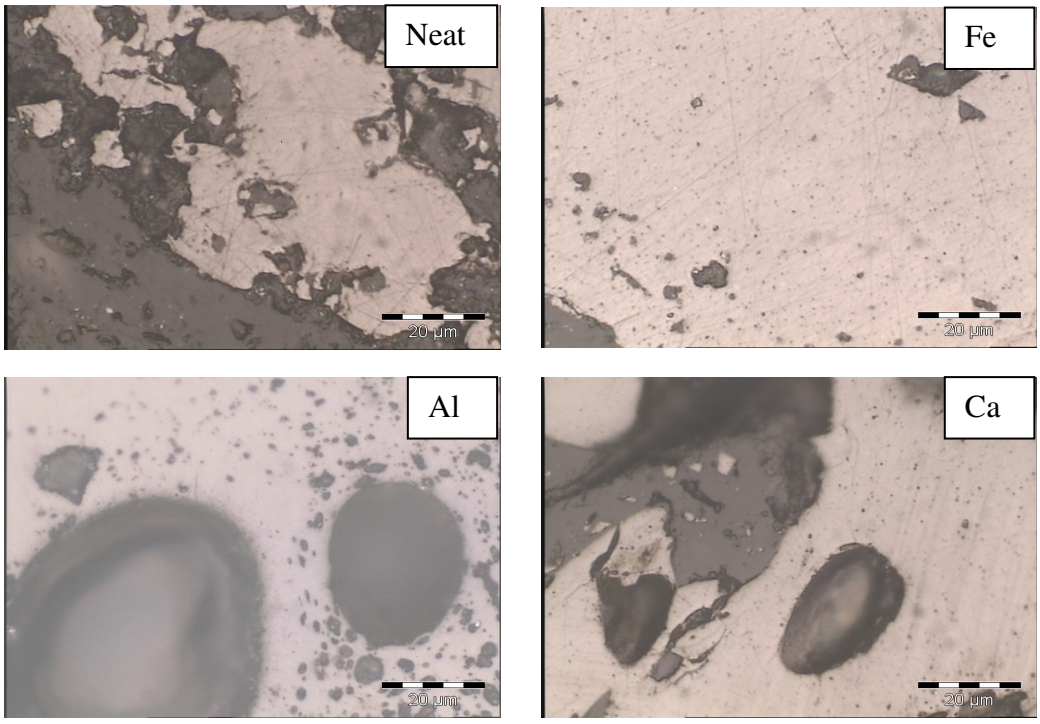

Figure 4.12(a): Optical micrographs of 3% M(acac)-containing cokes heat-treated for 2 hours at 1 600 ºC

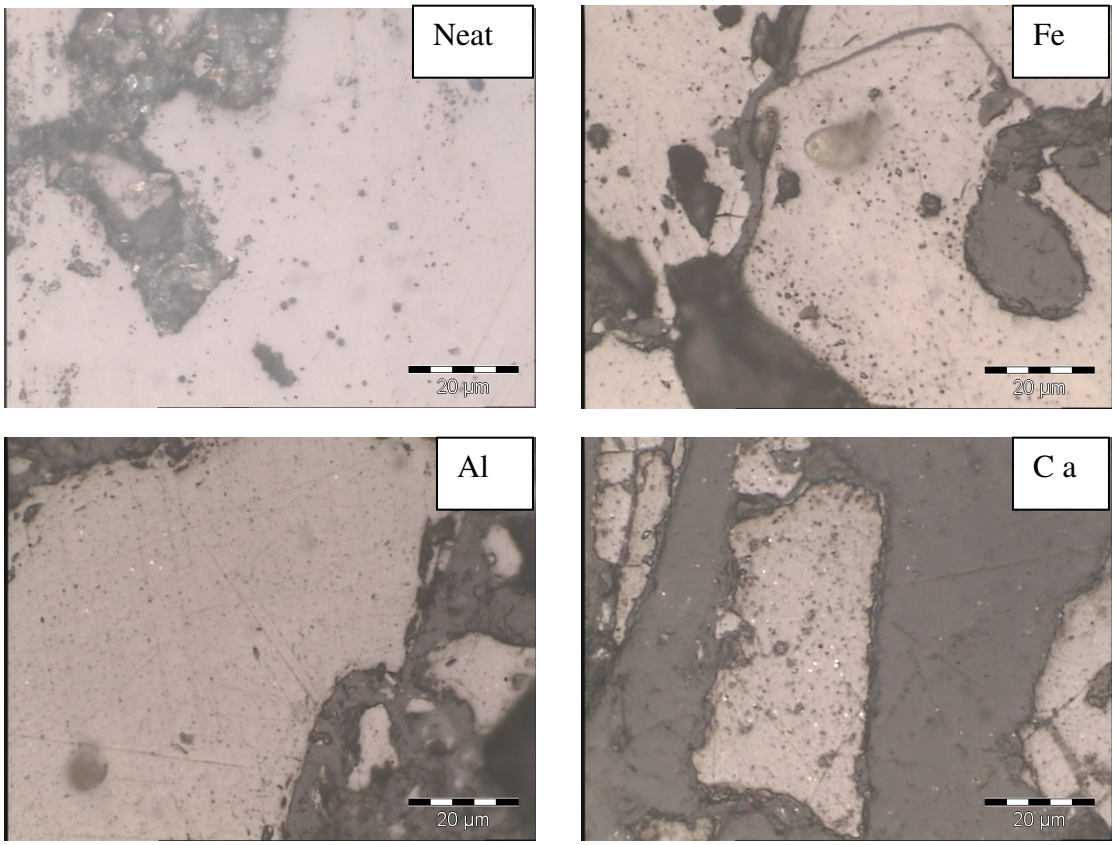

Figure 4.12(b): Optical micrographs of 3% M(acac)-containing cokes heat-treated for 6 hours at 1 600 ºC

Figures 4.12(a) and (b) show the optical micrographs of the cokes heat-treated at 1 600 ºC. Optical microscopy was used to study the changes in the optical texture of the cokes as they were heat-treated further to 1 600 °C. Since it may not be easy to observe the textural developments due to the fact that these were minor, a micrograph of synthetic graphite is given in the Appendix as a reference. The optical micrographs of the cokes heat-treated at 1 600 ºC show an improved texture compared with the cokes obtained at 900 ºC. The micrographs display the development of an anisotropic texture, even though the texture is composed of small, fine grains. The micrographs do not show the effect of catalyst composition and as a result only a few selected micrographs are given above. However, the micrographs of the copper-containing cokes showed an essentially isotropic texture. The aluminium-containing coke shows large devolatilisation pores, suggesting a considerable loss of volatiles. The micrograph of the neat coke heat-treated for six hours

has a fine to coarse anisotropic texture, and some regions are isotropic. The micrographs of the neat cokes demonstrate the effect of reaction time. However, it is noted that these developments are really minor. The micrographs of the coke heat-treated for six hours has a texture that is not observed with the neat coke heat-treated for two hours. This texture is not pronounced in the metal-containing cokes. The cokes containing iron, aluminium and calcium show a slight development of anisotropic texture. This indicates that the interaction of these metals with carbon at 1 600 ºC results in improvements in the structural ordering of cokes, but they obviously do not have a major effect.

4.4.3 X-ray diffraction of cokes heat-treated at 1 600 ºC

Table 4.7: XRD results of the graphitised cokes, listing angle 2θ, º and interlayer spacing (d_{002}), nm

Sample	Reaction conditions					
	1 600 ºC, 2 h		1 600 ºC, 6 h		2 000 ºC, 2 h	
	2θ,º	d_{002} (nm)	2θ,º	d_{002} (nm)	2θ,º	d_{002} (nm)
Neat coke	2θ,º	d_{002} (nm)	2θ,º	d_{002} (nm)	30.18	0.3437
3%Fe(acac) coke	29.99	0.3459	30.00	0.3458	30.07	0.3441
3%Al(acac) coke	29.40	0.3526	30.23	0.3482	29.99	0.3459
3%Ca(acac) coke	29.61	0.3502	29.65	0.3497	30.22	0.3433
3%Cu(acac) coke	29.99	0.3459	30.22	0.3453	29.80	0.3481
3%Zr(acac) coke	29.09	0.3563	29.62	0.3501	29.83	0.3477
3%Fe(ox) coke	29.80	0.3480	29.74	0.3480	29.60	0.3440
3%Al(ox) coke	29.87	0.3473	30.35	0.3469	29.84	0.3476
3%Ca(ox) coke	29.77	0.3484	29.60	0.3480	30.17	0.3438
3%Cu(ox) coke	29.72	0.3490	29.92	0.3467	29.60	0.3501
3%Zr(ox) coke	28.91	0.3585	29.62	0.3504	30.13	0.3443
0.5%Fe(acac) coke					30.15	0.3460
5%Fe(acac) coke					30.81	0.3369

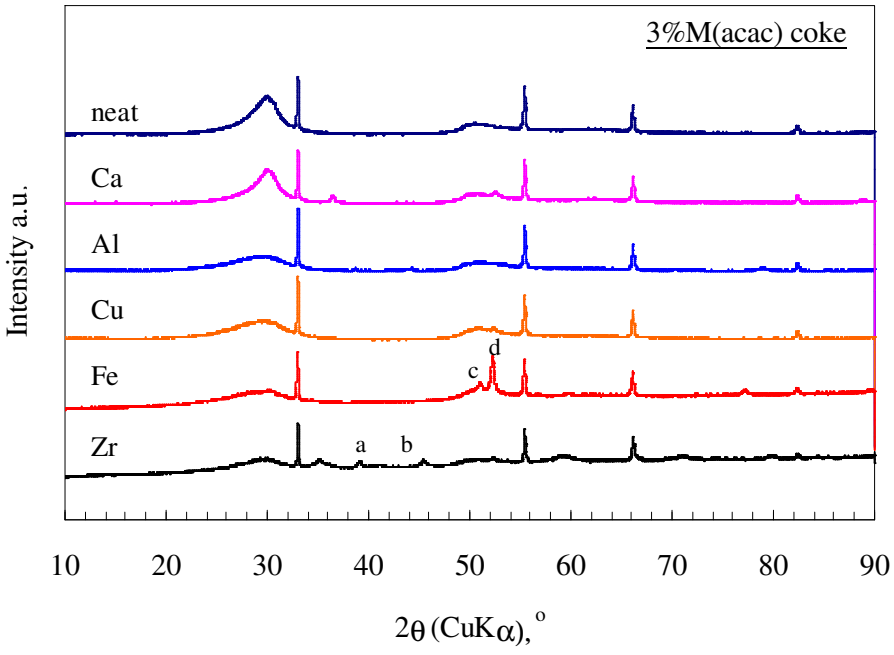

Figure 4.13(a): **X-ray diffraction patterns of 3% M(acac)-containing cokes heat-treated for 2 hours at 1 600 °C**

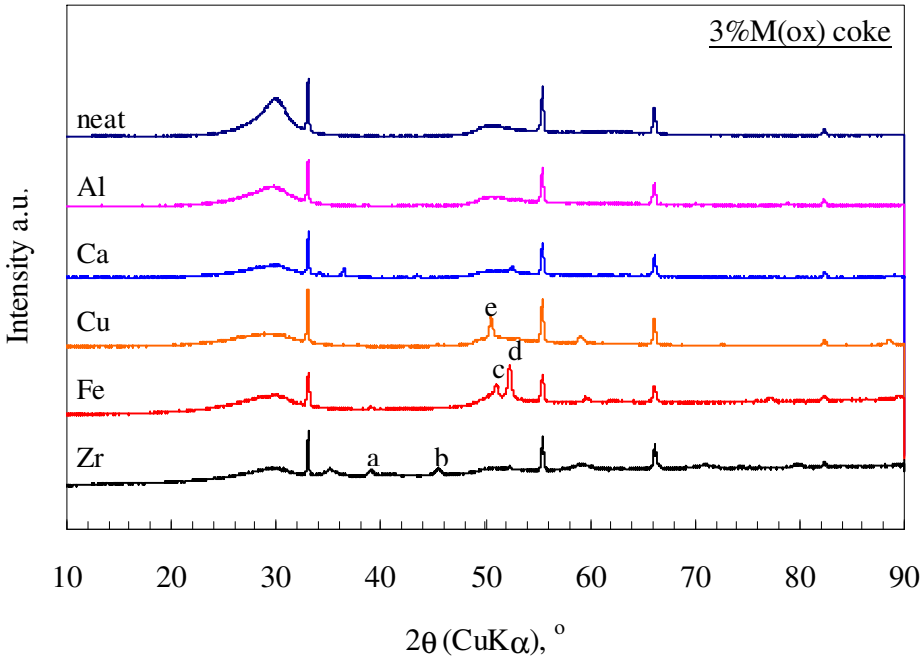

Figure 4.13(b): **X-ray diffraction patterns of 3% M(ox)-containing cokes heat-**

treated for 2 hours at 1 600 °C

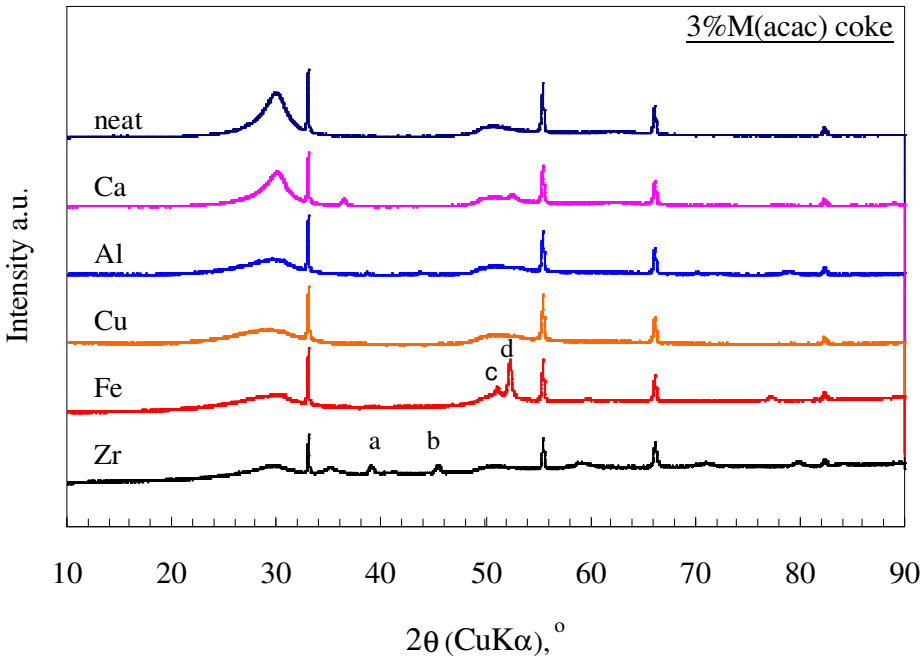

Figure 4.13(c): X-ray diffraction patterns of 3% M(acac)-containing cokes heat-treated for 6 hours at 1 600 °C

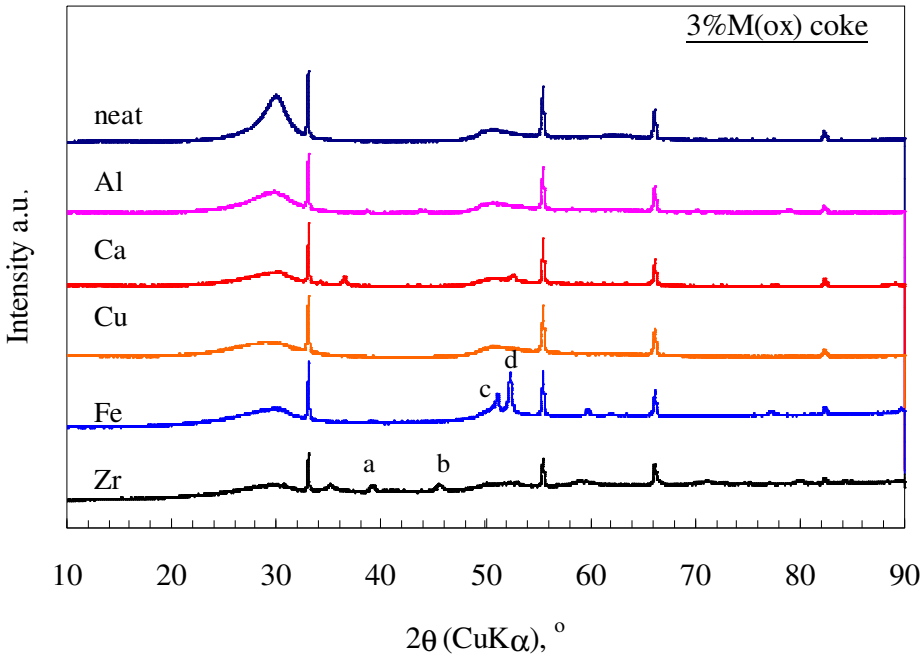

Figure 4.13(d): X-ray diffraction patterns of 3% M(ox)-containing cokes

heat-treated for 6 hours at 1 600 °C

Figures 4.13(a), (b), (c) and (d) show the X-ray diffraction patterns of the cokes heat-treated for two and six hours at 1 600 ºC. All the cokes show peaks at approximately 30º and 52º, corresponding to the (002) and (004) graphite planes. Generally, it is expected that the (002) peak will have a high intensity as the crystallinity increases in the structure. All the cokes show a broad (002) peak, indicating imperfect structures due to a low heat treatment temperature and impurities contained in the samples. However, in all the graphs the neat coke shows an improved (002) peak compared with those of the metal-containing samples. This means that at this stage the presence of metals leads to structural imperfection. However, the calcium-containing coke shown in Figures 4.13(a) and (c) shows an improved (002) peak, implying a pronounced calcium catalytic ability compared with the other metals.

The peaks labelled (a) and (b) in all the graphs represent ZrO_2, and those labelled (c) and (d) represent Fe_3C and Fe respectively. The phases observed in the iron-containing cokes demonstrate the metal carbide formation-decomposition mechanism. The metal carbide is expected to decompose to form graphite and metal crystals. Figure 4.13(b) also shows a peak labelled (e), which corresponds to metal copper. This peak confirms that there is no reaction between copper and the carbon network structure as shown in the SEM results. This means that copper has no positive impact on cokes, but leads to a disordered carbon structure. This peak is, however, not observed when the copper-containing coke is heat-treated at 1 600 ºC for six hours, presumably due to the loss of copper metal on prolonged heating as the SEM results suggested. These observations are confirmed by the results in Table 4.7. All the copper-containing cokes have the largest d_{002} values, implying that copper had the poorest catalytic ability towards graphitisation of Refcoal cokes.

The calcium(II)acetylacetonate-containing cokes have the smallest interlayer spacing (d_{002}) values, whereas the other metal-containing cokes have larger d_{002} values. This indicates a better performance of calcium in catalysing the graphitisation of Refcoal

cokes compared with other metals. The d_{002} value of the calcium(II)acetylacetonate-containing coke and the d_{002} value of the neat coke heat-treated at 1 600 ºC for two hours are equal, whereas the calcium(II)acetylacetonate-containing coke has the smallest d_{002} value compared with the neat coke value when heat-treated for six hours at 1 600 ºC. This shows the effect of reaction time on the catalytic graphitisation of Refcoal cokes. This means that the reaction is terminated before completion when the cokes are heat-treated for only two hours. It is also notable that all the metal-containing cokes, except the aluminium-containing coke, had small d_{002} values when the metals were coordinated to the acetylacetone ligand than when they were coordinated to the hydroxyquinoline ligand. This behaviour clearly demonstrates the effect of catalyst composition. It is assumed that the pronounced stability of the hydroxyquinolinate complexes retards the action of metals in the graphitisation of cokes.

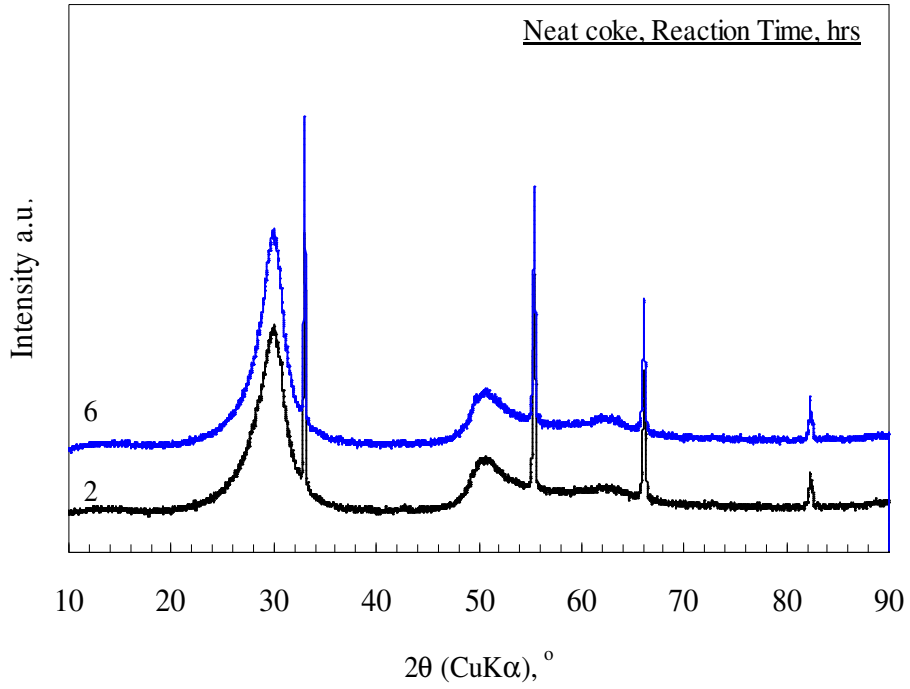

Figure 4.13(e): X-ray diffraction patterns of cokes graphitised for 2 and 6 hours at 1 600 °C

Figure 4.13(e) shows the X-ray diffraction patterns of the neat cokes that were graphitised at 1 600 ºC for two and six hours. The coke graphitised for six hours shows a sharp (002) peak with high intensity, compared with the coke graphitised for only two hours. This demonstrates that the reaction time has an effect on the degree of graphitisation of Refcoal cokes. The longer the reaction time, the better the degree of graphitisation.

4.4.4 Raman spectroscopy of heat-treated cokes at 1 600 °C

Table 4.8: Intensity ratio, R, of D-peak to G-peak for graphitised cokes

Sample	Reaction conditions		
	1 600 ºC, 2 h	**1 600 ºC, 6 h**	**2 000 ºC, 2 h**
	I_D/I_G (R)	**I_D/I_G (R)**	**I_D/I_G (R)**
Neat coke	1.34	1.14	0.67
3%Fe(acac) coke	1.57	1.03	0.98
3%Al(acac) coke	1.39	1.36	1.12
3%Ca(acac) coke	1.28	0.85	0.50
3%Cu(acac) coke	1.60	1.33	1.11
3%Zr(acac) coke	1.50	1.37	1.21
3%Fe(ox) coke	1.32	1.19	1.11
3%Al(ox) coke	1.12	1.30	0.85
3%Ca(ox) coke	1.28	1.24	1.06
3%Cu(ox) coke	1.37	1.26	1.19
3%Zr(ox) coke	1.38	1.35	1.25

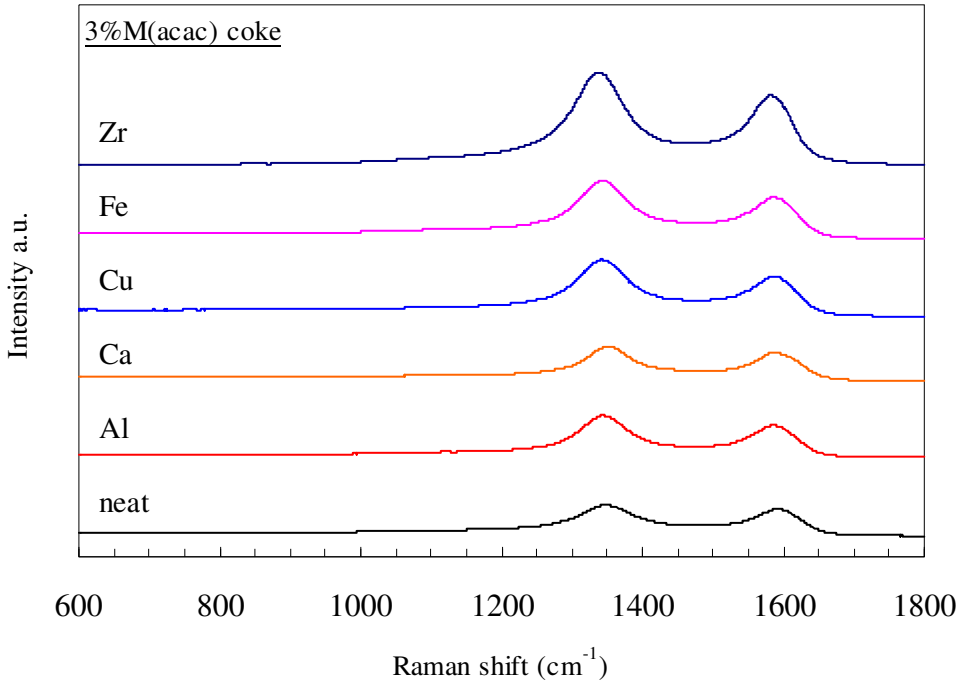

Figure 4.14(a): Raman spectra of cokes heat-treated for 2 hours at 1 600 °C

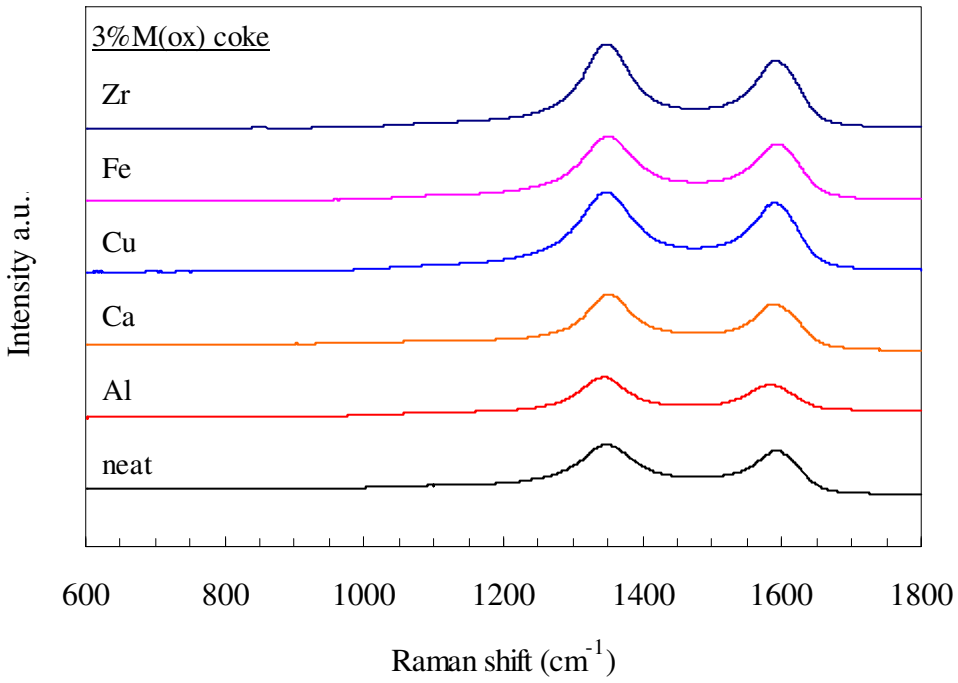

Figure 4.14(b): Raman spectra of cokes heat-treated for 2 hours at 1 600 °C

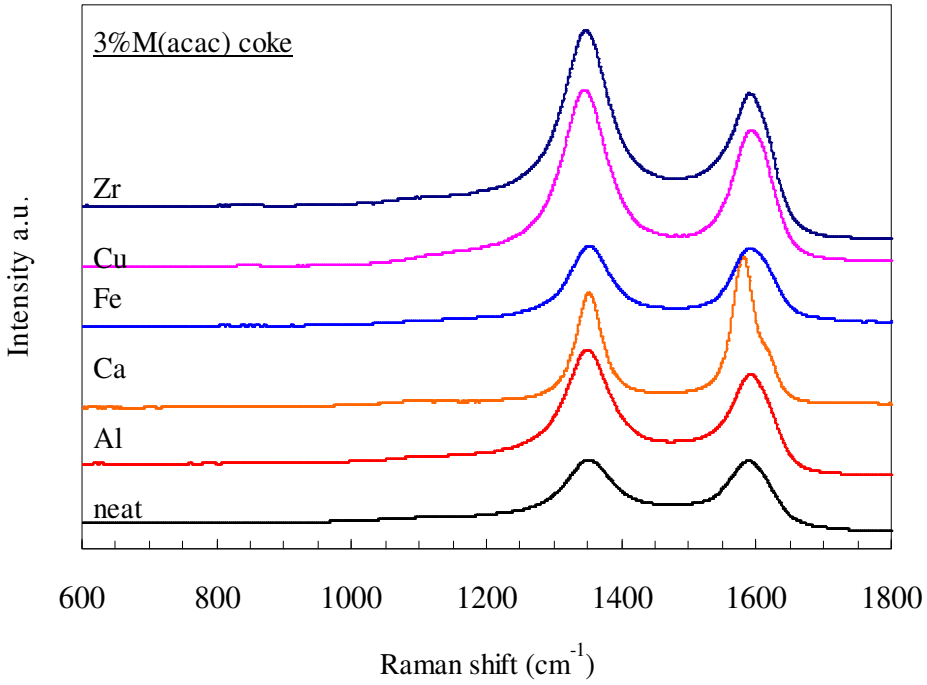

Figure 4.14(c): Raman spectra of cokes heat-treated for 6 hours at 1 600 °C

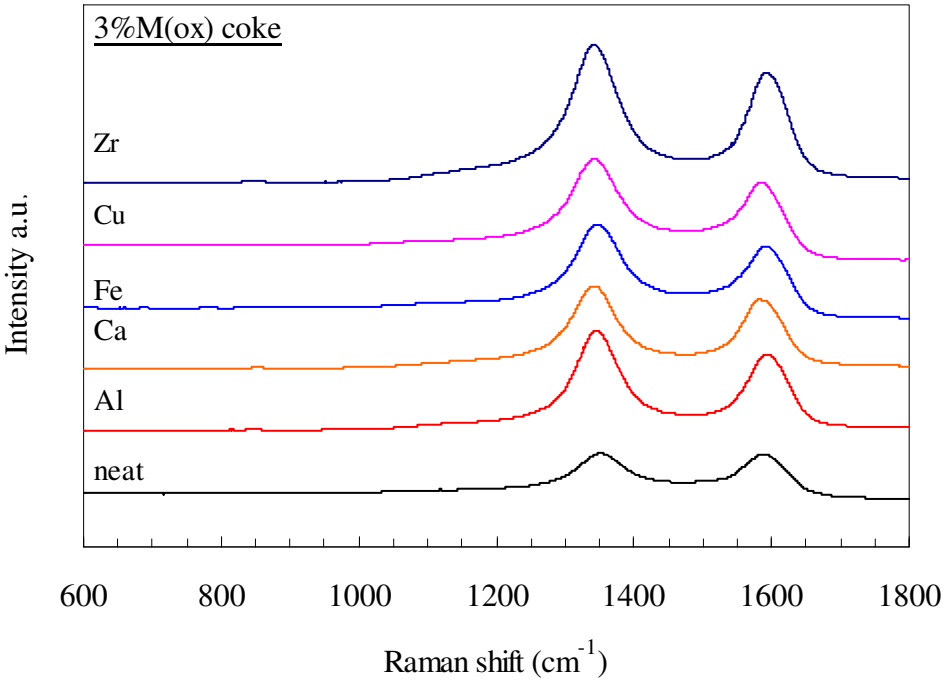

Figure 4.14(d): Raman spectra of cokes heat-treated for 6 hours at 1 600 °C

Figures 4.14(a), (b), (c) and (d) show the Raman spectra of cokes heat-treated for two and six hours at 1 600 ºC. They reflect the disorder-induced peak (D-peak) and the graphitic structure-induced peak (G-peak) centred around 1 345 and 1 580 cm^{-1} respectively. Both bands are due to the stretching of the sp^2 hybridised C-C bond. The intensities of the D- and G-peaks are almost equal, indicating that the cokes have both a disordered structure and a graphitic structure within. The metal-containing cokes show no evidence of catalytic action as the structure of the cokes remains disordered. The copper-containing and zirconium-containing cokes show a D-peak with a higher intensity than that of the G-peak. This intense structural disordering can be related to the X-ray diffraction of the cokes containing these two metals, as discussed in the previous section. It is also notable that the calcium(II)acetylacetonate-containing coke heat-treated at 1 600 ^{o}C for six hours has a G-peak with a higher intensity than that of the D-peak. This confirms the results obtained with X-ray diffraction, namely that calcium(II)acetylacetonate has a better catalytic ability towards graphitisation of Refcoal cokes than the other metal complexes in this study.

Table 4.8 lists the relative intensities of the D-band and G-band ($R=I_D/I_G$). The R-value is determined by crystal size: the smallest R-value indicates a graphitic structure, while a high R-value indicates a disordered structure. These results suggest that metals are not good catalysts for the graphitisation of Refcoal cokes. These observations also suggest finite crystal sizes and lattice strains in the coke structures. An exception is observed with the calcium(II)acetylacetonate-containing coke since this coke gives an R-value which is lower than that of the neat coke. All the cokes show improved structural ordering as the treatment temperature and reaction time are increased.

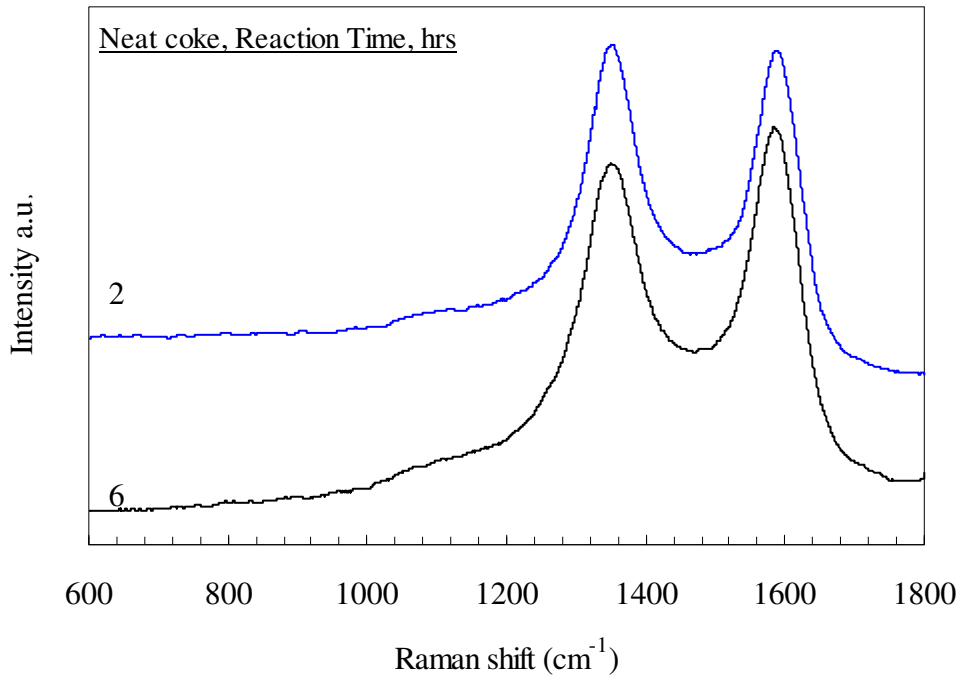

Figure 4.14 (e): Raman spectra of cokes graphitised for 2 and 6 hours at 1 600 ºC

Figure 4.14(e) shows the Raman spectra of the neat cokes graphitised for two and six hours at 1 600 ºC. This graph shows the effect of reaction time on the graphitisation of Refcoal cokes. The G-peak of the neat coke graphitised for six hours has a higher intensity than that of the D-peak, implying structural improvements after prolonged reaction time.

4.4.5 Scanning electron microscopy of cokes graphitised at 2 000 ºC

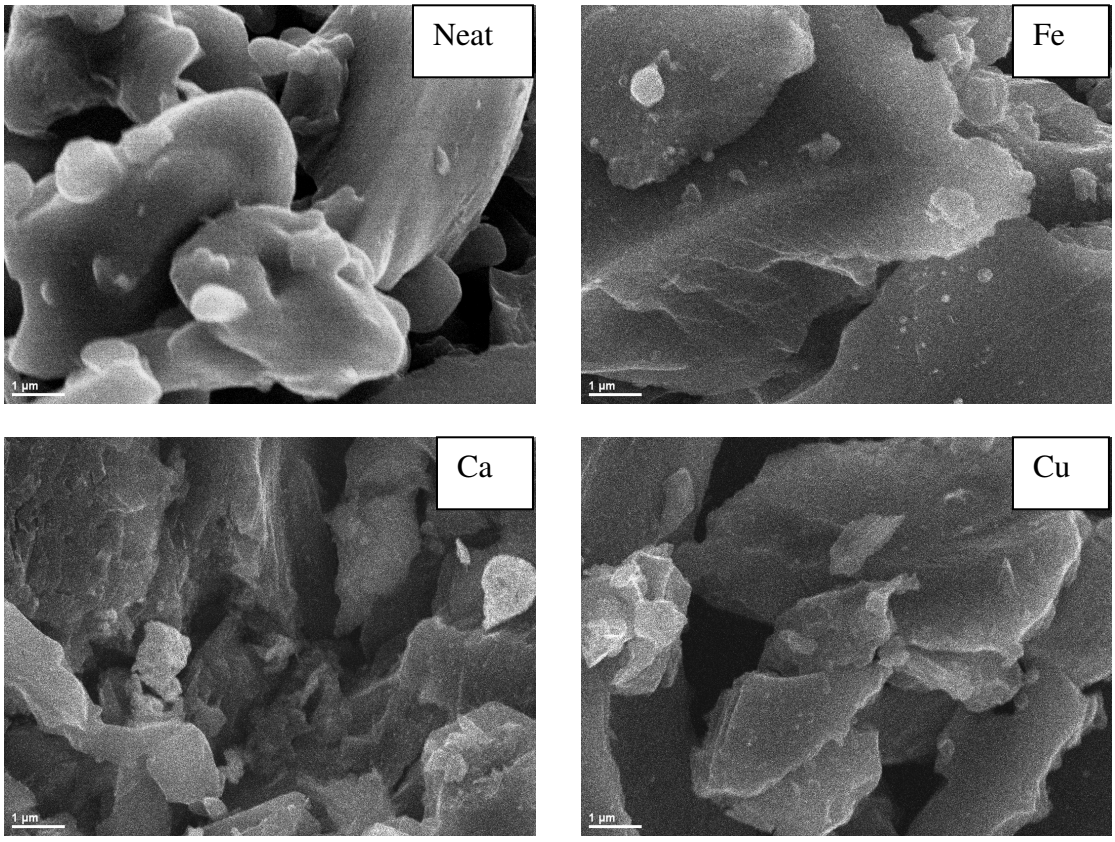

Figure 4.15(a): Scanning electron micrographs of 3% M(acac)-containing cokes graphitised for 2 hours at 2 000 ºC

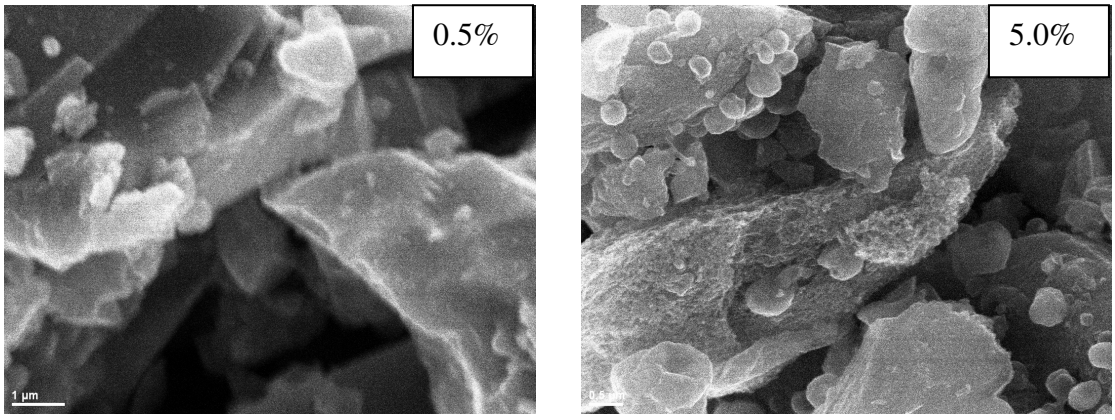

Figure 4.15(b): Scanning electron micrographs of cokes with different concentrations of Fe(acac), graphitised for 2 hours at 2 000 ºC

Figure 4.15 (a) shows the scanning electron micrographs of cokes graphitised at 2 000 ºC. The micrographs depict large grains with smooth regions, which show an improved ordering in the cokes. This is due to the improvement in the atomic rearrangement in the carbon layer planes. These large particles are not observable in the cokes heat-treated at 1 600 ºC. However, the neat coke shows large particles with smooth surfaces compared with those of the treated cokes. The micrograph of the calcium(II)acetylacetonate-containing coke shows a textured surface. Scanning electron microscopy shows no obvious effect of the catalyst composition on the morphology of the cokes graphitised at 2 000 ºC.

Figure 4.15(b) shows the micrographs of cokes with different concentrations of iron(III)acetylacetonate and graphitised at 2 000 °C. As the concentration of iron increases, the surface of the cokes becomes rougher and more textured. The micrograph of the coke containing 5% iron(III)acetylacetonate shows two different regions: there are smooth surfaces on the sides, whereas in between there is a coarsely textured region. The region with a texture is assumed to represent the graphitic structure of the coke, whereas the smooth surfaces with small grains represent a less-ordered carbon structure. This complements the X-ray diffraction pattern of this coke in that there is a well-ordered carbon structure and a less-ordered carbon structure within this coke, as is discussed in Chapter 5. This micrograph portrays a localised graphitisation in the material due to the lack of iron in some regions of the coke.

4.4.6 Optical microscopy of cokes graphitised at 2 000 °C

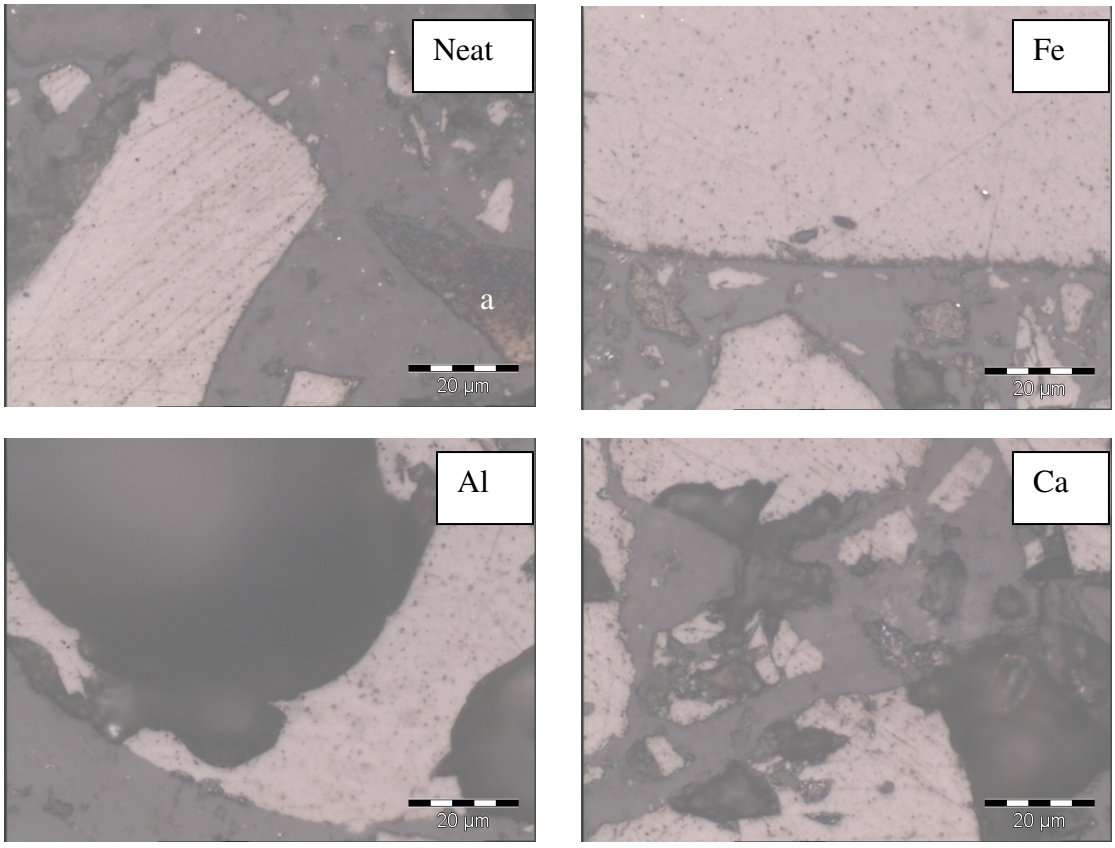

Figure 4.16(a): Optical micrographs of 3% M(acac)-containing cokes graphitised for 2 hours at 2 000 ºC

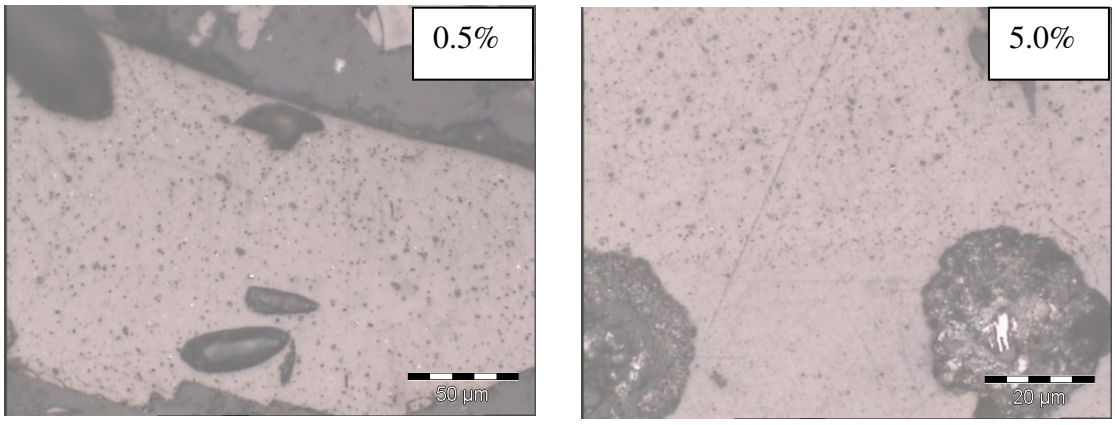

Figure 4.16(b): Optical micrographs of cokes with different concentrations of Fe(acac), graphitised for 2 hours at 2 000 ºC

Figure 4.16(a) shows the micrographs of the cokes graphitised at 2 000 ºC. These show an improved optical texture of the cokes compared with the texture of those heat-treated at 1 600 ºC. To enable description, a micrograph of synthetic graphite is given in the Appendix. The micrographs show that some regions contain large granular anisotropic grains, whereas other regions have a fine anisotropic texture. The micrograph of the neat coke shows a large region with large granular anisotropic grains. This region is labelled (a) in the micrograph. The micrograph of the calcium-containing coke shows many scattered anisotropic grains. This texture is not pronounced in the other metal-containing cokes. This implies that calcium indeed catalyses the graphitisation of Refcoal cokes. The micrographs of the aluminium-containing cokes show thin-walled structures due to large devolatilisation pores. The micrographs of the copper- and zirconium-containing cokes were found to have few anisotropic grains, with large parts of the micrograph showing the retention of fine anisotropic grains. Devolatilisation pores are also observed with the calcium- and zirconium-containing cokes.

Figure 4.16(c) shows the micrographs of cokes with different concentrations of iron(III)acetylacetonate and graphitised at 2 000 °C. These show an improvement in the structural texture as the concentration of iron increases. The anisotropic grains also become larger as the concentration of iron increases. The micrograph of the coke containing a 5% concentration of iron contains some regions with fine anisotropic texture and other regions with coarse anisotropic grains. This observation confirms that iron promotes the localised graphitisation of Refcoal cokes.

4.4.7 X-ray diffraction of cokes graphitised at 2 000 °C

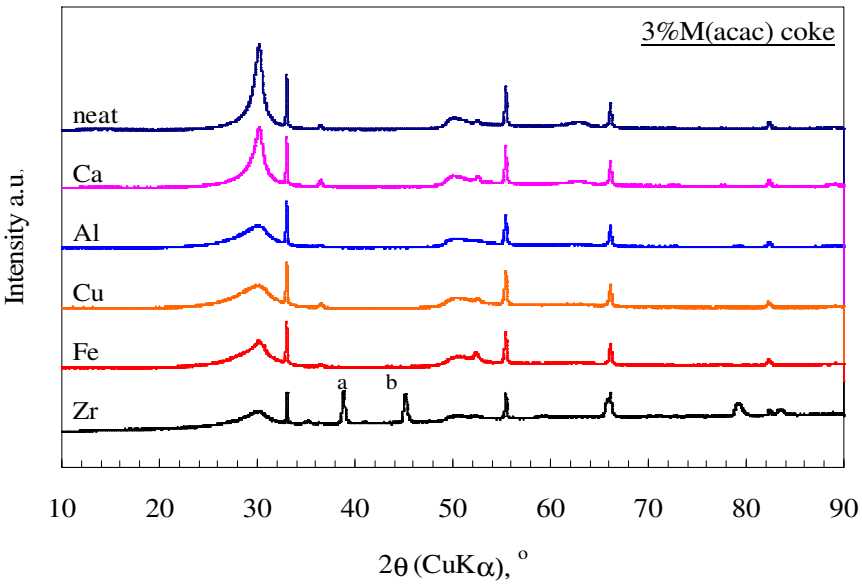

Figure 4.17(a): X-ray diffraction patterns of 3%M(acac)-containing cokes graphitised for 2 hours at 2 000°C

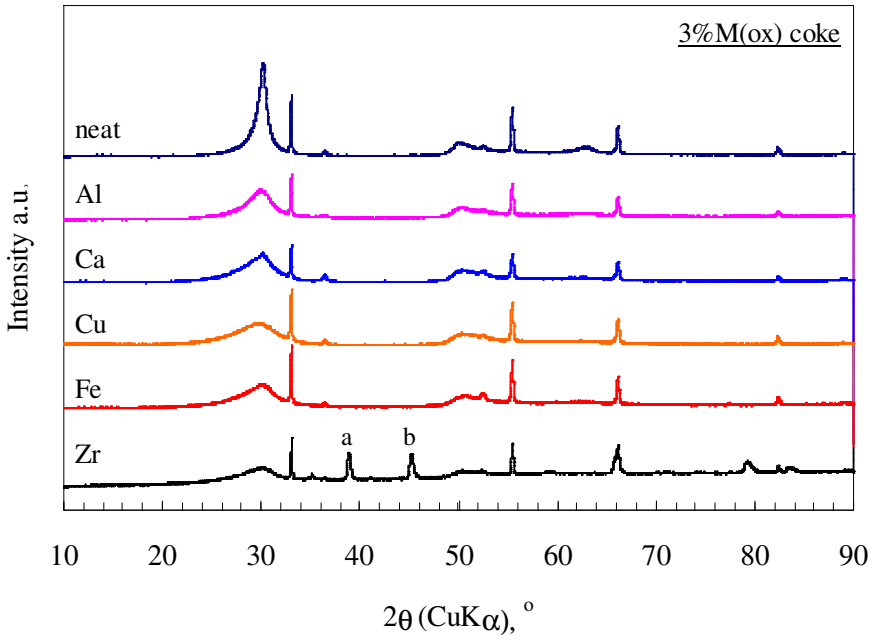

Figure 4.17(b): X-ray diffraction patterns of 3%M(ox)-containing cokes graphitised for 2 hours at 2 000 °C

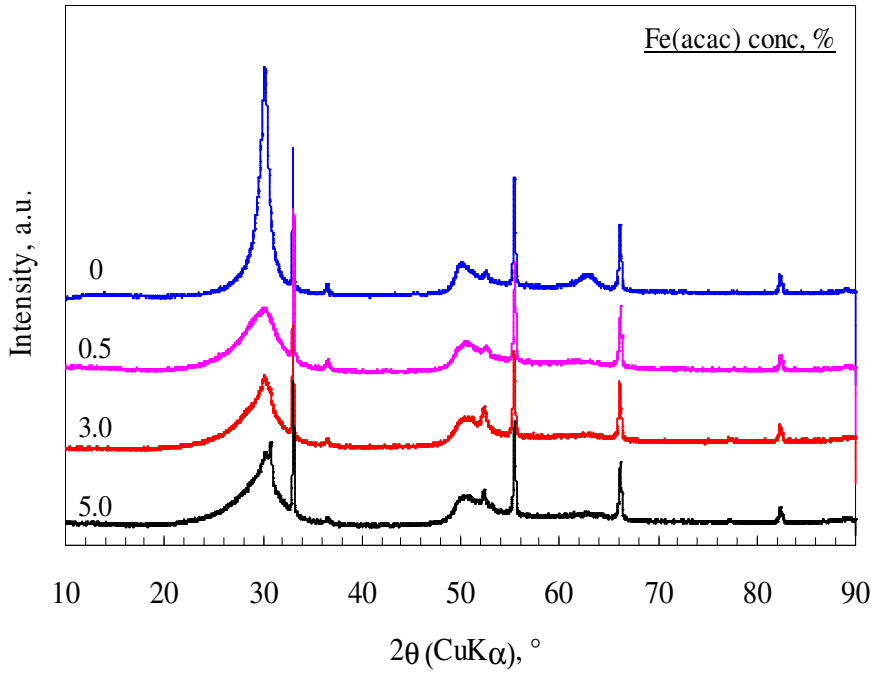

Figure 4.17(c): X-ray diffraction patterns of cokes treated with different concentrations of iron(III)acetylacetonate and graphitised for 2 hours at 2 000 ºC

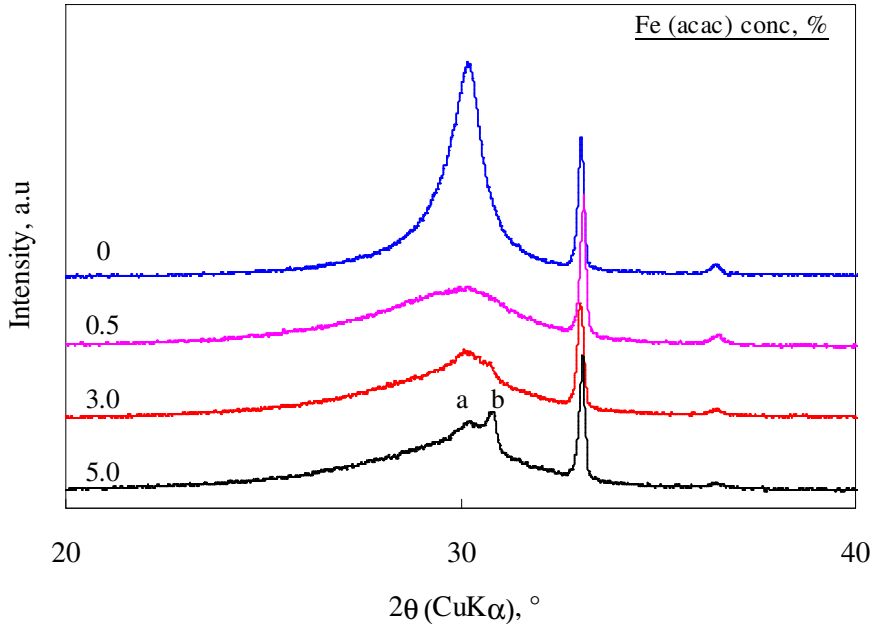

Figure 4.17(d): X-ray diffraction patterns of cokes treated with different concentrations of iron(III)acetylacetonate and graphitised for 2 hours at 2 000 ºC

Figures 4.17(a) and (b) show the X-ray diffraction patterns of the cokes graphitised for two hours at 2 000 ºC. All the cokes show peaks at approximately 30º and 52º, corresponding to the (002) and (004) graphite planes. Figure 4.17(a) suggests a catalytic action induced by calcium on the graphitisation of Refcoal cokes, whereas the other metals show poor catalytic ability. The neat coke shows a sharp (002) peak compared with the metal-containing cokes, except for the calcium(II)acetylacetonate-containing coke, indicating distortion of the structural lattice in the treated cokes. However, the iron-containing coke shows development of a shoulder on the (002) peak. This indicates the structural ordering attained through the catalytic effect of iron (Wang *et al*., 1995).

The development of a shoulder in the iron-containing coke suggests a localised and limited catalytic action of iron, leaving most portions of the structure disordered. Except in the zirconium-containing cokes, there is no evidence of the presence of metal in the cokes graphitised at 2 000 ºC. The peaks labelled (a) and (b) match zirconia (ZrO_2) in the graphitised cokes. The d_{002} values for the cokes graphitised at 2 000 ºC are given in Table 4.7. These results indicate that these cokes have a turbostratic structure since they have d_{002} values greater than 0.34 nm. (Turbostratic means that the carbon planes are only roughly parallel to each other.) The calcium(II)acetylacetonate-containing coke has the smallest d_{002} value of all the samples, including the neat coke. This shows a positive catalytic ability of calcium towards the graphitisation of Refcoal cokes. Since there is no evidence of calcium carbide formation, it is reasonable to conclude that in all the graphitisation runs calcium catalysed the graphitisation of Refcoal cokes through the dissolution-precipitation mechanism of catalytic graphitisation. The copper-containing cokes have the highest d_{002} value, indicating that copper has the poorest catalytic ability compared with the other metals. It is notable that the interlayer spacing value decreases with an increase in the heat treatment temperature and reaction time; this means that there is an improvement in the structural ordering with an increase in these two factors.

Figure 4.17(c) shows the X-ray diffraction patterns of the cokes with different concentrations of iron and graphitised for two hours at 2 000 ºC. All the samples show

peaks at approximately 30º and 52º, corresponding to the (002) and (004) graphite planes. The neat coke shows a sharp (002) peak compared with the heat-treated samples. However, as the concentration of iron increases, the (002) peak gradually shifts to high 2θ values. The development of a shoulder in the (002) peak of the coke containing 3% iron is noticed and the shoulder results in two peaks in the coke containing 5% iron. Figure 4.17(d) shows a short-scale graph of Figure 4.17(c), thus giving a clear view of the shoulder development and the ultimate formation of a small sharp peak. The broad peak, labelled (a), is attributed to the disordered carbon in the coke, whereas the sharp peak, labelled (b), represents the graphitic structure that is formed through the catalytic action of iron on graphitisation of coke (Wang *et al.*, 1995).

The short intensity of the sharp peak labelled (b) implies a localised catalytic action of iron. It is then assumed that the largest part of the coke is disordered, with only a small portion being graphitic. As shown in the X-ray diffraction patterns of the cokes graphitised at 1 600 ºC, iron reacts with carbon to form iron carbide (Fe_3C). It can therefore be concluded that the iron carbide decomposes to graphite and metal crystals when heated up to 2 000 ºC. Since there is no evidence of iron or iron compounds in the iron-containing cokes graphitised at 2 000 ºC, it is more likely that the iron dissolves in the carbon and becomes dispersed, making it difficult to detect it. From this observation it is reasonable to conclude that the increase in the concentration of iron leads to a pronounced catalytic action of iron towards the graphitisation of Refcoal cokes. The d_{002} values in Table 4.7 show that 5%Fe(acac) coke has the smallest interlayer spacing, which confirms that iron catalyses the graphitisation of Refcoal cokes when it is present in sufficient concentrations.

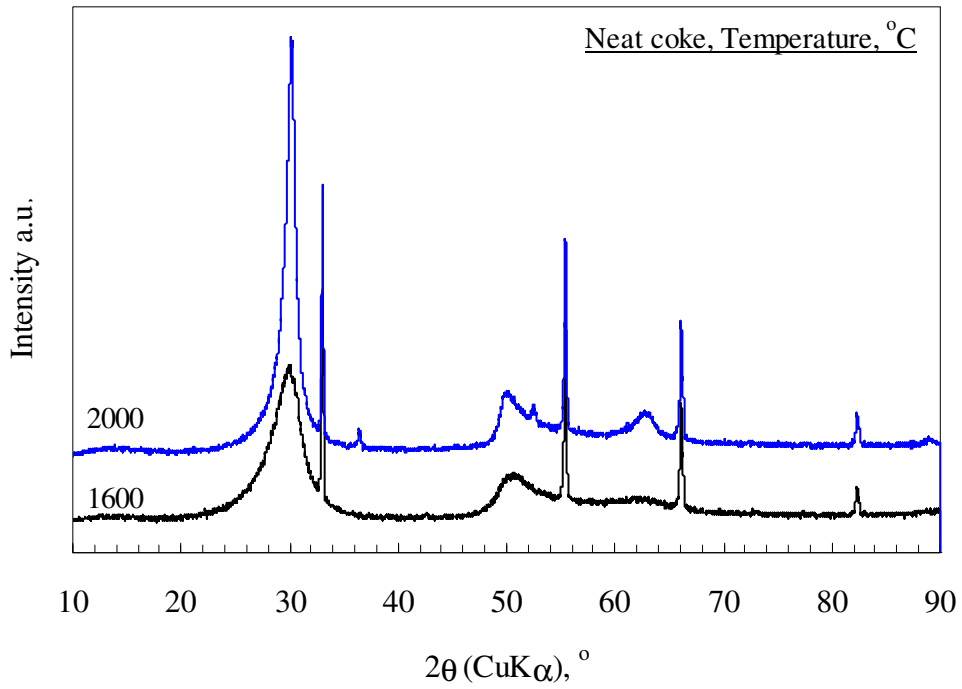

Figure 4.17(e): X-ray diffraction patterns of cokes graphitised for 2 hours at 1 600 and 2 000 °C

Figure 4.17(e) shows the X-ray diffraction patterns of the neat coke graphitised for two hours at 1 600 and 2 000 ºC. This coke has a sharp (002) peak with high intensity compared with the coke graphitised at 1 600 ºC. This also demonstrates the effect of the heat treatment temperature on the graphitisation of Refcoal cokes. Based on the above two graphs, it can be concluded that heat treatment temperature is a more important parameter than reaction time for the graphitisation of Refcoal cokes.

4.4.8 Raman spectroscopy of cokes graphitised for 2 hours at 2 000 °C

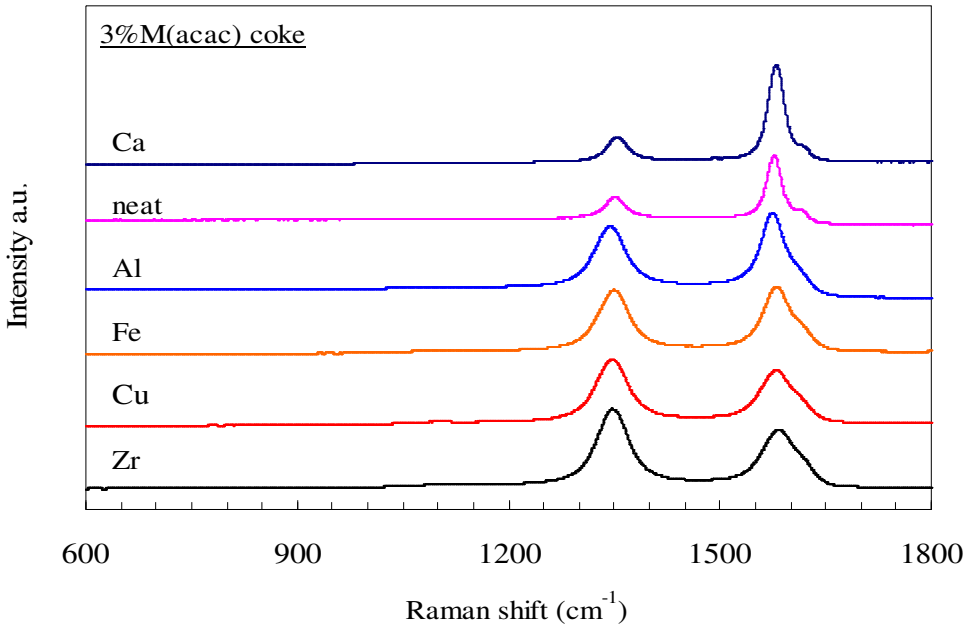

Figure 4.18(a): Raman spectra of 3%M(acac)-containing cokes graphitised for 2 hours at 2 000 °C

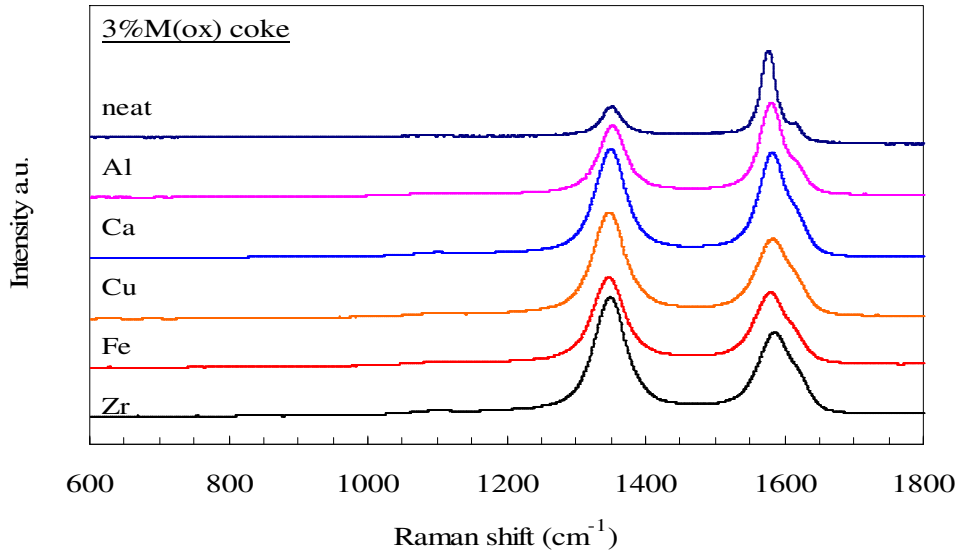

Figure 4.18(b): Raman spectra of 3%M(ox)-containing cokes graphitised for 2 hours at 2 000 °C

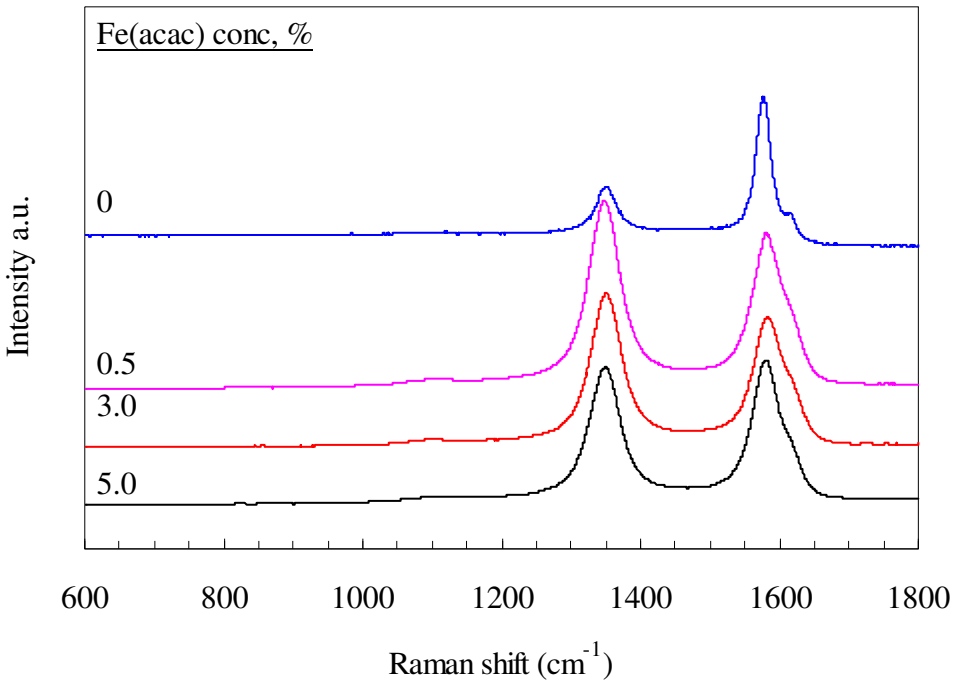

Figure 4.18(c). Raman spectra of cokes treated with different concentrations of iron(III)acetylacetonate and graphitised for 2 hours at 2 000 ºC

Figures 4.18(a) and (b) show the Raman spectra of the cokes graphitised for two hours at 2 000 ºC. These cokes show the D-peak and G-peak in the regions around 1 350 and 1 580 cm^{-1}. The peaks are intense and sharp compared with those obtained when the cokes are graphitised at 1 600 ºC. However, there is no doubt that the cokes still contain a considerable region with disordered structure. The calcium(II)acetylacetonate-containing coke shows a more pronounced G-peak compared with all the other cokes. This confirms the catalytic action of calcium(II)acetylacetonate towards the graphitisation of Refcoal cokes. As a result, this coke has a larger degree of graphitisation compared with the neat coke. These observations are confirmed by the R-values given in Table 4.8. The calcium(II)acetylacetonate-containing coke has the smallest R-value, whereas the copper-containing cokes have the largest R-values. These results complement the scanning electron microscopy and X-ray diffraction results.

Figure 4.18(c) shows the Raman spectra of the cokes containing various concentrations of iron. The effect of iron concentration is clear. There is a slight increase in the intensity of the G-band as the concentration of iron increases. However, the D-band competes strongly with the G-band, indicating that large portions of the graphitised cokes are disordered, as observed with the X-ray diffraction results.

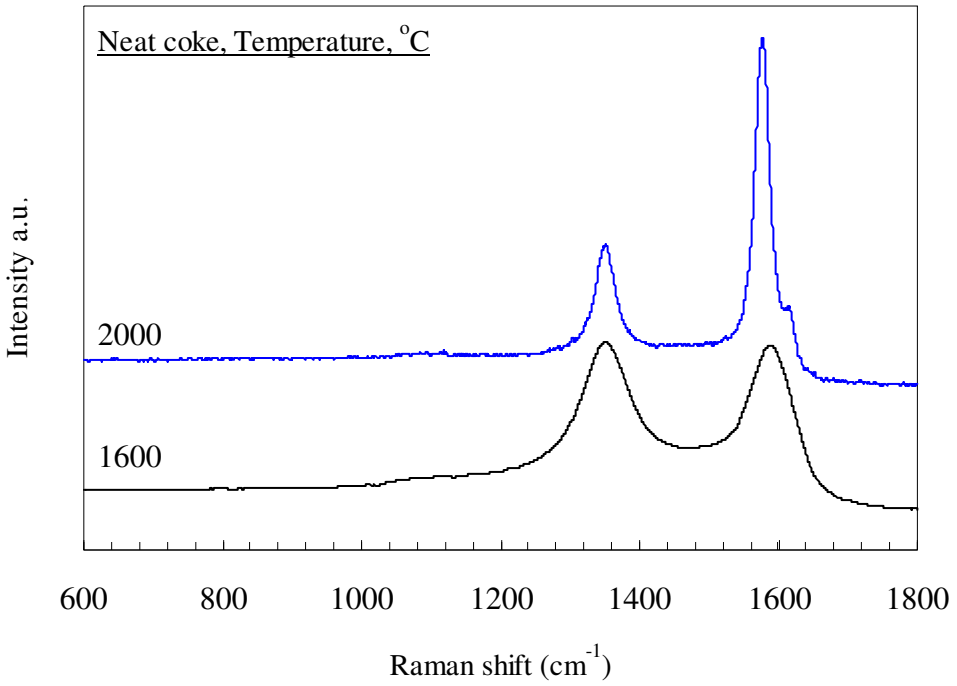

Figure 4.18(d): Raman spectra of cokes graphitised for 2 hours at 1 600 and 2 000 °C

Figure 4.18(d) shows the Raman spectra of the neat cokes graphitised for two hours at 1 600 and 2 000 ºC. The G-peak of the coke graphitised at 2 000 ºC has a very high intensity compared with that of the coke graphitised at 1 600 ºC. This means that the coke graphitised at 2 000 ºC has a much-improved structural organisation compared with the coke graphitised at 1 600 ºC. The coke graphitised at 2 000 ºC shows a more pronounced crystallinity, indicating that heat treatment temperature is an important factor in the graphitisation of Refcoal cokes, as expected.

CHAPTER 5: CONCLUSIONS

Graphitisation is the solid-state transformation of the disordered carbon atoms into a well-ordered hexagonal graphite structure, requiring temperatures as high as 2 600 ºC. Since this process involves major energy consumption, cost-effective methods of producing graphite are required and catalytic graphitisation is one of the methods that holds promise for this purpose. Catalytic graphitisation using metals or metal compounds promotes the ordering of carbon atoms within the carbon matrix towards the hexagonal at lower temperatures. The extent of catalytic graphitisation achieved is dependent on the structural ordering of the parent coke, the catalyst composition and the reaction conditions.

Solvent-refined coal-derivatives known as Refcoal cokes were investigated as potential precursors of graphite. Refcoal is a refined carbon precursor obtained by extracting coal using a combination of dimethylformamide (DMF) and sodium hydroxide. Previous work proved that the cokes derived from Tshikondeni coal are graphitisable (Kgobane, 2005). The main purpose of this study was to catalyse the graphitisation of such cokes extracted at 95 °C. Acetylacetonate and hydroxyquinolinate complexes of Fe, Al, Ca, Cu and Zr were investigated for their ability to catalyse the graphitisation of these cokes.

Metal complexes were dispersed in Refcoal solution such that the final cokes would contain 3 wt % of metal. Metal-containing cokes and neat coke were graphitised for two and six hours at 1 600 °C, and for two hours at 2 000°C under a nitrogen atmosphere. To study the effect of catalyst concentration on the catalytic graphitisation of Refcoal cokes, iron(III)acetylacetonate was dispersed in Refcoal to yield loadings of 0.5, 3 and 5 wt % Fe on the cokes. These cokes were then graphitised for two hours at 2 000°C under nitrogen.

The results show that the neat coke heat-treated at 1 600 °C has a much better structural ordering than the metal-containing cokes, except for the coke containing calcium(II)acetylacetonate. This means that most of the metals tested did not catalyse the

graphitisation of Refcoal cokes at 1 600 °C. Calcium(II)acetylacetonate appears to be effective at this stage, whereas calcium(II)hydroxyquinolinate does not display a similar ability. Moreover, except for aluminium, all the metals showed better catalytic activity when coordinated as acetylacetonates than when coordinated as hydroxyquinolinates. The results also show the effect of reaction time on the effectiveness of the metals in catalysing the graphitisation of Refcoal cokes. For example, an optical micrograph of a coke containing calcium(II)acetylacetonate showed large granular anisotropic grains when it had been heat-treated at 1 600 °C for six hours, whereas fine anisotropic grains were observed when it had been heat-treated for only two hours.

Samples graphitised at 2 000 °C showed improved structural ordering compared with cokes heat-treated at 1 600 °C. This is generally due to the atomic rearrangement induced by high-temperature heat treatment. With X-ray diffraction analysis, the added metals were not observed in cokes graphitised at 2 000 °C, except for zirconium, which appeared as zirconia (ZrO_2). Even at this temperature the metals, including calcium, did not show much catalytic activity towards the graphitisation of Refcoal cokes. The metal-containing cokes graphitised at this temperature did not show substantial structural improvement, i.e. they remained largely amorphous. The coke containing calcium(II)acetylacetonate coke graphitised at 2 000 °C showed some evidence of a well-ordered phase structure compared with the neat coke graphitised at the same temperature. The copper-containing cokes had the highest structural disorder.

The results also show an improvement in structural ordering with an increase in the concentration of iron. Iron catalyses the graphitisation of Refcoal cokes through the metal-carbide formation mechanism. However, the cokes containing different concentrations of iron, and graphitised at 2 000 °C, show only a localised graphitisation. This means that some parts of the structure are crystalline, whereas other parts are disordered. Thus the method of metal dispersion is of critical importance.

It is therefore concluded that, for the Refcoal cokes studied here, calcium catalyses graphitisation to some extent, provided it is coordinated to acetylacetonate. It is suspected

that there may have been a significant difference in the metal contents of the Refcoal treated with metal acetylacetonate and that treated with metal hydroxyquinolinate. The pronounced stability of hydroxyquinolinate complexes is viewed as one of the factors that lead to the poor catalysing ability of metals when coordinated to the hydroxyquinoline ligand. The poor activity of metals towards graphitisation of Refcoal could also be possibly be due poor dispersion of metals in Refcoal carbon. It is also assumed that poor activity of the tested metals, was due the evaporation of metals before they effectively enhance graphitisation of Refcoal carbon.

There is an increase in the degree of graphitisation as the concentration of iron increases. Iron also promotes a localised graphitisation, thus leaving some regions of the material disordered. Iron catalyses graphitisation of Refcoal cokes through metal-carbide formation mechanism. Both reaction time and heat treatment temperature are important parameters in the catalytic activity of metals towards the graphitisation of Refcoal cokes. The employment of a short reaction time may result in the termination of reactions before they reach completion, thus having an effect on the structure of the resultant carbon product. However, although the heat treatment temperature and the reaction time are important, homogeneous dispersion of the catalyst particles is also vital.

The study has been able to create a background on catalytic graphitisation of Refcoal cokes. For future work, it is recommended that the method of dispersion be evaluated in details. Other parameters that determine the degree of graphitisation on a metal catalysed graphitisation should be studied on individual basis. More work should be done in studying the catalytic activity of calcium and iron, so as to reinforce their positive ability as shown on results and discussion.

CHAPTER 6: REFERENCES

Austerman S. B. (1968), *Chemistry and Physics of Carbon*. Ed, P.L. Walker Jr., New York.

Bouska, V. (1981). *Destruction and Decomposition of Plant Matter,* Elsevier: Amsterdam.

Brown, M. E. (1988). *Introduction to Thermal Analysis,* New York: Chapman Hall.

Charles, R. G. (1961). Heat stabilities of the alkaline earth chelate derived from 8-hydroxyquinoline. *J Inorg Nucl Chem,* 20**:** 211-221.

Cottinet, D., Couderc, P. & Roman, J. L. S. (1988). Raman microprobe study of heat-treated pitches. *Carbon,* 26: 334-339.

Crespi, M. S., Ribeiro, C. A., Greenhalf, V. C. M. & He, Z. J. (1999). Preparation and thermal decomposition of copper (II), zinc (II), and cadmium (II) chelates with 8-hydroxyquinoline. *Quimica Nova,* 22: 41-46.

Davidson, R. L., Natusch, D. F. S., Wallace, J. R. & Evans Jr, C. A. (1974). Trace elements in fly ash dependence of concentration on particle size. *Environ Sci Technol,* 8: 1107-.1113.

Derbishire, F. E., Presland, A. E. B. & Trimm, D. L. (1975). Graphite formation by the dissolution-precipitation of carbon in cobalt, nickel and iron. *Carbon,* 13: 111-113.

Dryden, I. G. C. (1945). *Chemical constitution and reactions of coal,* In: H. H. Lowry (Ed), Chemistry of Coal Utilization, New York: Wiley.

Ellington, R. T. (1977). *Liquid Fuels from Coal,* London: Academic Press.

Erdey, L. (1965). *Gravimetric Analysis*, Part II, London: Pergamon Press.

Firtzer, E. & Kegel, B. (1968). Reaktionen von Kohlenstoffgesattigter Vanadiumcarbidschemelze mit ungeordenetem Kohlenstoff (Beitrag zur katalytischen graphitierung), *Carbon,* 6: 433-441.

Fischbach, S. B. (1972). *Chemistry and Physics of Carbon,* P.L. Walker (Ed), London: Edward Arnold.

Forrest, M. & Marsh, H. (1983). Growth and coalescence of mesophase in pitches with carbon black additives and in coal. *Fuel,* 62: 612-615.

Francis, W. (1961). *Coal,* London: Edward Arnold.

Franklin, R. E, (1951). X-ray study of the graphitisation of CB, *Acta Cryst*, 4: 253-255.

Fuchs, W. (1942). *Thermodynamics and coal formation*, Int Min Met. Eng Trans, New York.

Gerhartz, W. (Ed) (1986). *Ullman's Encyclopedia of Industrial Chemistry.* London

Given, P. H. (1960). *The Distribution of Hydrogen in Coals and its Relation to Coal Structure.* London: Edward Arnold.

Guan, R., Li, W. & Li, B. (2003). Effects of Ca-based additives on desulphurisation during coal pyrolysis. *Fuel,* 82: 1961-1966.

Hata, T., Vystavel, T., Bronsveld, P. & Dehosson, J. (2004). Catalytic carbonisation of wood charcoal: Graphite or diamond? *Carbon,* 42: 961-964.

Hoffman, E. J. (1978). *Coal Conversion,* USA: Morden Printing Company.

Hollingshead, R. G. W. (1954). *Oxine and its Derivatives,* London: Butterworth.

Hong, S. E., Kim, D. K., Jo, S. M., Kim, D. Y., Chin, B. D. & Lee, D. W. (2007). Graphite nanofibres prepared from catalytic graphitisation of electrospun poly(vinylidene fluoride) nanofibres and their hydrogen storage capacity. *Catalysis Today,* 120: 413-419.

Inagaki, M., Harada, S., Sato, T., Nakajima, T., Horino, Y. & Morita, K. (1989). Carbonization of polyamide film “Kapton”, *Carbon,* 27: 253-257.

Ishikawa, T. & Yoshizawa, S. (1963). Some factors affecting the strength of carbon fibers. *J. Chem. Soc. Japan, Ind. Sec*. 66: 933-940

Jeffery, G. H., Basset, J. & Denney, R. C. (Eds) (1989). *Vogel's Textbook of Quantitative Chemical Analysis*, 5th edition, London.

Jenkins, G. M. & Kawaramura, K. (1976). *Polymeric Carbons,* Cambridge: Cambridge University Press.

Kanno, K., Fernandez, J. J., Fortina, F., Korai, I., & Mochida, I. (1997). Modification to carbonisation of mesophase pitch by addition of carbon black. *Carbon,* 35: 1627-1637.

Kanno, K., Yoo, K. E., Fernandez, K. E. J. J., Mochida, I., Fortina, F. & KORAI, Y. (1994). Effect of carbon black on the carbonisation of mesophase pitch. *Carbon,* 32: 801-807.

Kgobane, B. L. (2005). *Preparation and Characterisation of Graphitisable Carbon Prepared from Coal Solution.* PhD thesis, University of Pretoria, South Africa.

Khan, M. R., Walker, P. L. & Jenkins, G. R. (1988). Swelling and plastic properties of coal devolatilized at elevated pressures of H_2 and He. *Fuel,* 65: 693-699.

Kiebler, M. W. (1945). *The Action of Solvents on Coal,* In: H. H. Lowry (Ed), *Chemistry of Coal Utilisation,* New York: Wiley.

Kirk-Othmer (1996). *Encyclopedia of Chemical Technology,* 4th edition, Kroschwitz J, (Executive Editor), New York: Wiley, Vol. 6: 424–594.

Klug, H.P. (1984). *X-Ray Diffraction Principles*. London

Kokkonen, P., Palmu, L. & Lajunen, L. H. J. (1987). Thermal decomposition of 8-hydroxyquinoline complexes with aluminium, cobalt, manganese and nickel. *Thermochimica Acta,* 114: 329-336.

Lamber, R., Jaeger, N. & Schulz-Ekloff, G. (1988). Electron microscopy study of the interaction of Ni, Pd and Pt with carbon. *Surf Sci,* 197: 402-414.

Macherzysnska, B. & Blazewicz, S. (2004). Effect of intercalation on electrical and mechanical properties of C/C composite. *J Phys Chem Solids,* 65**:** 1745-1750.

Madswen, L. D., Charavel, R., Birch, J. And Svedberg, E. B. (2000). Assessment of MgO (100) and (111) substrate quality by X-ray diffraction. *J Crystal Growth,* 209: 91-101.

Maitre, A. & Lefort, P. (1997). Solid state reaction of zirconia with carbon. *Solid State Ionics,* 104: 109-122.

Mantell, C. L. (1968). *Carbon and Graphite Handbook,* New York: Interscience.

Marsh, H. & Menendez, R. (1988). Carbons from pyrolysis of pitches, coal and their blends. *Fuel Proc Tech,* 20: 269-296.

Marsh, H. & Warburton, A. P. (1970). Catalysis of graphitisation. *J Appl Chem,* 20: 133-142.

Marsh, H. & Warburton, A. P. (1976). Catalytic graphitisation of carbon using titanium and zirconium. *Carbon,* 14: 47-52.

Marsh, H. (1989). *Introduction to Carbon Science,* London: Pergamon, Butterworth.

Mochida, I., Itoh, I., Korai, Y., Fijubu, H. & Takishita, K. (1981). Catalytic graphitisation of fibrous and particulate carbons. *Carbon,* 19: 457-465.

Morgan, D. L. (2000). *Nuclear Graphite from Refcoal*. CSIR Report 86DC/Ht002, Pretoria.

Nasibulin, A. G., Moisala, A., Brown, D. P. & Kauppinen, E. I. (2003). Carbon nanotubes and anions from carbon monoxide using $Ni(acac)_2$ and $Cu(acac)_2$ as catalyst precursors. *Carbon,* 41: 2711-2724.

Nicholls, D. R. (2001). The Pebble Bed Modular Reactor, *Trans Roy Soc S Afr,* 56: 125-130.

Nicholls, D. R., (1996). The Pebble Bed Modular Reactor, *Eskom*, 25-26.

Nicholls, D. R., (2000). The Pebble Bed Modular Reactor, *S Afr J Sci*, 98: 31-35.

Noda, T., Inagaki, M., Amanuma, H. & Kamiya, K. (1965). Heat treatment of carbon under pressure, *Carbon,* 3: 336-339.

Otani, S., Oya, A. & Akagami, J. (1975). The effects of nickel on structural development in carbons, *Carbon,* 13: 353-356.

Oya, A. & Marsh, H. (1982). Phenomena of catalytic graphitisation, *J Mat Sci,* 14: 309-322.

Oya, A. & Otani, S. (1979). Catalytic graphitisation of carbons by various metals, *Carbon,* 17: 131-137.

Oya, A. & Otani, S. (1979). Effect of particle size of calcium and calcium compounds on catalytic graphitisation of phenolic resin carbon, *Carbon,* 79: 125-129.

Oya, A. & Otani, S. (1981). Influence of particle size of metal on catalytic graphitisation of non-graphitizing carbons. *Carbon,* 19: 391-400.

Oya, A. & Otani, S. (Eds) (1978). *Proc 5th Int Conf on Carbon and Graphite Conf,* London.

Park, S. H., Jo, S. M., Kim, D. Y., Lee, W. S. & Kim, B. C. (2005). Effect of iron catalyst on the formation of crystalline domain during carbonisation of electrospun acrylic nanofibre, *Synthetic metals*, 150: 265-270.

Parker, W. E., Merk, R. W. & Woodriff, E. M. (1965). Use of additives for graphite densification and improve neutron radiation stability, *Carbon,* 2: 395-406.

Preiss, H., Berger, L. & Szulzewsky, K. (1996). Thermal treatment of binary carbonaceous/zirconia gels and formation of Zr(C,N,O) solid solutions, *Carbon,* 134: 109-119.

Renganathan, K., Zondlo, J.W., Stiller, J.W., Phillips, A.H., and Mintz, E.A. (1987). Extraction studies on bituminous coal using N-methylpyrrolidinone. *International Conference on coal science*, Amsterdam.

Schilnder, H. D. (1989). *Coal Liquefaction Research Needs,* US Dept of Energy.

Schrader, B. (1995). *Infrared and Raman Spectroscopy,* New York: VCH Publishers.

Sevilla, M. & Fuertes, A.B. (2006). Catalytic graphitisation of templated mesoporous carbons. *Carbon*, 44: 468-474

Shevkoplyas, V. N. (2002). Coal carbonisation and addition of hydrochloric acid as a way of improving coke quality, *Fuel,* 81: 947-950.

Shoko, L. (2005). *The Chemistry of the Alkali-induced Solubilisation of Coal,* MSc Thesis, University of Pretoria, South Africa.

Starch, E., Mackowsky, H. T., Teichmuller, Tailor, G. H., Chandra, D. & Teichmuller, R. (1982). *Starch's textbook of coal petrology*. Berlin, Eddward Arnold Stuttgart

Taylor, G. H., Pennock, G. M., Fitz, Gerald, J. D. & Brunckhorst, L. F. (1993). Influence of QI on mesophase structure, *Carbon,* 31: 341-354.

Tohji, K., Goto, T., Takhashi, H., Shinoda, Y., Shimizu, N., Jeyadevan, B., Matsuoka, I., Saito, Y., Kasuya, A., Ohsuna, T., Hiraga, K., Nishina, Y., (1996). Purifying single-walled nanotubes, *Nature,* 383: 679-679.

Tsubruchi, N., Xu, C. & Ohtsuka, Y. (2003). Carbon crystallisation during high-temperature pyrolysis of coal and enhancement by calcium. *Energy and Fuels,* 17: 1119-1125.

Tuinstra, F. & Koenig, J. L. (1970). Raman spectrum of graphite, *J Chem Phys,* 53: 1126-1130.

Urbach, J. (2006). *Nuclear Power for South Africa.* The Free Market Foundation of Southern Africa.

Valkovic, V. (1983). *Trace Elements in Coal,* Vol. 1, Boca Raton, Florida, USA: CRC Press.

Van Krevelen, D. W. (1961). *Coal: Typology Chemistry-Physics Constitution,* Elsevier: Amsterdam.

Wang, W., Thomas, M., Poultney, R. M. & Willmers, R. R. (1995). Iron catalyzed graphitisation in the blast furnace, *Carbon,* 33: 1525-1535.

Wang, Y., Korai, Y., Mochida, I., Nagayama, K., Hatano, H. & Fukuda, N. (2001). Modification of synthesis of mesophase pitch with iron oxide, Fe_2O_3, *Carbon,* 39: 1627-1634.

Weisweiler, W., Subramainan, N. & Terwiesch, B. (1971). Catalytic influence of metal melts on the graphitisation of monolithic glasslike carbon. *Carbon,* 9: 755-781.

Wilson, P. J. & Wells, J. H. (1950). *Coal, Coke and Coal Chemicals*, New York: McGraw-Hill.

Yokokawa, C., Hosokawa, K. & Takegami, Y. (1967). A kinetic study of catalytic graphitisation of hard carbon, *Carbon,* 5: 475-480.

APPENDIX

Table A1: Mass changes in Refcoal samples on carbonisation for 2 hours at 900 °C under N_2

Sample	Mass (g) before carbonisation	Mass (g) after carbonisation	Yield (%)	Volatiles (%)
Neat coke	2.81	2.15	76.63	23.75
3%Fe(acac) coke	2.80	2.03	72.25	27.75
3%Al(acac) coke	2.86	2.07	72.73	27.27
3%Ca(acac) coke	2.76	1.98	71.74	28.26
3%Cu(acac) coke	2.62	1.90	72.51	27.49
3%Zr(acac) coke	2.96	2.17	73.31	26.69
3%Fe(ox) coke	2.14	1.57	73.36	26.64
3%Al(ox) coke	2.88	2.10	72.91	27.09
3%Ca(ox) coke	2.99	2.26	73.26	26.74
3%Cu(ox) coke	2.88	2.15	74.65	25.35
3%Zr(ox) coke	2.74	2.03	74.08	25.92
0.5%Fe(acac) coke	2.75	2.09	76.00	24.00
5%Fe(acac) coke	2.77	1.97	71.11	28.89

Table A2: Mass changes in coke samples on graphitisation for 2 hours at 1 600 °C

Sample	Sample ID	Mass (g) before graphitisation	Mass (g) after graphitisation	Yield (%)	Volatiles (%)
Neat coke	C162	2.48	2.15	86.69	13.30
3%Fe(acac) coke	FeaC162	2.50	2.00	80.00	20.00
3%Al(acac) coke	AlaC162	2.51	2.18	86.88	13.15
3%Ca(acac) coke	CaaC162	2.54	2.23	87.79	12.20
3%Cu(acac) coke	CuaC162	2.47	2.10	85.02	14.97
3%Zr(acac) coke	ZraC162	2.51	2.19	87.25	12.75
3%Fe(ox) coke	FeoC162	2.51	2.18	86.85	13.14
3%Al(ox) coke	AloC162	2.51	2.12	84.46	15.52
3%Ca(ox) coke	CaoC162	2.52	2.16	85.71	14.28
3%Cu(ox) coke	CuoC162	2.54	2.07	81.49	18.50
3%Zr(ox) coke	ZroC162	2.52	2.09	82.92	17.06

Table A3: Mass changes in coke samples on graphitisation for 6 hours at 1 600 °C under N_2

Sample	Sample ID	Mass (g) before graphitisation	Mass (g) after graphitisation	Yield (%)	Volatiles (%)
Neat coke	C166	2.48	2.22	89.52	10.48
3%Fe(acac) coke	FeaC166	2.37	2.07	87.34	12.68
3%Al(acac) coke	AlaC166	2.42	2.09	86.36	13.63
3%Ca(acac) coke	CaaC166	2.32	2.07	89.22	10.77
3%Cu(acac) coke	CuaC166	2.34	2.00	85.47	14.53
3%Zr(acac) coke	ZraC166	2.31	2.04	88.31	11.68
3%Fe(ox) coke	FeoC166	2.40	2.06	85.83	14.16
3%Al(ox) coke	AloC166	2.33	1.95	83.69	16.30
3%Ca(ox) coke	CaoC166	2.47	2.12	58.82	14.17
3%Cu(ox) coke	CuoC166	2.52	2.05	81.34	18.65

3%Zr(ox) coke	ZroC166	2.40	2.02	84.16	15.83

Table A4: Mass changes in coke samples on graphitisation for 2 hours at 2 000°C under N_2

Sample	Sample ID	Mass (g) before graphitisation	Mass (g) after graphitisation	Yield (%)	Volatiles (%)
Neat coke	C22	2.60	2.26	86.92	13.07
3%Fe(acac) coke	FeaC22	2.62	2.25	84.90	14.12
3%Al(acac) coke	AlaC22	2.66	2.22	83.46	16.54
3%Ca(acac) coke	CaaC22	2.61	2.28	87.35	12.64
3%Cu(acac) coke	CuaC22	2.59	2.18	84.16	15.83
3%Zr(acac) coke	ZraC22	2.58	2.23	86.43	1.56
3%Fe(ox) coke	FeoC22	2.64	2.24	84.85	15.15
3%Al(ox) coke	AloC22	2.65	2.16	81.51	18.49
3%Ca(ox) coke	CaoC22	2.68	2.22	82.83	17.16
3%Cu(ox) coke	CuoC22	2.65	2.21	83.39	16.60
3%Zr(ox) coke	ZroC22	2.74	2.37	86.49	13.50
0.5%Fe(acac) coke	1/2FeaC22	1.28	1.17	89.84	10.16
5%Fe(acac) coke	5FeaC22	1.33	1.16	87.21	12.79

Table A5: Masses used in sample preparation for X-ray diffraction measurements (List 1)

Sample	Mass of sample (g)	Mass of silicon (g)
Neat coke	0.66426	0.035442
3%Fe(acac) coke	0.66706	0.033353
3%Al(acac) coke	0.67094	0.033547
3%Ca(acac) coke	0.66366	0.033183
3%Cu(acac) coke	0.66256	0.033128
3%Zr(acac) coke	0.67444	0.033722
3%Fe(ox) coke	0.66097	0.033048
3%Al(ox) coke	0.66240	0.033119
3%Ca(ox) coke	0.66448	0.033224
3%Cu(ox) coke	0.67378	0.033821
3%Zr(ox) coke	0.66255	0.662552
0.5%Fe(acac) coke	0.66579	0.032895
5%Fe(acac) coke	0.64155	0.032077

Table A6: Masses used in sample preparation for X-ray diffraction measurements (List 2)

Sample	Mass of sample (g)	Mass of silicon (g)
C162	0.60522	0.03185
FeaC162	0.60906	0.03205
AlaC162	0.57341	0.03017
CaaC162	0.57810	0.03030
CuaC162	0.61668	0.03245
ZraC162	0.58533	0.03080
FeoC162	0.60710	0.03191
AloC162	0.59216	0.03266
CaoC162	0.61618	0.03143
CuoC162	0.60516	0.03186
ZroC162	0.60522	0.03166

Table A7: Masses used in sample preparation for X-ray diffraction measurements (List 3)

Sample	Mass of sample (g)	Mass of silicon (g)
C166	0.62685	0.03299
FeaC166	0.60906	0.03205
AlaC166	0.57341	0.03017
CaaC166	0.62376	0.03282
CuaC166	0.61521	0.03254
ZraC166	0.59821	0.03132
FeoC166	0.62269	0.03227
AloC166	0.62875	0.03309
CaoC166	0.61793	0.03251
CuoC166	0.60048	0.03160
ZroC166	0.62819	0.03306

Table A8: Masses used in sample preparation for X-ray diffraction measurements (List 4)

Sample	Mass of sample (g)	Mass of silicon (g)
C22	0.62226	0.03275
FeaC22	0.59926	0.03154
AlaC22	0.63086	0.03320
CaaC22	0.62376	0.03282
CuaC22	0.62962	0.03313
ZraC22	0.59679	0.03141
FeoC22	0.62269	0.03227
AloC22	0.59456	0.03129
CaoC22	0.62677	0.03298
CuoC22	0.59605	0.03137
ZroC22	0.62092	0.03268
1/2FeoC22	0.50660	0.02666
5FeoC22	0.49020	0.02581

Table A9: Operating parameters of X-ray powder diffraction

Target element	Cu
Temperature	25 ˚C
Sample	Flat-plate, rotating (30 r/min)
Power setting	45 kV, 40 mA
Soller slit	2˚ (diffraction beam side)
Divergence slit size	1˚
Receiving slit	0.05˚
Monochromator	Secondary, graphite
Detector	Scintillation counter
Range of 2θ	10-90˚, 2θ
Step width	0.008˚ 2θ
Time per step	5 seconds

Table A10: Operating parameters of Raman spectroscopy

Laser power	200 mW
Excitation line	568.2
Objective lens	x50
Accumulation	2
Time	60

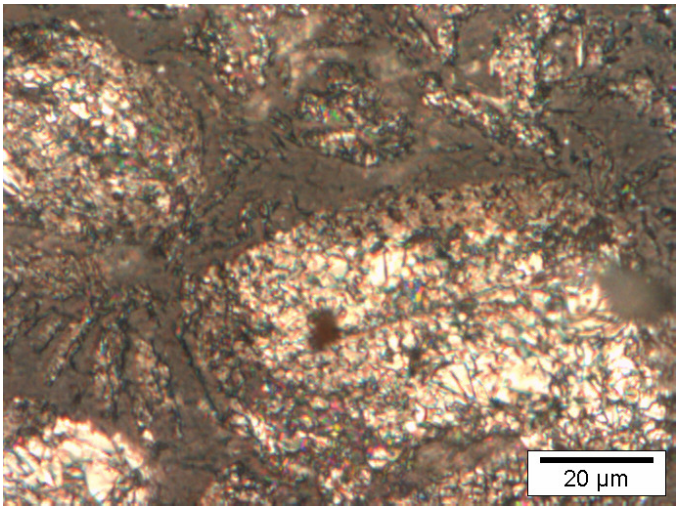

Optical micrograph of a synthetic graphite